Longterm, high resolution records of climate variability from cave speleothems in Cold Air Cave, Makapans Valley, Limpopo Province

FINAL REPORT TO THE WATER RESEARCH COMMISSION

2004

Julia A. Lee-Thorp

Department of Archaeology and Quaternary Research Centre
University of Cape Town

ISBN 1-77005-205-4
WRC REPORT NO 1013/1/04

PREFACE

This project was initiated following the success of a pilot study that developed proxy records from stalagmites in the Makapansgat Valley. Professor Karin Holmgren, Department of Geography and Quaternary Geology, Stockholm University, co-led the pilot project with Professor Peter Tyson, Climate Research Unit, University of the Witwatersrand. Out of a number of stalagmites sampled from several sites in Gauteng and the Limpopo Province, stalagmites from the Cold Air Cave, Makapansgat Valley, showed greatest promise. The shortest "T5" stalagmite was discontinuous and began growing about 4.5 Ky ago. It was analysed as a Masters project and published (Repinski et al, 1999). A small stalagmite from nearby Ficus Cave was analysed as an Honours project at the University of Cape Town (Spreckley 1998). The "T7" stalagmite provided a magnificent 6.5 Ky record with oxygen and carbon isotope ratios performed in the University of Cape Town Stable Light Isotope Facility, grey scale and incremental analysis (supervised by Holmgren at Stockholm University), and a chronology from α-spectrometry Uranium series in Professor Lauritzen's laboratory, Bergen University. The first set of results were published as Holmgren et al (1999). Analysis of T5 and T7 provided good experience in sampling and interpreting the proxy data from these unusual aragonite stalagmites. Both showed high frequency oxygen isotope variability that precluded conventional interpretation as temperature fluctuations, but T5 provided inadequate corroboration for the T7 record.

Stronger corroboration and validation of the proxy records was urgently required. Hence the proposal to the Water Research Commission included two main components - to provide corroboration by further analyses of these and an additional stalagmite from Cold Air Cave, and to set up a monitoring study of the cave climate and environment to develop sounder interpretive tools. First, more precise dates were obtained for T7 by means of Thermal Ionisation Mass Spectrometry analysis in the Bergen laboratory, and dates were established for a third stalagmite, T8, by the same method in Dr Toni Eisenhauer's Geochronology Laboratory, GEOMAR, Kiel. The full results for T7 were published with the new age model (Lee-Thorp et al, 2001), providing a comparison for the results from the slightly taller T8, recovered a few metres away from T7.

The regional team as initially constituted for the present project consisted, apart from me, of Associate Professor Chris Harris and Mr Craig Stevenson at the University of Cape Town, and Professors Tim Partridge and Peter Tyson at the University of the Witwatersrand. The collaboration continued with Professor Karin Holmgren, who supervised the chronological and colour analyses. Some changes were effected along the way. Associate Professor Harris, who performed the isotope analyses of water samples in the monitoring study, left to take up a post in France (he has since returned to UCT). Subsequently these analyses were performed by Dr Jodie Miller from the same laboratory, and on one occasion by Professor Balt Verhagen, Witwatersrand University Hydrology

Laboratory. Excepting the latter set, all stable light isotope measurements of waters and carbonates were carried out in the Stable Light Isotope Facility, University of Cape Town. The monitoring study was extended to include trace element analyses on cave waters, by Dr Andreas Spath of the ICP-MS Unit, Geological Sciences, University of Cape Town, guided in the early stages by Dr Stephanie de Villiers until her departure from UCT. Pressure on Professor Lauritzen's laboratory caused us to shift the U-series dating programme to Dr Toni Eisenhauer's laboratory in GEOMAR, Kiel. Hence dates on T8 were performed at two laboratories: the first set of α-spectrometry dates in Bergen, and the high resolution dates in Dr Eisenhauer's lab.

A number of South African and Swedish students were involved in the project, either in the form of research projects (Mr Simon Gear, Wits) or as student assistantships (Ms Riashna Sithaldeen, Ms Shaun Spreckley, Mr Ian Newton at UCT and Ms Katarina Lundblad at Stockholm University).

ACKNOWLEDGEMENTS

I am sincerely grateful to the many people who contributed to this study. Firstly, I express my thanks to the 'core' team members who helped to guide this project: Professor Karin Holmgren of Stockholm University, and Professors Peter Tyson and Tim Partridge of the University of the Witwatersrand. Professor Stein-Erik Lauritzen permitted the use of his dating laboratory and provided many snippets of advice. Dr Toni Eisenhauer provided prompt U-series TIMS analyses and assisted in interpreting the data. Associate Professor Chris Harris, together with Dr Jodie Miller, performed isotope analyses on all cave waters, apart from one set which was kindly performed by Professor Balt Verhagen, University of the Witwatersrand. Dr Andreas Spath and Dr Stephanie de Villiers either performed, or helped to interpret, the trace element analyses of water. I thank Mr John Lanham, Stable Light Isotope Facility at UCT, for his help and patience, and Drs.Amanda Rau and Jean-Luc Melice for their help with continuous wavelet analyses. Professor Paul Shaw (Luton University) hosted a small workshop about trace element distributions, and his and Dr Adrian Finch's high resolution elemental analyses of T8 helped us to interpret the mineralogy.

For assistance in both laboratory and field, I thank Mr Craig Stevenson, Miss Riashna Sithaldeen, and Mr Ian Newton from UCT, and Mr Pedro Boshoff, now at the Palaeoanthropology Unit Research (PURE), University of the Witwatersrand. Mr Boshoff ensured our safety on numerous cave trips. Ms Sithaldeen managed most of the sampling and analysis, field excursions and data management while Mr Newton nursed the climate station and extracted the data. I am grateful to Mr Walter Mertzl, Zwartkrans Farm, for access to his meticulous rainfall records. The South African Weather Services responded efficiently to requests for climate data for Polokwane and elsewhere. The Limpopo Province Conservation Dept. and the Scientific Committee chaired by Professor Bruce Rubidge, Director of the Bernard Price Institute for Palaeontology, granted permission to carry out the cave monitoring study in the Valley, which is a National Heritage site. I thank conservation officer Mr Stan Rodgers, Limpopo Province, for his assistance with permits and in the field.

This project would not have been possible without funding from the Water Research Commission, and the support of the Steering Committee and its Chairman, Dr George Green. In addition to Dr Green, the Steering Committee consisted of Professor Peter Tyson, Dr Peter Zawada, Dr E.C. February, Mr E.A. Nel (alternate Mr F. Cornelius), Mr A.S. Talma, Dr Stephan Woodborne, Dr D. Hudson, Professor Louis Scott, Professor Partridge, Mr J.F. Tjaljaard, and Mrs C.M. Smit. Without wishing to diminish the valuable contributions of *all* the steering committee members, I would like to thank particularly Mr Siep Talma and Dr Stephan Woodbourne, QUADRU, CSIR; for their enthusiasm, advice, and generosity in sharing ideas. During the extended phase of the project, funding to complete the project was provided by the National Research Foundation.

EXECUTIVE SUMMARY

This project built on the results of a pilot study using proxy records from stalagmites in the Cold Air Cave, Makapansgat Valley, Limpopo Province, to establish longterm, high resolution proxy climate records. Such records can provide a more holistic perspective of the behaviour of the South African climate over longer time-scales, and hence, a more comprehensive understanding of variability and forcing over the longer term, and greater predictive power. At present, the two outstanding features of the South African climate - low rainfall and high variability - together with relatively short instrumental records, conspire to limit understanding of climate patterns and variability over decadal and centennial scales. Short sequences can provide no indication about longer-term climate cycles and position of the current climate within those cycles, inherent harmonic modes, or dominant forcing mechanisms over these time-scales. Proxy data series from continuous cave speleothems present significant new opportunities for addressing these gaps.

OBJECTIVES

The overall goal of the current project was to extract continuous, long-term, and highly resolved records of climate and environmental variability in the north-eastern, summer rainfall region of South Africa, and to improve our understanding of the interpretation of the proxies. In the pilot project the Cold Air Cave aragonitic stalagmites showed promise as a source for palaeoclimate proxy data from oxygen and carbon isotope ratios, grey scale, incremental and trace elements. In the current project the aims were to validate and expand the existing record and the interpretations, by means of a cave climate monitoring study and further study of new and existing stalagmites. The aims, as set out in the original proposal, can be summarised as follows.

> The construction of a regional, sub-decadal scale record of precipitation, temperature and vegetation response in the north-eastern, summer rainfall region, to be accomplished through the following aims:
>
> 1. Precise validation of the chemical signals in speleothems pertaining to moisture availability, nature of rainfall, temperatures, and vegetation responses.
>
> 2. Amplify and strengthen existing speleothem records for the Makapan Valley.
>
> 3. Improve chronological resolution to achieve sub-decadal scale records.
>
> 4. Integration and statistical interrogation of the palaeoclimate time series to establish (i) variability of precipitation, temperatures and vegetation, (ii) regional comparisons and detection of forcing, and (iii) occurrence and impact of extreme events.

There were thus essentially two connected arms to the project, one focused on understanding current processes, and the other on the stalagmite records. In the final report the methods and results are

considered in 4 chapters in addition to the introduction, a descriptive chapter about the site and materials, and the conclusions. The contributors to the project are given in the preface to the report, along with brief indications of their contributions.

METHODS AND RESULTS

Cave climate monitoring

In August 1999 a data-logger was placed in the cave's interior near the collection point of the stalagmites. We sought to establish, by measurement of temperature, relative humidity, seepage flow (via a rain gauge) and drip rate in the cave, whether the requirements for isotopic equilibrium and stalagmite growth were met, whether the cave interior did in fact reflect external mean annual temperatures, and a better understanding of the controls in this cave site. Conditions were monitored, intermittently because of some instrument difficulties in the corrosive cave atmosphere, for almost 3 years. The results showed that relative humidity remained at 100% throughout the year and that temperature did not fluctuate diurnally or on short time scales, although there is a small negative inflexion in the winter months. The mean value of 18.8^{o}C accurately reflects mean annual temperature for the area. We monitored the amounts of drip-water and periodically analysed seepage, pool and river water from a variety of locations. Amounts of drip-water measured by the rain gauge reasonably reflected the pattern in the cave. Drip-water amounts exaggerated the annual cycle, with large amounts in mid-late summer, and minimal to none in winter.

The variability of isotopic and trace element composition of seepage water from different points was established. The results showed that water in the cave pool was distinct from dripwater, and that small local scale variability occurred as a result of different fissure tracks through the roof. One clear effect is due to the amount of roof thickness through which the water travels. The record is too short to establish direction of shifts with regional rainfall, but it did establish that cave waters, and others in the region, undergo effects which shift the relationship between δD and $\delta^{18}O$ above the international meteoric water line. Trace element analysis showed that calcium, magnesium and sodium ions were super-abundant, and that amounts of strontium, barium, potassium and manganese fluctuated in complex ways, but most notably at the beginning and ends of wet and dry seasons.

Chronology

High resolution dating methods were required in order to establish sound age models congruent with the high resolution of the proxy data sampling, and to allow comparisons with other high resolution series such as ice cores. The T7 stalagmite was re-dated, and the new stalagmite T8, dated by means of Thermal Ionisation Mass Spectrometry uranium series. Both stalagmites are now *extremely* well-dated. The new dates for T7 showed that it had grown continuously, regularly and relatively quickly. The same was true of the upper aragonitic section of T8, which gave ages of 0 to 10 200 years.

Dates for the lowermost calcitic section had far larger errors due to a change in uranium chemistry, and showed far slower growth from 12 700 to 24 600 years ago. The hiatus between 10 200 and 12 700 is well-constrained. Age models were constructed by linear interpolation between dated points for the aragonitic sections, and by linear regression over the whole period for the calcite section. Excellent dating precision of ± 6 to160 years was obtained for the period 0-12 700 years; thereafter precision declines from about ± 500 yr at 13 Ky to about ±3000 years at 24 400 years. The age models suggest that average sampling intervals were about 10 - 20 years for T7, for T8 9 years on average for the aragonite growth and ≥50-100 years for the calcite growth although the latter does not take into account the large errors.

Stalagmite proxy data

The proxy data series outlined in the report concern mainly the oxygen and carbon isotope series. Samples were drilled at as close a spacing as possible using a handheld drill. Analysis for isotopes of oxygen and carbon followed standard procedures. The results for T8 show similar high variability behaviour as for T7 (and unlike the previously published Cango Cave data) and the two series are reasonably concordant. The longer view provide by the T8 record, however, provides a far more comprehensive perspective. By this stage we were able to argue with some confidence that the stalagmite oxygen isotope values are *not* inversely related to temperature fluctuations based on the thermodynamic fractionation between seepage water and carbonate. Rather, they are directly, although more distantly, related via the effects of rainfall patterns - whether there is proportionately more input from high altitude convective storms and hail (hence cold, leading to depletion in ^{18}O), or from medium altitude, continuous rain and generally warmer atmospheric conditions.

Overall trends and several pronounced excursions are visible in the records. A marked depletion excursion in ^{18}O, common to both records, occurs at AD 1700 at about the time of the Little Ice Age, suggesting that this period was cooler, stormier and possibly drier. The rapid shifts observed in these stalagmite records provide a strong indication about the rapidity of climate changes in rainfall and vegetation patterns, which are on the order of years to decades. Further back, another surprise is the lack of a pronounced Last Glacial Maximum signal in $\delta^{18}O$, rather the LGM seems to be merely one of a series of modest quasi-periodic shifts. The ^{13}C records provide indications of the evolutionary series of shifting amounts of C_4 grasses within the vegetation, and a useful complement to the $\delta^{18}O$ record. These data indicate that C_4 grasses were always abundant in the environment. Lower amounts in the early and late Holocene periods respectively suggest lower grass coverage, probably as a result of aridity. A pronounced peak in C_4 grasses is seen in both records, and the distant Cango Cave stalagmite, about 2200 years ago. This is likely due to occurrence of optimal conditions for C_4 at this time, namely high solar radiation in the growing season, and might also reflect stronger seasonality or shorter, more intense growing seasons.

Variability and longterm trends

The main trends for $\delta^{18}O$ and the $\delta^{13}C$ records in the late Pleistocene are low frequency quasi-periodic shifts, but the Holocene records show stronger directional trends. In the Holocene the $\delta^{18}O$ trend is from more positive to more negative values culminating at AD 1700. Trends for $\delta^{13}C$ are different, from lower values in the early Holocene to higher values at 2000-2500 years.

Variability was interrogated by multi-taper spectral analysis and continuous wavelet transform (CWT) analysis on T7, and CWT analysis on T8. The results underscore the complexity of the climate variability suggested by visual observation. All bands showed strong frequency and amplitude modulation. Amongst the lower frequency bands, frequency modulation occurs from longer periods in the Pleistocene to shorter periods in the Holocene. For $\delta^{18}O$ this is from moderate ~4000 to stronger but discontinuous ~3000 year bands, and weak, intermittent ~1000 to intense, intermittent ~750 year bands. For $\delta^{13}C$, an intense, continuous band at ~4000 modulates to a weaker band at ~2500 years, and a moderate, discontinuous ~750 band becomes broader and intense in the Holocene. Also observed in the $\delta^{13}C$ Holocene series is intermittent power at ~300 years, in agreement with the T7 spectral analysis. The higher frequency Holocene spectrum is noisy for both isotope series, showing intermittent variability in broad bands between ~50-150 years. The results suggest that most power occurs in the lower frequency bands, especially at multi-centennial (1000-700 years), scales. These data suggest that variability in rainfall patterns (from $\delta^{18}O$) and proportions of tropical C_4 grasses in the floral mix (from $\delta^{13}C$) is more predictable at lower frequencies than at high frequency, multi-decadal scales.

Although not well-understood, variability in the multi-millennial to multi-centennial scales may relate to non-linear responses of the precession cycle, solar forcing, and the global thermohaline conveyor system. The greater intensity of $\delta^{13}C$ variability at these scales supports the importance of solar factors, since proportions of C_4 grasses in the floral environment are sensitive to solar radiation and seasonality (that is, when pCO_2 is held constant). No evidence exists for the presence of Dansgaard/Oeschger events, so prominent in the Greenland ice cores and North Atlantic marine records.

Comparison of the stalagmite $\delta^{18}O$ records with Antarctic ice core records, such as Byrd and Taylor Dome, and with the nearby Wonderkrater pollen cores, indicate similar trends over longer and shorter time scales. The general “flatness” of the late Pleistocene is a surprising feature in the stalagmite curve but closer inspection of a variety of regional and Antarctic records suggests that it is less unusual than first apparent. The results suggest strong and rapid teleconnections with Antarctic climate patterns, most likely related to the intensity and extent of the circumpolar vortex.

However leads, or rather, lags, are difficult to detect given that they are of the same kind of magnitude as errors in the stalagmite age models.

Conclusions

We have made considerable progress in understanding and interpreting the proxy data archived in these cave stalagmites. A watertight interpretation of the marked isotopic depletion episodes observed in the palaeo-records still eludes us, although we have eliminated a number of competing explanations. Isotopic records for the two stalagmites agree well on the whole, and this gives far greater confidence that the climate records are robust. The $\delta^{18}O$ and $\delta^{13}C$ series from T8 and T7 undoubtedly confirms high climate variability on multi-decadal, centennial and millennial scales. The patterns for these proxies, therefore suggests that rainfall and vegetation patterns have continuously shifted in the past, often extremely rapidly. But the variability is noisy at higher frequencies (multi-decadal and to a lesser extent centennial scales) while the overall trends and low frequencies are more predictable. This means that the original goals of achieving greater predictability cannot be met using the methods we used, at least for the short term.

EXTENT TO WHICH OBJECTIVES WERE MET

1. Our understanding of the relationships between climate parameters such as rainfall and temperature, the cave environment and contents, and the stalagmite proxy data are enormously improved. However a number of grey areas remain, most notably the *exact* nature of the relationship between isotopic composition of rainfall under different conditions, and precisely how this is reflected in the stalagmite records.
2. We now have two (three counting the intermittent T5) stalagmite records which agree, making for a very robust proxy climate series.
3. These two series are extremely well-dated with highly robust age models, far exceeding anything which has previously been achieved for a long South African climate record.
4. We reached the limit of resolution for isotopic analyses using handheld drilling methods, at ~9 years. We had aimed for up to 5 years. Preliminary ultra high resolution trace element analyses suggest that sub-*annual* precision is possible for the strontium and barium proxy series, the same may be true for stable isotopes if higher resolution sampling and analytical techniques are applied (for instance, laser ablation isotope analysis which is not available in SA).
5. An important goal was to test variability over longer time periods; the results suggest that low frequency variability is more important and predictable, and that the high frequency spectrum at the multi-decadal, and to a lesser extent the centennial, level is very noisy.
6. Comparisons with high resolution Antarctic cores reveal strong similarities especially at centennial scales, and indicate strong teleconnections over long time scales between atmospheric circulation in the two regions.

7. Stronger, quasi-periodic cycles of proportions of C_3 and C_4 plants exist than has previously been suspected. It would seem that solar forcing (impacting on radiation and seasonality) has had a marked effect on the abundances of C_4 grasses, and that of pCO_2 perhaps rather less than expected.

RECOMMENDATIONS FOR THE FUTURE

We have demonstrated that we can extract robust high resolution, continuous climate records from cave stalagmites. The challenge for the future is to expand the application to other locations in South Africa by establishing further similar records. It would be useful to check whether another location in the summer rainfall area follows the same pattern, including the high variability. A good high resolution record from the Western Cape would be highly desirable, as it would allow us to test whether the two regions really remain anti-phase for rainfall as suggested by some analyses of the meteorological records. The Cango Cave stalagmite records in the Southern Cape should be revisited for higher resolution sampling.

A continuous programme monitoring the relationship between isotopic composition of rainfall with temperature and rainfall variability is necessary for further developing understanding of these tools. Such a programme should be located in more than one location in South Africa. Spin-offs would provide fundamental data important not only for the interpretation of stalagmites, but also for other high resolution records.

The surprising observations for cyclical variability of C_4 grasses over the longterm, in response apparently to solar radiation changes (although this is not certain) to solar radiation changes, deserve further investigation, either from stalagmites at other locations, or even better, using independent proxies.

Finally, the findings for long-distance connections between the Antarctic climate system, shown to exist over the long-term in addition to recent work demonstrating similar connections in the present-day, deserves a great deal more attention, as it likely holds a key to understanding a major influence on South African climate.

STALAGMITE ARCHIVES AND DATA STORAGE

At present, one section of the T8 stalagmite is housed in the Stable Light Isotope Facility, Archaeology Department, University of Cape Town, and another in the Geography and Quaternary Department, Stockholm University. The remaining section of T7 is held in the latter department. Applications for access can be made to Associate Professor Julia Lee-Thorp (jlt@science.uct.ac.za) or to Professor Karin Holmgren (karin.holmgren@natgeo.su.se). When all analyses are complete, the remaining material will be housed in the Bernard Price Institute for Palaeontology, University of the Witwatersrand.

The complete set of data for T7 is available from the NOAA National Palaeoclimatic Data Center archive, available online at http://www.ngdc.noaa.gov/paleo/data.html. The data for T8 will be placed in the same repository as soon as publications are completed (2004). The NOAA NPDC has a mirror site at the University of the Witwatersrand.

TABLE OF CONTENTS

LIST OF TABLES

LIST OF FIGURES

CHAPTER 1

INTRODUCTION AND BACKGROUND TO LONGTERM CLIMATE CHANGE IN SOUTH AFRICA, CONTRIBUTIONS OF STALAGMITE RECORDS TO CLIMATE RESEARCH.

It is a truism that water resources in our largely arid country are a crucial limiting factor in development. Two outstanding features of the southern African climate - low rainfall and high variability - taken together with relatively short instrumental records, conspire to limit understanding of climate patterns and variability over decadal and centennial scales. Short sequences can provide no indication about longer-term climate cycles and position of the current climate within those cycles, inherent harmonic modes, or about dominant forcing mechanisms over these time-scales. Proxy data series from continuous cave speleothems present significant new opportunities for addressing these gaps. At the time of writing the proposal to the Water Research Commission, very few speleothem records had been obtained for southern Africa; where they existed resolution was poor. As outlined in the proposal, the aims of this project were as follows.

> The construction of a regional, sub-decadal scale record of precipitation, temperature and vegetation response in the north-eastern, summer rainfall region, to be accomplished through the following aims:
>
> 1. Precise validation of the growth and chemical signals in speleothems that pertain to moisture availability, nature and amount of rainfall, temperatures, and vegetation response, in order to separate and elucidate these signals.
>
> 2. Amplify and strengthen existing speleothem records for the Makapan Valley, in order to establish consistency of the signals and record on a broader regional scale, by reconstructing further similar high resolution stalagmite proxy record.
>
> 3. We seek to improve our chronological resolution, in order to achieve sub-decadal scale records. In principle these are achievable to perhaps 5 year scales, duing periods of favourable growth of stalagmites, as long as optimal sampling and analytical measurements can be obtained.
>
> 4. Integration of this data, and its statistical interrogation to establish (i) variability of precipitation, temperatures and vegetation, (ii) amplitude, and (iii) rate, of change, (iv) quasi-periodicities at various scales, (v) regional comparisons and detection of forcing, and finally (vi) occurrence and impact of extreme events.

The rest of the introduction chapter identifies the gaps for long-term climate records, and outlines the rationale for proxy data from speleothems as presently understood.

GAPS IN EXISTING SOURCES OF CLIMATE AND ENVIRONMENTAL DATA

Climatologists and meteorologists rely extensively on data from a nationwide network of hundreds of climate stations, available through the South African Weather Service. An extensive and complex data-base now exists for more-or-less the entire country; this has been extensively used for analysis of recent climate patterns. However, records for many stations include only the last 20-30 or so years of data, and only a handful record information for about 100 years (Tyson, 1986). Hence the instrumental record for South Africa is relatively short.

Palaeoclimate proxy records are recognised as providing the means for extending climate records further back into the past. Not only do longer records allow us to determine trends, patterns and variability in the natural system, they offer opportunities for comparisons across space and time, for detecting periodicity, and hence ultimately for a better understanding of forcing and hence prediction. They further provide a basis for testing General Circulation Models in climate systems with conditions completely unlike those operating today. Hence palaeoclimate records provide information otherwise hidden from us. They are particularly important where climate records are short, as they are in southern Africa.

Establishing good continental proxy records further back in time presents considerable challenges in this region. Ideal proxy records would be located in appropriate places, stratigraphically reliable and continuous yet with accumulation rates sufficient for high resolution , yield quantifiable proxies, and be amenable to precise age-dating. All these qualities are extremely rare in the southern African Quaternary record because the landscape is generally arid and erosive with a tendency to erase deposits. With the notable exception of the Tswaing Crater Saltpan (Partridge et al, 1997), there are no continuous lake sequences that offer opportunities for continuous incremental sequences. Further, the climate has never offered the extremes in terms of temperature that can be readily observed, and as experienced in the more intensively studied northern hemisphere.

A further considerable challenge lies in the interpretations of the proxy data themselves. Almost without exception understanding of the various proxies commonly used in palaeoclimate studies everywhere is still under development and refinement.

CAVE SPELEOTHEMS AS SOURCES OF CLIMATE PROXY DATA

In low or mid-latitude regions, secondary precipitates in the form of cave speleothems constitute one of the few archives with the potential for encoding a continuous climate record spanning a long period of time. Caves offer protection from the forces of destruction on the surface – such as weathering and erosion - and temperatures within a cave system even out diurnal and intra-annual fluctuations, thereby reflecting mean annual temperatures. Cave speleothems are calcium carbonate

formations re-precipitated *in situ* from carbonate-rich seepage waters by degassing of CO_2. They form in limestone or dolomite karst (Fig 1). Speleothems include flowstones, stalactites, and stalagmites - formations that form in irregular sheets, from the ceiling downwards and from the floor upwards, respectively. Only stalagmites are capable of providing useful proxies in incremental growth layers so as to reflect a continuous and reliable record of conditions.

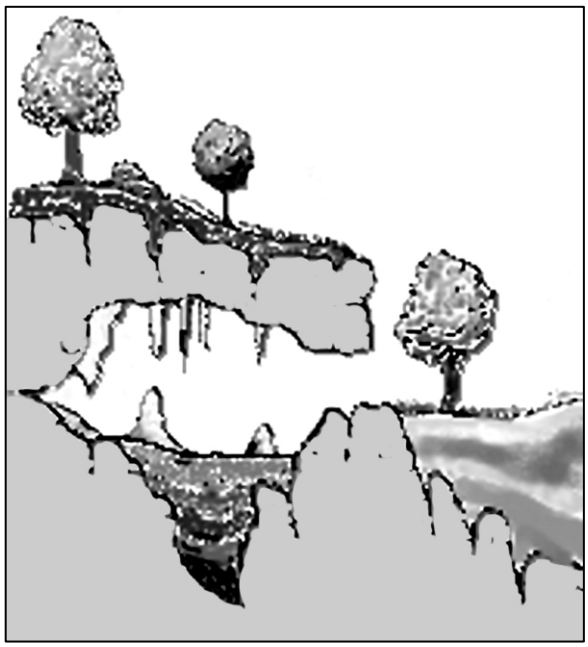

Figure 1. A schematic diagram showing the essential features of a typical karst cavern with deposition of secondary speleothems as stalactites (from the roof), a flowstone (to the left, at the rear of the 'cave'), and stalagmites (on the floor), and activation of the system by vegetation.

Chronological control is of paramount importance in all palaeoclimate studies. An important attribute of speleothems is that they can be readily and precisely age-dated by one of several methods, in strict stratigraphic context. Radiocarbon (^{14}C) determinations are now less frequently used for speleothems because of their limited time-range back to about 40 Ky, errors due to random nature of radioactive decay, fluctuations in the production rate of ^{14}C, and lack of clarity about the proportion and effects of "old" carbon from the karst system on the observed age. Thorium-uranium (Th/U) disequilibrium dating is a more appropriate method for speleothem chronology, yielding ages in calendar years, provided sufficient uranium is present, the carbonate fabric has remained a closed system with respect to uranium, and the material is free of contaminants, for instance those introduced by dust or soil (Schwarcz, 1986). $^{230}Th/^{234}U$ ratios are determined either by measurement of radioactive decay (using α-particle spectrometry), or by means of thermal ionisation mass spectrometry (TIMS). The latter requires far less material and yields more precise dates.

Because they are formed of calcium carbonate increments, stalagmites can be analysed in a time series for a number of proxies including stable carbon and oxygen isotope ratios, trace elements, humic acid content, colour and growth layers. Constraints exist for extraction of valid proxy records. Firstly, stalagmites must form deep in the cave system where there is little or no movement of air and high (~100%) relative humidity, conditions required to allow slow precipitation of carbonate and isotopic equilibrium. Disequilibrium conditions lead to kinetic fractionation, yielding isotope ratios unconnected to environmental conditions. The best candidates are flat-topped – again for promoting isotopic equilibrium. Stalagmites should be growing continuously and growing actively at the time of removal so that analytical results for the tip may be matched with isotopic composition of modern dripwater and cave conditions.

STABLE LIGHT ISOTOPE RATIOS, TRACE ELEMENTS, COLOUR

Stable isotope, trace element and growth layer analyses of well-dated stalagmites may provide continuous palaeoclimate records of temperature, precipitation and vegetation shifts, subject to constraints (Schwarcz, 1986; Talma and Vogel, 1992; Baker et al, 1993; Bar-Matthews et al, 1997).

Stable light isotope ratios

Stable light isotope ratios of oxygen ($^{18}O/^{16}O$) and carbon ($^{13}C/^{12}C$) are by convention expressed in the differential (δ) notation relative to an international standard in per mil (per thousand, or $^{o}/_{oo}$, as given in the following example for oxygen isotope ratios:

$$\delta^{18}O\ (^{o}/_{oo}) = (R_s\text{-}1)/R_{ref} \times 1000 \qquad (1)$$

R = $^{18}O/^{16}O$ of the sample and standard respectively. A similar expression pertains for $\delta^{13}C$. Standard Mean Ocean Water (SMOW) is the international standard for $\delta^{18}O$ from water, while the standard for $\delta^{18}O$ and $\delta^{13}C$ from carbonates is Peedee Belemnite (PDB).

When stalagmite carbonate is deposited under equilibrium conditions, the oxygen isotope composition of the carbonate, $\delta^{18}O_c$ may be related to both temperature conditions at formation of the carbonate, and to isotopic composition of dripwater obtained ultimately from rainfall conditions, in the following speleothem delta function:

$$\delta^{18}O_c = e^{(a/t2\ -b)}[F(T,t,g)+10^3]\text{-}10^3 \qquad (2)\ \text{(Lauritzen, 1995)}$$

T = absolute temperature, t = time, g = geographical position, a and b are constants governing the fractionation factor between carbonate and water ($\alpha_{c\text{-}w}$).

The expression has two components: the thermodynamic fractionation $e^{(a/t2\ -b)}$, and the dripwater function $F(T,t,g) + 10^3$. Thermodynamic fractionation increases with decreasing temperature, so

that cooler temperatures lead to inclusion of relatively more ^{18}O and hence higher $\delta^{18}O$ values. It is this relationship which underpins the empirically determined *palaeotemperature equation* that has been used as the basis for many stalagmite-derived palaeotemperature records, including the Cango Cave stalagmite sequence.

$$T\ (^{o}C) = 16.9 - 4.2(\delta^{18}O_c - \delta^{18}O_w) + 0.13(\delta^{18}O_c - \delta^{18}O_w)^2 \qquad (3)\ \text{(Craig, 1965)}$$

This expression holds for calcite; the expression for aragonite is similar in slope, but offset:

$$T\ (^{o}C) = 19 - 3.52(\delta^{18}O_c - \delta^{18}O_w) - 0.03(\delta^{18}O_c - \delta^{18}O_w)^2 \qquad (4)\ \text{(Grossman \& Ku, 1986)}$$

For equations (3) and (4)

$\delta^{18}O_c = {}^{18}O/{}^{16}O$ composition of the carbonate (expressed versus PDB)

$\delta^{18}O_w = {}^{18}O/{}^{16}O$ composition of the dripwater (expressed versus SMOW).

The value for $\delta^{18}O_c$ is determined by analysis. The value for $\delta^{18}O_w$, however, is more elusive, and difficulties in estimating this value represent a severe problem for all speleothem palaeotemperature studies. The approach employed to circumvent the problem for the Cango Cave stalagmite was to insert isotopic values for the Uitenhage aquifer (Talma and Vogel, 1992) (see below). An approach currently under development is the extraction and isotopic analysis of water inclusions, but this approach is not always applicable or viable.

Considering the importance and complexity of the dripwater function in (1), a more inclusive approach is preferable in any case. Meteoric water isotope values vary for a variety of reasons that are well-studied but nevertheless complex. As first laid out by Dansgaard (1964) and later refined by others (eg. Rozanski et al, 1993), $\delta^{18}O_{mw}$ varies according to the following significant factors:

(a) Conditions at the source of the moisture including both $\delta^{18}O_{seawater}$ and temperature which affects the fractionation factor (α) between seawater and vapour.

(b) Latitude (lower $\delta^{18}O_{mw}$ with increasing latitude)

(c) Distance the moisture travels over the continent before being released as precipitation. This is known as the "continental effect"; Rayleigh distillation occurs so that precipitation containing more ^{18}O is released first, leaving a cloud depleted in ^{18}O to travel further inland.

(d) Conditions at the site of precipitation, including amount of water released (the "amount effect" in which heavy downpours tend to release most of the water at once); altitude and air temperatures which are linked (rain more depleted in ^{18}O occurs with cool temperatures, high altitude). A counter-effect is related to warm conditions and strong updrafts, in which evaporation occurs repeatedly during formation of rain droplets, leading to increase in ^{18}O.

Further effects relate to conditions on, and within, the soil and epikarst. Rain must penetrate both before entering the cave as seepage water; during these processes evaporation may occur at the surface (leading to isotopic enrichment), and during passage, mixing or exchange and further fractionation. These processes as well as those in (a) to (d) are included in the F(T,t,g) component of expression (2). Hence the storm-track history of a cloud mass *plus* events at the site leads to a complex series of shifts which affect isotopic composition of dripwater reaching a stalagmite.

The carbon isotope composition of speleothem carbonate is related to that of the plant biomass overlying a cave catchment (Schwarcz, 1986). Plant-derived dissolved CO_2 forms the acidic medium for dissolution of the dolomite or limestone, forming bicarbonate in the seepage water which is subsequently re-precipitated as carbonate in the cave (Hendy, 1971). Carbon isotope composition of seepage water bicarbonate is highly dependent on the plant-derived soil CO_2, which derives from the carbon isotopic composition of the vegetation.

In the summer rainfall woodland savannas and grasslands of South Africa, most grasses follow the C_4 photosynthetic pathway, while trees, herbs and shrubs follow the C_3 pathway (Vogel et al, 1978). These pathways are distinguished by formation of different primary carbon compounds and carbon isotope compositions, because C_3 plants discriminate markedly against ^{13}C during photosynthesis whereas C_4 plants discriminate to a lesser degree (Smith and Epstein, 1971). Today $\delta^{13}C$ values for the former average about -26 $^{o}/_{oo}$ whereas the latter average about -12 $^{o}/_{oo}$,; hence the two groups are isotopically distinct (Smith and Epstein, 1971). C_4 grasses are favoured in regions with warm, high radiation, growing seasons (Ehleringer et al, 1997). A third group, mostly succulents following the Crassulacean Acid Metabolism (CAM) pathway show a more complex $\delta^{13}C$ distribution, exhibiting a range of values approximating either the C_3 or C_4 ranges. CAM plants are, however, abundant only in particular habitats (such as the Succulent Karoo biome for instance), and their influence is usually disregarded in dietary and environment studies. In most of the summer rainfall regions of Southern Africa, barring high altitude mountain, carbon isotopes in soils and carbonate formations reflects to a large degree the proportion of the biomass made up from C_4 grasses.

The signal is influenced by carbon bedrock composition (Schwarz, 1986). Degassing processes may also influence the isotopic signal. In at least one study, degassing processes likely contributed to higher $\delta^{13}C$ thus producing a "pseudo-C_4" signal clearly impossible at the relatively high latitude location in Britain (Baker et al 1997).

Increment analysis, humate content and grey scale

Very small increments are added annually to stalagmites as a result of precipitation of calcium carbonate from thin films of water rich in bicarbonate and other ions. Where visible (frequently not

the case), growth increments can be observed in a polished section. It has been shown that increments are deposited annually, and that layer thickness can be a proxy for rainfall, or at least for conditions optimal for promoting stalagmite growth (Baker et al, 1993, Railsback et al 1994). Growth rates for stalagmites can be anywhere between 0.02 to 1mm per year, depending on conditions. The limits for growth have been calculated from first principles (Dreybrodt, 1980) and verified from field observations. Aragonite speleothems can sustain a higher growth rate, but they are poorly studied. Apart from counting increments, which is only feasible for certain stalagmites or sections where sub-annual bands are coloured, for instance by humates (Baker et al, 1993), growth rate is best calculated from the chronology. Annual laminations were visible and studied earlier on small sections of the 6.5 Ky-old stalagmite, T7 (Svanered, 1998) but increment analysis *sensu stricto* was not further pursued in the study reported here.

Increased humate levels appear as dark, slightly translucent layers; they reflect enhanced production of organic matter and increased humate mobilisation from overlying soils. Mobilisation may occur on a sub-annual basis in response to seasonally enhanced water throughput at the beginning of the rainy season, or it may also continue across broader time scales. Humate mobilisation has also been tentatively correlated with higher temperatures by comparison with the historical instrumental record in the T7 Cold Air Cave stalagmite (Holmgren et al, 2001). Humate content is usually measured by means of ultra-violet fluorescence (Baker et al, 2000). In stalagmites which are uncontaminated by dust or soil additions, or colour-producing trace elements, a reasonable measure of the humate content is provided by fluctuations in colour. These can be measured as a grey scale series which are easy to produce using standard equipment and free software. Moreover, the grey scale can be determined at high resolution. The T7 stalagmite showed large visible shifts in humate content; in this case changes in humates as measured by the grey scale provided a useful adjunct for interpretation of vegetation changes (Lee-Thorp et al, 2001). However, grey scale is less useful for T8 because of lower humate levels.

Trace elements and mineralogy

Both aragonite and polymorph calcite can be modelled as ionic solids, and understood in terms of simple ionic theory. Since Ca^{2+} has a moderately large ionic radius, and larger ionic radii tend to stabilise aragonitic structures, $CaCO_3$ can exist in the two different crystal forms of calcite or aragonite (Finch et al, 2001; Finch pers.com.). These two forms differ in the crystal form, aragonite crystallites being more needle-like, and in the size of ionic radii which can be tolerated in the unit cell. Simple substitution of divalent alkali earth metals (Mg^{2+}, Sr^{2+}, Ba^{2+}) for Ca^{2+} occurs in the calcium carbonate crystal lattices. In agreement with predictions from ionic radii, Sr followed by Ba are the principal trace elements in aragonite, while Mg (smaller ionic radius) remains low (Finch et

al, 2001). In contrast Mg tends to be high in calcite speleothems. Other ions of environmental interest are Cd, Cu, Pb, U, Zn, Fe and P from soils which may either be substituted in a more complex manner, or occupy interstitial spaces.

Variations in concentrations of Sr, Ba, and Mg are believed to reflect environmental conditions at the time of deposition, but the environmental correlates are not yet well understood. Fluctuations in the supply of these solutes provide one constraint, while other considerations are the effects of growth rate coupled with seepage water supply, as well as temperature. In temperate regions, solute acquisition by seepage waters depends on residence time in the soil and epikarst, hence trace element ratios of Mg/Ca, and Sr/Ca tend to increase during drier spells (Baldini et al, 2002). However, in warmer regions with dolomite karst, such as in the Makapans Valley, where these ions are always abundant and not limiting, the question becomes whether growth rate as mediated by dripwater supply, or temperature, is the dominant control. This question is not resolved.

Most studies use bulk analysis by means of ICP-MS, which combines material from several annual cycles. However, since trace elements may now be measured with high precision on very small (μm) scales, recent studies have attempted to gauge variation on annual to sub-annual scales using techniques such as Ion Microprobe (eg. Baldini et al, 2002), or Secondary Ion Microprobe (eg. Finch et al, 2001; Fairchild et al, 2001). In these high resolution studies it becomes important to understand the quantities of trace elements in seepage waters, and their spatial, seasonal and annual fluctuations.

PREVIOUS CAVE STALAGMITE RESEARCH IN SOUTHERN AFRICA

Several stalagmite records have been obtained in southern Africa. The chronology of growth or activity in Namibian speleothems has been proposed as indicative of wetter episodes while cessation of growth indicates arid episodes (Brook et al, 1990). The Lobatse II stalagmites from eastern Botswana, active for periods during the late Pleistocene, provided records of $\delta^{18}O$ and $\delta^{13}C$ variability showing periods with strong C_4 grass cover peaking at about 22 Ky (Holmgren, 1995).

The best known record is that of the Cango Cave speleothem. An oxygen and carbon isotope record was obtained from a 2.7 m calcitic stalagmite deep in the Cango Caves, near Oudtshoorn in the Southern Cape (Fig 2) (Talma and Vogel, 1992). The chronology, established by radiocarbon, and Uranium disequilibrium from α-spectrometry (Vogel, 1983), showed that it grew continuously for 47 Ky apart from a significant hiatus between 15 Ky and 6 Ky. Sampling resolution was approximately centennial for the Holocene section, but with lower resolution for the Pleistocene section. Substitution of the appropriate oxygen isotope values for a dated aquifer from the coastal plain to the east (Heaton et al, 1986) allowed calculation of a palaeotemperature record for 30 Ky

using equation 3 (Craig, 1965). The $\delta^{18}O$ record is remarkably uniform throughout, and the shifts in temperature derive largely from the aquifer $\delta^{18}O$ substitutions. A shift of about 5-6^{o}C from the Pleistocene to the Holocene is suggested.

The $\delta^{13}C$ record shows a variable, mostly depleted, series for the Pleistocene section, indicating dominance of C_3 plants. After the hiatus a steep increase to maximum values at about 2000 radiocarbon years BP indicates increasing proportions of C_4 grasses. $\delta^{13}C$ values for the tip show values consistent with the modern ~40% C_4 grass cover. The $\delta^{13}C$ trends suggest that this region, which presently experiences a bimodal distribution of rainfall in winter and summer, formerly fell within a winter rainfall distribution area, and that this situation had changed by the Holocene period. A second, mostly older, stalagmite has been sampled from the Cango Cave but remains unpublished.

More recently, a series of stalagmites from Cold Air Cave in the Makapans Valley, near Polokwane in the Limpopo Province have been analysed with the aim of establishing high resolution records over extended periods. The first of these, T5, was dated by α-spectrometry Uranium disequilibrium and found to be relatively young and discontinuous (Repinski et al, 1999). However, the fairly high resolution $\delta^{18}O$ and $\delta^{13}C$ series provide corroboration for the other stalagmites, T7 and T8. In the preceding, pilot study, a highly variable $\delta^{18}O$ and $\delta^{13}C$ series was determined (Stevenson et al, 1999) at approximately 10 year resolution, as was a grey scale series reflecting humate fluctuations for the 1m tall T7 stalagmite (Holmgren et al, 1999). The dates, obtained by α-spectrometry, indicated continuous growth for the last 6 500 years; at the same time the age model suggested that the isotopic determinations were at approximately 10 year resolution. The results were revised after re-dating the stalagmite using TIMS methods; the implications are best discussed together with those for the taller 1.4m T8 stalagmite reported in the present study.

THIS STUDY

Analysis of T5 and T7 revealed some unusual features in the chemistry and records. They are entirely aragonitic, the isotope series showed high amplitude short-term variability in comparison to previously known examples from the region, and $\delta^{18}O$ fractionation did not, apparently, correspond inversely with temperature. Some well-known climate events, particularly the “Little Ice Age”, stood out as major isotopic excursions. Higher resolution dating of T7 was required to establish firm ages for the features and better understand the variability. A further good, well-dated, proxy record was required to corroborate and further understand these features and others visible in a longer record. As in all speleothem studies, the proxies needed to be validated. This turned out to be particularly important in this case where aragonitic mineralogy and isotopic proxies seemed non-standard. This was the rationale for the monitoring study of cave conditions and seepage waters.

CHAPTER 2

THE SETTING: MAKAPANSGAT VALLEY INCLUDING PRESENT CLIMATE AND VEGETATION COVER, AND COLD AIR CAVE INCLUDING THE STALAGMITES.

THE ENVIRONMENT AND CLIMATE

Cold Air Cave is located in the Makapansgat Valley (24°1'S; 29°11'E) on the interior plateau, about 30km southwest of Polokwane (formerly Pietersburg) in the Limpopo Province, South Africa (Fig 2.1).

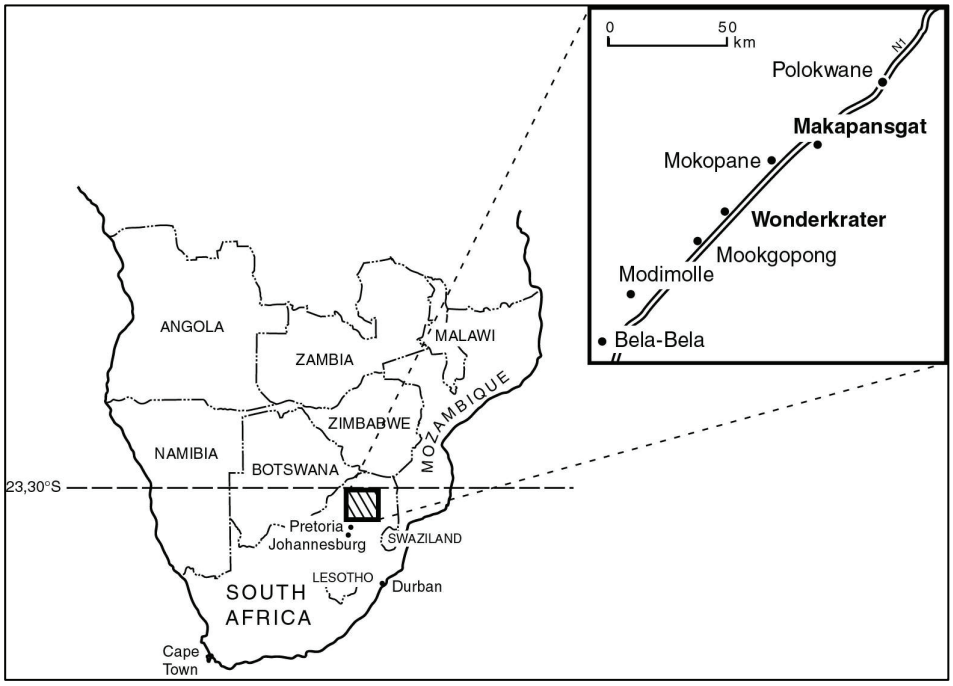

Figure 2.1. Map of southern Africa showing the location of the study area. Inset, position of the Makapansgat Valley in relation to Polokwane (formerly Pietersburg,) and the Wonderkrater spring site. Map reproduced from Holmgren et al (2003).

The cave itself lies at an altitude on 1420m. It is one of a series of karst caves of moderate size that occur along a 1000m stretch of the northern slope of the valley, within a band of lower Precambrian dolomite, the Monte Christo Formation of the Malmani Subgroup, Transvaal Supergroup. Most of these caves have formed through collapse into underlying phreatic cavities within the dolomite. Cave entrances are linked via steep debris cones to the water table with a mean elevation of about 1390m. Many of the collapsed cave sediments contain fossil-rich breccias of high palaeontological and palaeoanthropological significance, while a number of the existing caves contain archaeological

and palaeontological deposits. The Valley has an extremely long and rich history of human occupation, spanning an evolutionary history from Australopithecines to modern hunter-gatherers to recent occupation by Iron Age and then European farmers. The earliest fossil-bearing breccias in the Makapansgat Limeworks that contain the hominid *Australopithecus africanus*, are in excess of ~3.2 million years old (Partridge, 2000). On the other hand the archaeological deposits in Historical Cave reflect occupation in an historically known siege with tragic consequences in the late 19th century.

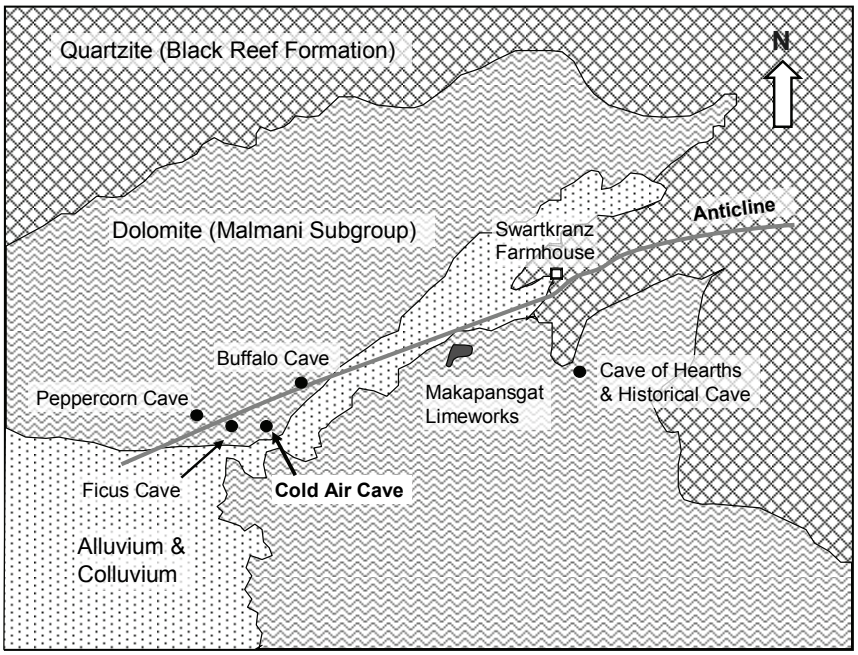

Figure 2.2. Plan of the Makapan Valley showing the geology and position of Cold Air Cave in relation to other caves and sites, and Zwartkrans farm from which the rainfall series was obtained. Adapted from a sketch by Prof. T.C. Partridge.

The climate is mild. Mid-summer daily maximum temperatures average 28°C, while the mean mid-winter daily minimum temperature is 4.2°C over the decade 1991-2002 (South African Weather Service). Winter minimum temperature routinely falls below 6°C from May to September. The diurnal range is 11.3°C and 17.1°C in midsummer and midwinter respectively. The extreme range between the hottest and coolest summers, and between the warmest and coldest winters on record for the twentieth century is ~17°C in both cases.

In this north-eastern region, rainfall is strongly seasonal with well over 90% of rainfall occurring in summer months. Mean annual rainfall at Polokwane (the nearest official climate station) is ~520mm/year, while winter rain from May to September does not exceed 24mm (Schulze, 1984). Rainfall is increased locally in the Valley as a result of the proximity of the Highlands and

Buffelshoek mountains which attain elevations of 2010m within 7.5km of the site. Over the twentieth century the summer rainfall region of southern Africa has experienced a significant 18.6 year oscillation in rainfall (Tyson, 1986) that is also reflected in the Polokwane climate station record. An inverse relationship exists between summer season rainfall and occurrence of high altitude thunderstorms with hail (Harrison, 1986). Hence a feature of seasons with lower-than-average rainfall is that a relatively higher proportion of the rainfall comes from convective storms. Tyson et al (1975) detected a weak inverse relationship between rainfall and mean annual temperatures, ie. an inverse relationship between temperature and rainfall on decadal scales. The southwestern Indian Ocean is the major atmospheric moisture source area. Fluctuations in sea surface temperatures in this area are one of the factors believed to influence the uptake of moisture into the atmosphere and hence transport of moisture onto the continent.

The mountain slopes in the vicinity of the valley are characterised by a Northeastern Mountain Sourveld type (Acocks, 1953) or *Loudetia simplex- Diheteropogan flilifolius*. Closer to Cold Air Cave it is transitional to Sourish Mixed Bushveld – a mixed grassland and woodland (Acocks 1953). Both types are dominated by C_4 grasses but the tree and shrub component is larger in the Sourish Mixed Bushveld and approaches a closed woodland on some of the steeper protected slopes. Soils are skeletal and thin with extensive areas of rock outcrop. Mean regolith thickness is less than 300mm. Frequent solutionally widened joints in the dolomite contain pockets of sandy soil which sustain the vegetation cover.

THE CAVE AND STALAGMITES

The entrance to Cold Air Cave is located nearly halfway up the valley slope. The entrance is small (<700mm in diameter), which results in poor ventilation particularly in the inner reaches of the cave. The stalagmites were recovered *in situ* from the flanks of a large debris cone, in an area >100m from the entrance and at elevations of about 13-20m below the cave entrance (Fig 2.3). They were collected within 10m of each other but beneath different fissure lines in the dolomite roof. Each fissure is marked by a line of small stalactites, and acts as a separate conduit from a surface catchment above the cave to the growing speleothems below. The roof thickness at this point is at least ~25m. All three stalagmites were active at the time of collection.

As outlined in the Preface, analysis of the smallest (300mm) stalagmite, T5, was completed as part of a Masters study during an earlier phase of the project (Repinski et al, 1999) and is not described further here. The analysis of T7 was already well underway by the start of this project, but work continued during the earlier part of the current project (specifically, completion of the isotope analyses, TIMS Uranium series determinations, and the write-up). Hence, stalagmite T7 and the main, relevant results are included in this report.

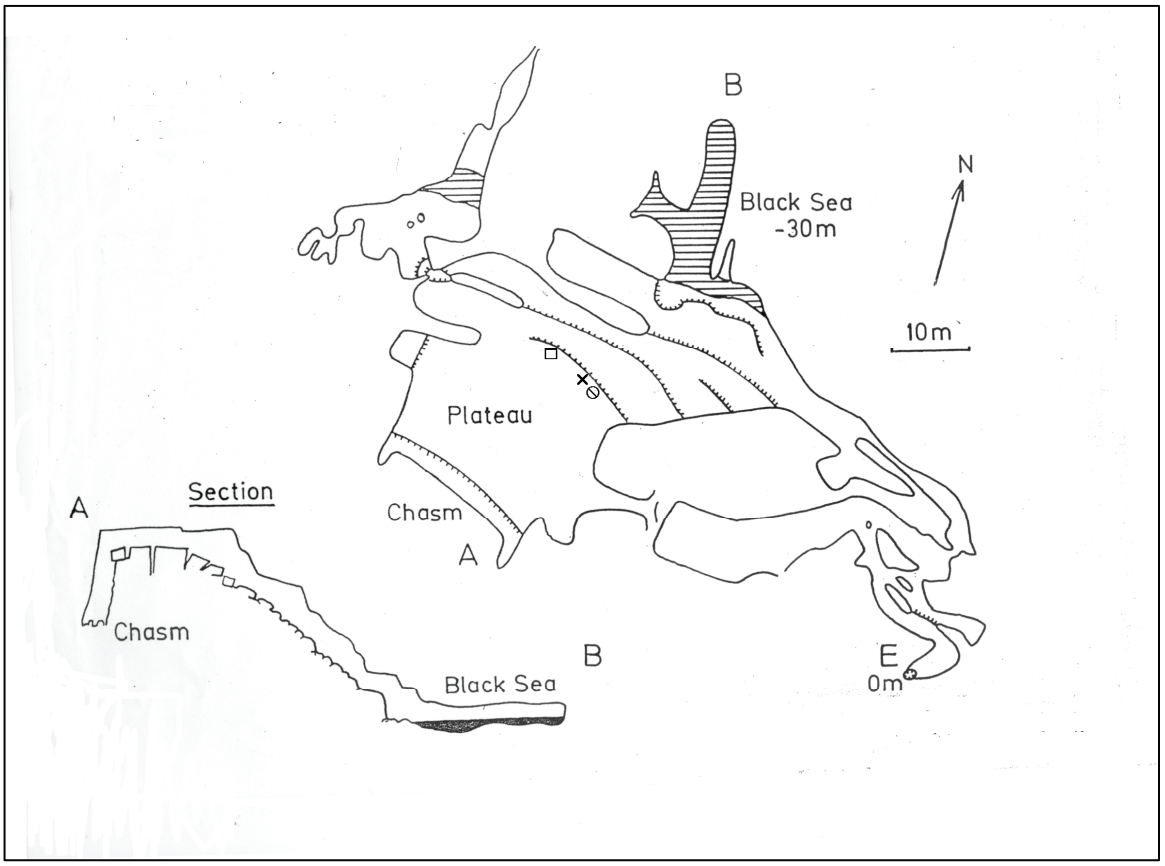

Figure 2.3. Plan of Cold Air Cave from the original map drawn up in 1980 by Prof T.C. Partridge and the S.A. Speleological Association. The entrance is labelled E. The vertical section shown on the lower left reflects a section of the main cavern from points A to B. The positions of the two stalagmites and the climate station on the slope of the cone are marked as a crossed circle for T7, square for T8, and an "x" for the data-logger. The "Black Sea" shown here is referred to simply as the "pool" elsewhere in this report.

T7 is 1m tall, with diameters of 102mm at the base and 67mm near the top (Fig 2.4). On sectioning, the stalagmite was observed to be composed of compact growth layers made up of needle-like aragonite crystals. There were no signs of any hiatus or significant change in the carbonate. Distinct dark and light banding was visible throughout, but the dark bands were more significant in the lower section.

At 1.4 m, T8 is taller, but otherwise it has similar dimensions to T7. On sectioning (Fig 2.5), the upper 1.15m appeared to be very similar with alternate dark and light banding (although humic staining was less pronounced) and needle-like crystals of aragonite. The lowermost section, however was markedly different. There was a clear, sharp change in mineralogy at 25 cm from the base. The material below the change was far denser and lacked needle crystals.

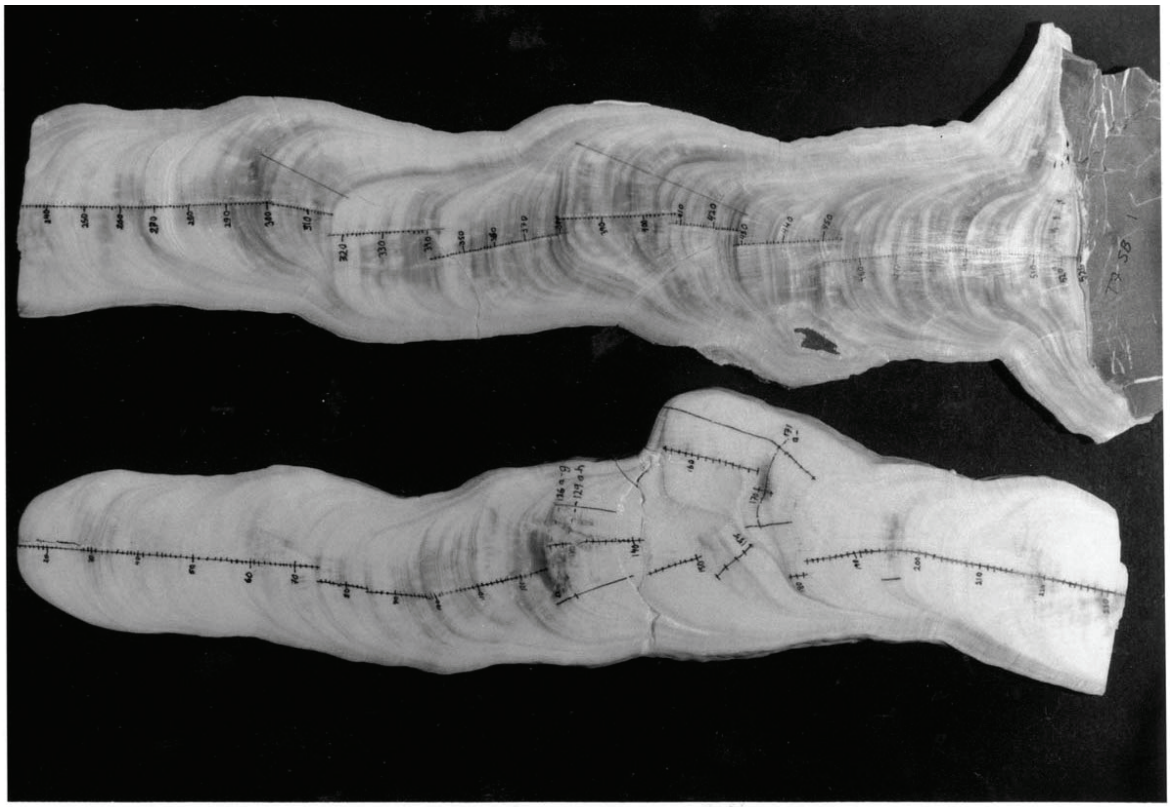

Figure 2. 4. Sectioned stalagmite T7 shown in two halves – the basal section is uppermost, and the upper section below. An irregular piece of dolomite is still attached to the base. The slightly altered sampling directions are marked in ink along the growth axes, and small, numbered sample holes. Where complexity was observed in the growth direction, several lines were sampled. Humate staining is clearly visible, particularly in the lower half, and in a limited section of the upper half.

Banding was present but more densely packed and clearly dissimilar in character to the upper section. These bands are dark grey and enhanced on the flanks of the stalagmite, while the central portion retains some of the slightly translucent brown staining associated with humates. The grey staining on the flanks is more plausibly ascribed to manganese, which is abundant in the local dolomite and causes similar staining in fossil bones and teeth.

The fact that the T8 stalagmite clearly consists of two sections with different mineralogy implies strongly that these sections were laid down under markedly different conditions. The chronology and origins of these differences are investigated in Chapter 4 and 5 respectively.

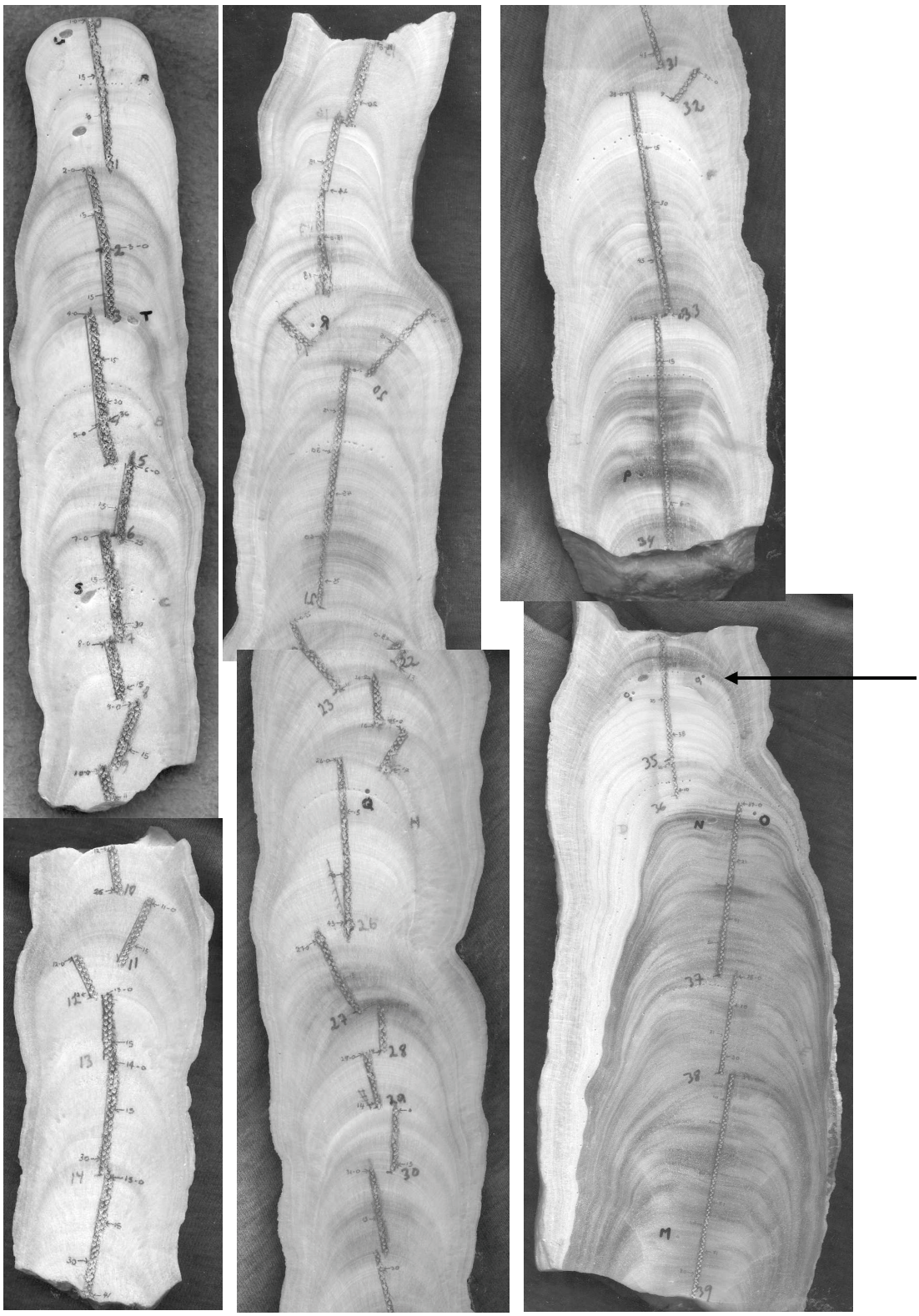

Figure 2.5. Scans of stalagmite T8 in six pieces, showing banding and colour changes. The tip is shown in the upper left column, followed by sequential sections ending with the base section in the lower right. The change from calcite to aragonite is marked by an arrow. Growth trajectories and sampling points are marked for visibility. The larger sampling holes were used for XRD determinations.

CHAPTER 3

THE MONITORING STUDY OF CONDITIONS IN COLD AIR CAVE.

A number of constraints exist for the establishment of sequences from stalagmites that can be interpreted reliably. Ideal conditions for obtaining records from stalagmites by means of isotope thermometry include the following. The cave environment should have poor ventilation and high humidity, conditions which are normally found relatively deep within a cave system. These conditions are essential for isotopic equilibration of oxygen and carbon isotopes between dripwaters, the cave atmosphere, and carbonate as noted in Chapter 1. Too rapid a process leads to kinetic fractionation of both isotopes and meaningless results. Precipitation as a result of drying (evaporation) has a similar effect. The "ideal" stalagmite should be flat-topped for the same reason as run-off is minimised down the flanks with accompanying evaporation. Testing of single growth layers in stalagmites by means of the "Hendy" test provides a useful check. It is also essential to check that these conditions hold at the present-time. Another requirement, that cave interiors preserve mean annual temperatures and do not fluctuate markedly, can also be easily verified.

The Cold Air stalagmites were chosen with a reasonable expectation that these conditions would be met. They were located deep within the cave system where observations indicated no air movement and high humidity. Both T7 and T8, although not strictly flat-topped, had rounded tips, and moisture on the tips indicated that they were still growing. The monitoring study aimed to verify these cave conditions. Hendy tests of individual layers can address the remaining requirements. This section describes the cave monitoring study; the stalagmite tests are described in Chapter 5.

Few monitoring studies have been conducted for caves in mid-latitude regions with warm climates. The importance of understanding the hydrochemical system that supplies water and trace elements for speleothem growth, in addition to processes during precipitation of the carbonate, has been stressed frequently (eg. Baker et al, 1997; Roberts et al, 1999). Understanding the influence of these supply processes is nascent – especially for trace elements - even for the better studied calcitic speleothem locations in Europe. They are extremely poorly understood in warmer mid- to low-latitude regions. The effects of a highly seasonal rainfall and temperature regime (also variable on annual and decadal scales) on the supply of light isotopes and trace elements are very poorly understood. Although the present study is limited, it should provide some insights into unknowns such as residence time for waters in the epikarst zone, and spatial variability in isotopic and trace element composition of water supply within the cave. Moreover it may be possible to use patterns for the dry winter/moist summer regime to reflect the kinds of changes to be expected in the proxies for longer dry and wet spells. This information is essential to help understand the patterning of isotopic and trace element variation through time, and their interpretation as palaeoclimate proxies.

CAVE MONITORING

Data-logger

A Thomson multi-channel data logger was placed in the interior of the cave in August 1999, near the point of collection of the 3 stalagmites T5, T7, and T8. The logger was set up in a stable area of the debris cone in the interior cavern, with channels for measurement of the logger temperature, the cave temperature, relative humidity, a drip-counter, and a rain gauge. The logger itself was placed into a sealed Tupperware container in an effort to protect the contacts from the corrosive cave atmosphere with its high levels of CO_2. The rain gauge was connected to multiple stalactite dripwater sources by means of Tygon tubing, and the drip-counter was set under one active source. Warning tape was circled around the area to ensure that the delicate tubing and wiring was not disturbed in subsequent visits. We returned at intervals of approximately 3 months over the next ~3 years, as frequently as possible, to download the data and to change the long-life battery.

Collection and analysis of water samples

On each visit, water was sampled at different but strictly demarcated points in the cave. The aim was to determine spatial and chronological variability for both isotope ratios and trace elements. Therefore a wide range of sampling stations was chosen, including different parts of the cave from near the entrance to the lowest point at the pool. On subsequent occasions the number of sampling stations was reduced based on their relevance and on availability of water (the cave has been getting steadily drier). On each occasion the Makapan Valley stream was sampled as well.

Separate samples were collected for stable light isotope analysis in larger glass bottles (~10-50 ml sizes), and for trace elemental analysis in 2 ml polycarbonate, self-stoppered, disposable centrifuge tubes. The containers were rinsed in an acid solution prior to use. Water samples were sealed and brought back to the University of Cape Town for analysis. An attempt was made to fill the sample bottles to the brim prior to sealing with stoppers and tape, to prevent exchange with air when the container was exposed outside, but this was frequently impossible because there were simply not enough drips (unless one stood under a source for hours, and this was simply not feasible). In an attempt to sample cave waters between visits, ie over several months, several small clean glass bottles were attached to active stalactites by means of plain condoms. This method was suggested by Prof. Stein-Erik Lauritzen as providing a means for securing the bottles, without damaging the stalactites. At the time he was engaged in a cave monitoring study in Norway using a similar approach.

Water samples were analysed for oxygen and hydrogen isotopes, and for trace elements. Oxygen isotopes in water samples were determined following the CO_2 equilibration method of Socki et al

(1992) employing disposable pre-evacuated 7ml glass vials. Approximately 0.5 atmosphere of medical-grade CO_2 of known isotopic composition was equilibrated with about 2ml water sample for a minimum of 2hrs at 25 C, thereafter CO_2 was removed, dried by cryogenic distillation and sealed into a glass tube.

For hydrogen isotope analysis (D/H) a variant of the Zn closed tube reduction method of Coleman et al. (1982) was used to reduce water to H_2. The water sample was drawn into a 2 µl capillary tube which was placed into a glass tube containing a few grains of "Indiana" zinc and heated at 500^{o}C for 2 hours. The glass tube was attached to a vacuum line, immersed in liquid nitrogen until the capillary tube containing the water sample had frozen and then evacuated and sealed using an oxy-propylene torch. The sealed tubes were then placed in a furnace at 450 C to reduce the water to H_2.

Isotope ratios of CO_2 and H_2 were measured using a Finnigan MAT 252 mass spectrometer. The fractionation factor between CO_2 and water at 25^{o}C is assumed to be 1.0412 (Coplen 1993). The standards V-SMOW and SLAP were analysed to determine the degree of compression of raw data and the equations of Coplen (1988) were used to convert raw data to the SMOW scale. An internal water standard (CTMP) which has been calibrated against V-SMOW and SLAP, and independently analysed, was run with each batch of samples and used to correct for drift in the reference gases. Electrical conductivity (EC) was measured using a Crison CM2201 micro-conductivity meter. These determinations were done by Dr Chris Harris in the Geochemistry Isotope Laboratory, and later by Dr Jodie Miller. One small batch was analysed by the University of the Witwatersrand Hydrogeology Isotope Laboratory. Where samples were too small only D/H was determined.

Determinations of trace element water sample concentrations were performed by Dr Andreas Spath, using a Perkin Elmer Elan 6000 ICP-MS instrument. All samples were diluted 10 times with ultra-clean 5% HNO_3 before analysis. Calibration was accomplished by external standardisation using artificial multi-element standard solutions. Instrument drift was corrected by internal standardisation using Y, Rh and Bi.

RESULTS

Cave conditions

From the outset, problems were experienced with the data-logger. We had anticipated some, as concerns were voiced by the supplier about the corrosive effects of the cave atmosphere with its high humidity and [CO_2]. And indeed the electrical contacts did deteriorate over time, until eventually the cave temperature probe had to be replaced and the relative humidity probe contacts repaired. The drip counter calcified and ceased to work after several months; after several attempts we gave up since there seemed no way around the problem and in any case the dripcounter was not

essential since we had also installed a rain gauge. A further problem was experienced with the batteries. Although the logger functioned on first installation, it ceased to function soon after we left the cave; the problem was not detected until our return months later. The net result is that the logger results have long gaps.

Nevertheless the results provide a reasonable view of conditions and timing of events in the cave. The first important result is that relative humidity in the cave interior remains 100% or more at all times; the relative humidity counter actually gave a mean reading of 109.8±0.10%. This is an *overestimate* related to the problem of calibrating relative humidity beyond the limits of the instrument. Data obtained from the rain gauge and temperature channels are shown in Fig 3.1. The mean temperature is 18.8 ± 0.22^{o}C, which compares very well with a mean annual temperature of 18.6 ± 0.56^{o}C for the Polokwane weather station, for the decade 1991-2002 (data supplied courtesy of the South African Weather Service). There is a hint that winter temperatures (July-August) are slightly lower but the amplitude of the winter shift is within the error for the probe, which moreover occasionally and inexplicably missed data or gave spikes greater than the overall trends. These results demonstrate that two of the essential requirements for useful speleothem proxies are met in this cave: that relative humidity remains high and that interior temperatures mirror external mean annual temperatures.

The rain gauge results are shown as millilitres per 6 hourly measurements, per day (Fig 3.1). Therefore, although the data are quantitative, the actual total for each *day* is underestimated in Figure 3.1. But because of the way in which it was connected to several stalactite sources, the gauge essentially 'exaggerates' water quantities. This is certainly the case in times of high flow, but not in periods of low flow. The latter is evident from some discrepancy between the quantities of water indicated by the rain gauge and the drip-counter (measuring number of drops) when it operated, during the dry months. Therefore these results must be interpreted with caution. What the rain gauge data clearly shows is a strong seasonality in the amount of seepage water reaching the cave interior. The difference between winters and wet summers are marked; the data suggest that very little dripwater is present in winter. This is an important observation, because it implies that stalagmite growth could cease, or at least be very much reduced, in winter. By extrapolation, stalagmite growth could also cease during more prolonged droughts, perhaps on sub-decadal scales impossible to detect in the stalagmite. A further implication is that the rainfall or temperature proxies would represent mainly summer conditions. Such a situation would also depend on the conditions and amount of time which seepage water and its solutes spend in the soils and overburden, ie the residence and release time.

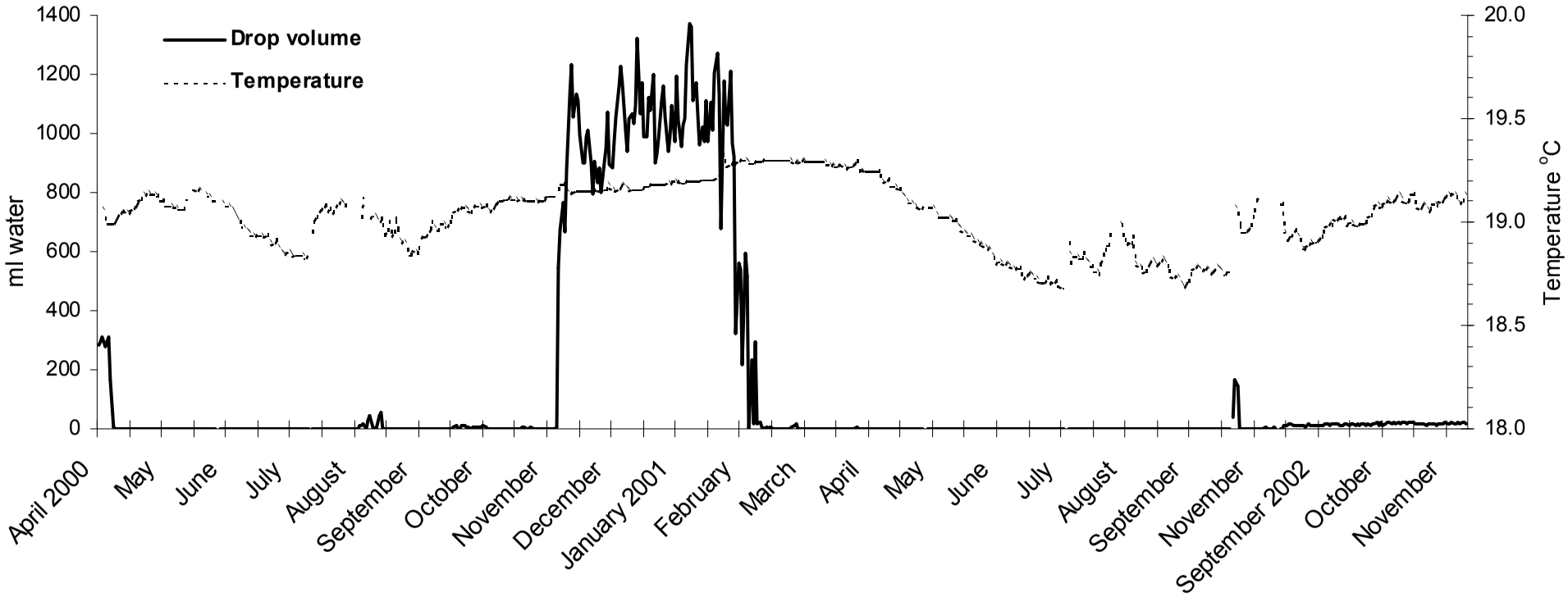

Figure 3.1. Logger results for 2000-2002 show essentially consistent temperature (given in ^{o}C on the right Y axis) throughout the year, but highly variable amounts of dripwater according to the rain-gauge counts (given as ml/6hours on the left Y axis). The overall pattern, however, of large amounts of dripwater in the summer months, and mostly negligible amounts in the winter months, seems secure. Only the end of the 2000 flood was captured but the pattern shows how soil/epikarst moisture was prolonged to the end of April.

This question of residence and release times of water in the overburden cannot be addressed directly without tracer studies of groundwater. Nevertheless it is instructive to compare the timing of seepage water increase, and the onset of the rainy season each year. We were given access to the monthly rainfall records (from 1996) from the Zwartkranz farm up the Valley (Fig. 3.2). Although there were some gaps in the cave rain gauge data, a comparison between Fig 3.1 and Fig 3.2 suggests that appearance of significant quantities of water in the cave is delayed by about 6 weeks following the onset of significant rain in the Valley. The higher rainfall and a longer rainy season for 2000 are reflected in the cave waters. The offset, however, does not necessarily show a *residence* time of 6 weeks, but rather the period for a response by ground and soil waters.

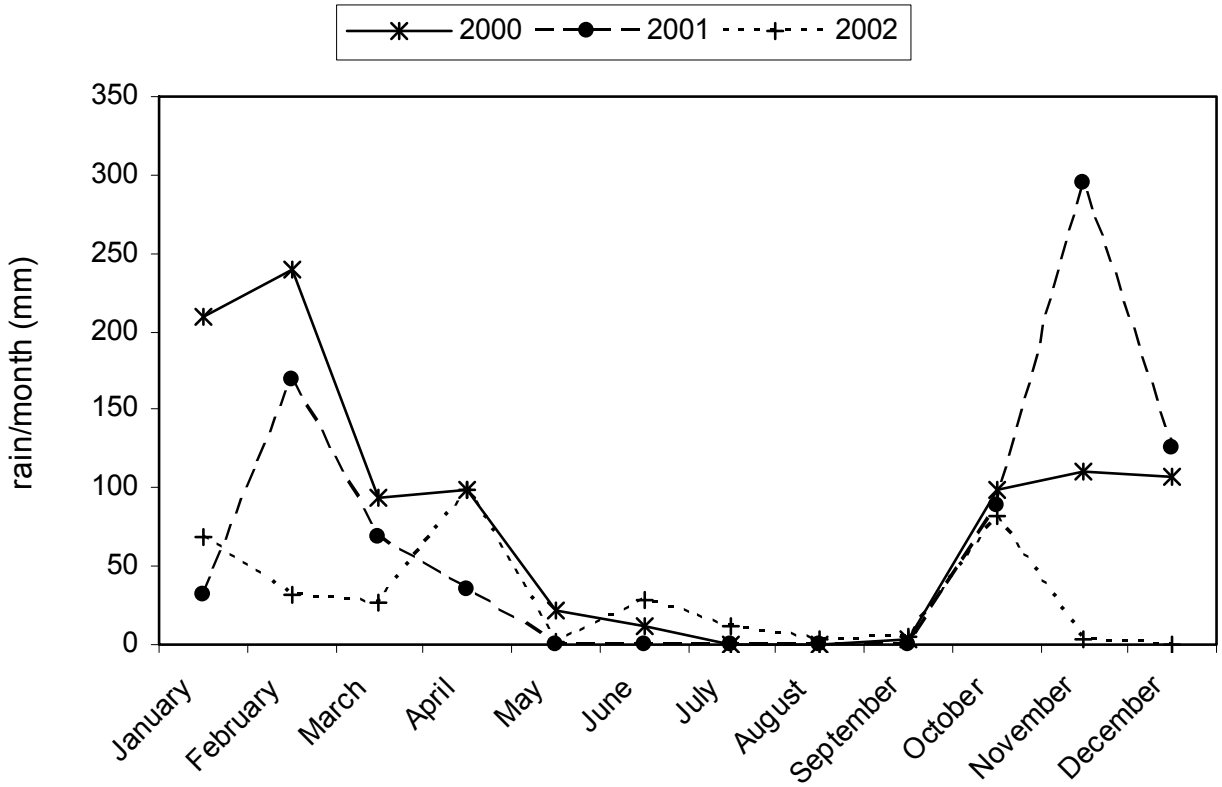

Figure 3.2. Local monthly and annual rainfall records from Zwartkranz farm. Data are plotted from January to December rather than for the rainfall year Oct. to Sept., for easier comparison with the logger data. Rainfall is a little higher in the Valley compared to the nearest South African Weather Services station in Polokwane.

The floods of early 2000 and longer rain season for that year are reflected in the data. The logger data for 2000 also reflects the prolonged rain season, but it seems that cave waters fell sharply and immediately the rain ceased. Hence cave dripwater lags rainfall onset by ~6 weeks at the start of the season, but not at the end, suggesting both a piston effect and a threshold below which little water enters the cave as seepage.

Isotopic and trace element variation in cave waters

The results of the $\delta^{18}O$ and δD cave water analyses for the various sampling stations, their dates and locations are given in Table 3 (following page). The results are variable in space and time. The pool water tracks the stream water closely in response time and in isotopic composition, while the seepage waters are somewhat different (Fig 3.3). The first $\delta^{18}O$ values obtained for dripwater from near the logger and stalagmites cluster near -3 $^{o}/_{oo}$, but lower values occurred at or just after the 2000 flood. The drips at the lowest point in the cave near the pool took longer to respond. Surprisingly, no significant excursion is seen in the stream and pool water at this time. Stream and pool water become more enriched in ^{18}O during winter, likely due to evaporation effects, and slightly more depleted in summers in comparison (Fig 3.3). Apart from the small flood-linked depletion episode, and the suggestion that slightly more depleted values for dripwaters occur in late summers, there are no noticeable patterns in the seepage waters. Seepage waters fluctuate between -3 and -4 $^{o}/_{oo}$, offset from the summer pattern of the river and pool by an amount ranging from 1-2 $^{o}/_{oo}$ in the earlier part of the record to ~0.5 $^{o}/_{oo}$ in the latter part.

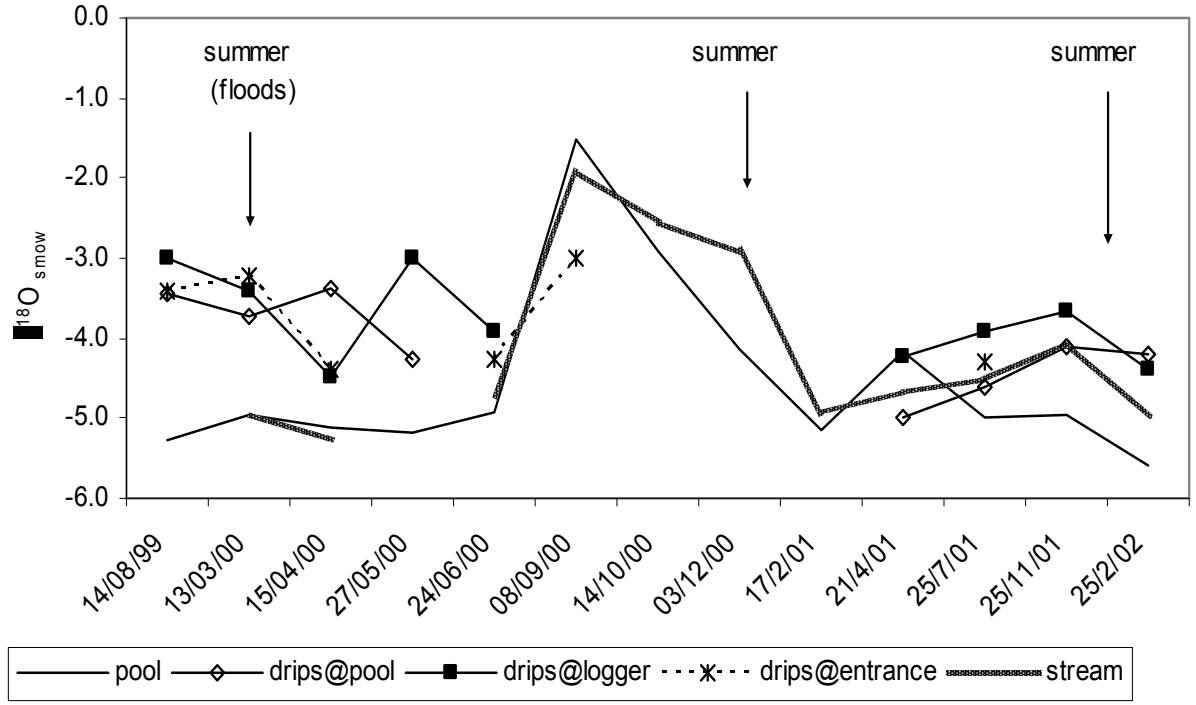

Figure 3.3. Trends in $\delta^{18}O$ of waters collected from designated stations within the cave and the stream at different periods. Summers have pointers, winters lie in-between. The largest isotopic excursion is the enrichment in stream and pool water during winter 2000.

Date	CA1 pool water		CA2 (dw) pool area		CA3 (accum) logger area		CA3 (dw) logger area		CA4 (accum) logger area		CA4 (dw) logger area		CA5 (dw) 50m fm entr.		CA6 (dw) 25m fm entr.		Stream	
	δD	$\delta^{18}O$	δD	$\delta^{18}O$	δD	$\delta^{18}O$	δD	$\delta^{18}O$	δD	$\delta^{18}O$	δD	$\delta^{18}O$	δD	$\delta^{18}O$	δD	$\delta^{18}O$	δD	$\delta^{18}O$
14/08/99	-26	-5.3	-10	-3.4			-6	-3.0			-6	-3.0	-7	-3.4				
13/03/00	-25	-5.0	-20	-3.7	-11	-3.4							-18	-4.0	-16	-3.2	-28	-5.0
15/04/00	-22	-5.1	-17	-3.4	-9	-4.5	-15	-4.8	-11	-4.4	-18	-4.5	-11	-4.3	-10	-4.4	-22	-5.3
27/05/00	-30	-5.2	-19	-4.3	-13	-3.8	-18	-2.7			-21		-24	-0.4				
24/06/00	-26	-4.9	-19		-11	-4.0	-16	-3.9	-7	-4.1	-16	-3.9	-24	-3.9	-15	-4.3	-26	-4.7
05/08/00	-21	-0.6	-16						-5				-16	-2.1	-7		-24	
08/09/00	-16	-1.5	-11		-15	-4.1	-8							-3.0	-6		-22	-1.9
14/10/00	-23	-2.9			-14	-4.3	-12		-13	-3.4	-8						-23	-2.6
03/12/00		-4.1			-4	-4.0			-14	-4.3					-8		-19	-2.9
17/2/01	-26	-5.2	-14		-15				-14	-4.2	-14	-4.2					-23	-4.9
21/4/01	-14	-4.2	-26	-5.0	-14	-4.3	-12	-4.3			-15	-4.2					-22	-4.7
25/7/01	-23	-5.0	-22.5	-4.6					-18.9	-3.9					-15.5	-4.3	-30	-4.5
25/11/01	-25	-5.0	-17.5	-4.1							-9.9	-3.7					-17.3	-4.1
25/2/02	-27	-5.6	-15	-4.2				-4.4			-15	-4.5					-25	-5.0

Table 1. $\delta^{18}O$ and δD data for the series of cave waters collected from Aug 1999, giving the dates and sampling locations. Isotopic values are expressed relative to SMOW. Dripwater collected during a visit is denoted (dw), while accumulated dripwater collected in bottles is denoted (accum). Samples dated Nov 2001 were analysed in the Wits University laboratory. Missing values are due to insufficient sample.

The relationship between δD and $\delta^{18}O$ in (moisture) precipitation should follow the International Meteoric Water Line (MWL) relationship:

$$\delta D_{mw} = 8.1 \times \delta^{18}O_{mw} + 11 \qquad \text{(Dansgaard, 1964)}$$

The relationship between δD and $\delta^{18}O$ compared with the MWL can give an indication of the history of a water body. In general, a slope significantly <8 implies evaporative effects, while a slope of >8 implies condensation effects.

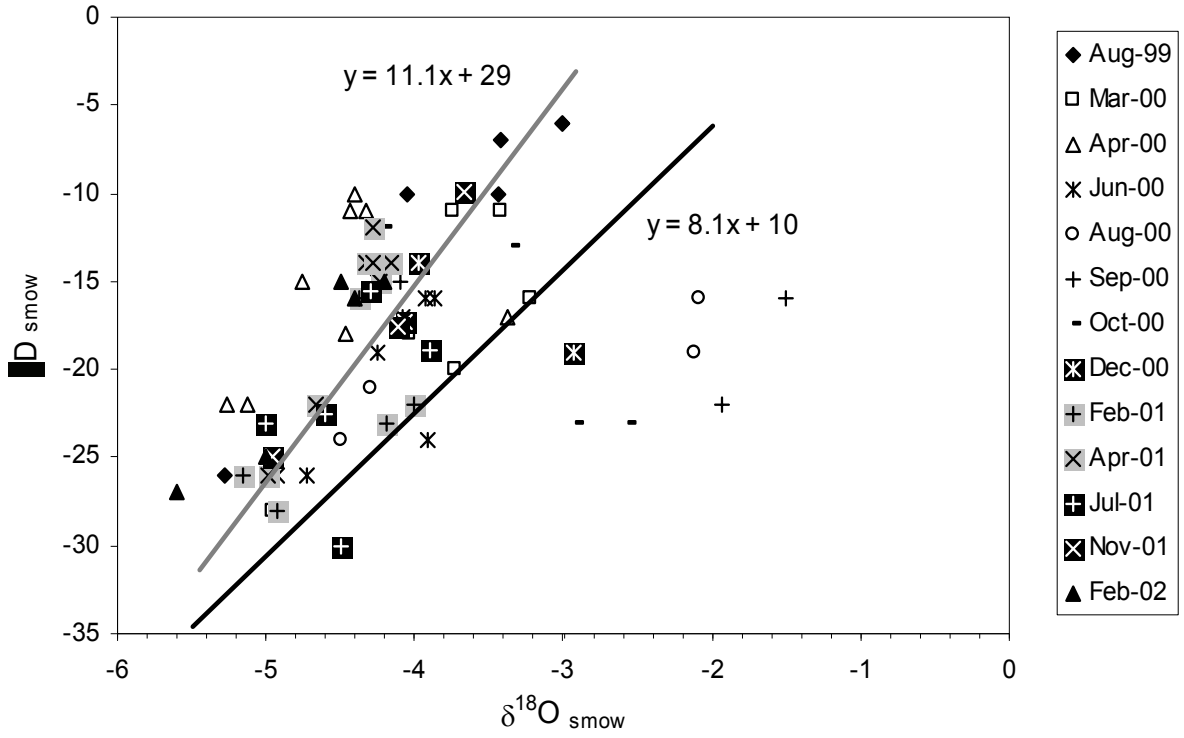

Figure 3.4. Isotopic values for cave-waters collected at various times, expressed as δD versus $\delta^{18}O$. The MWL is shown as a solid line, while the regression for Nov 2001 (as an example) is shown as a dotted line with the regression expression. Points representing the stream and pool waters cluster on the lower left with the exception of the a few points to the right of the MWL most of which are from Aug, Sept, and Oct 2000.

Most δD vs. $\delta^{18}O$ points fall above the MWL, with just a few points below (Fig 3.4). This general position may be partly attributable to anomalously enriched δD values for all waters (for given values of $\delta^{18}O$), since the $\delta^{18}O$ values are reasonably consistent with values obtained in the Pretoria series (IAEA, 1992). A number of samples suffered from isotope exchange because the bottles could not be filled, or because they could be analysed immediately – the results have been discarded where this effect could be noted. Those samples from the accumulated dripwaters (bottles held in condoms) that were believed to have been contaminated during overflow were also discarded. Hence these problems cannot account for a slope > MWL across all waters including directly

sampled stream, pool and drips. We considered, but discarded, an explanation of analytical error since all analyses were standardised and moreover, data from the Wits laboratory shows the same pattern. The offset from the MWL in all local waters, including the stream and pool, suggests that both environmental and cave waters have undergone processes resulting in higher δD values and/or slightly lower $\delta^{18}O$ values. The higher slope suggests condensation effects, possibly reflecting the tropical nature of the rainfall. However, since the effect seems more pronounced in the cave waters (excluding the pool) which have travelled through the overburden, exchange with soils and bedrock during passage must also be considered. The nature of these processes remains unclear. Surprisingly, although water samples collected nearer the entrance are likely to have condensed, no strong trends are observable from the inner cave towards the entrance.

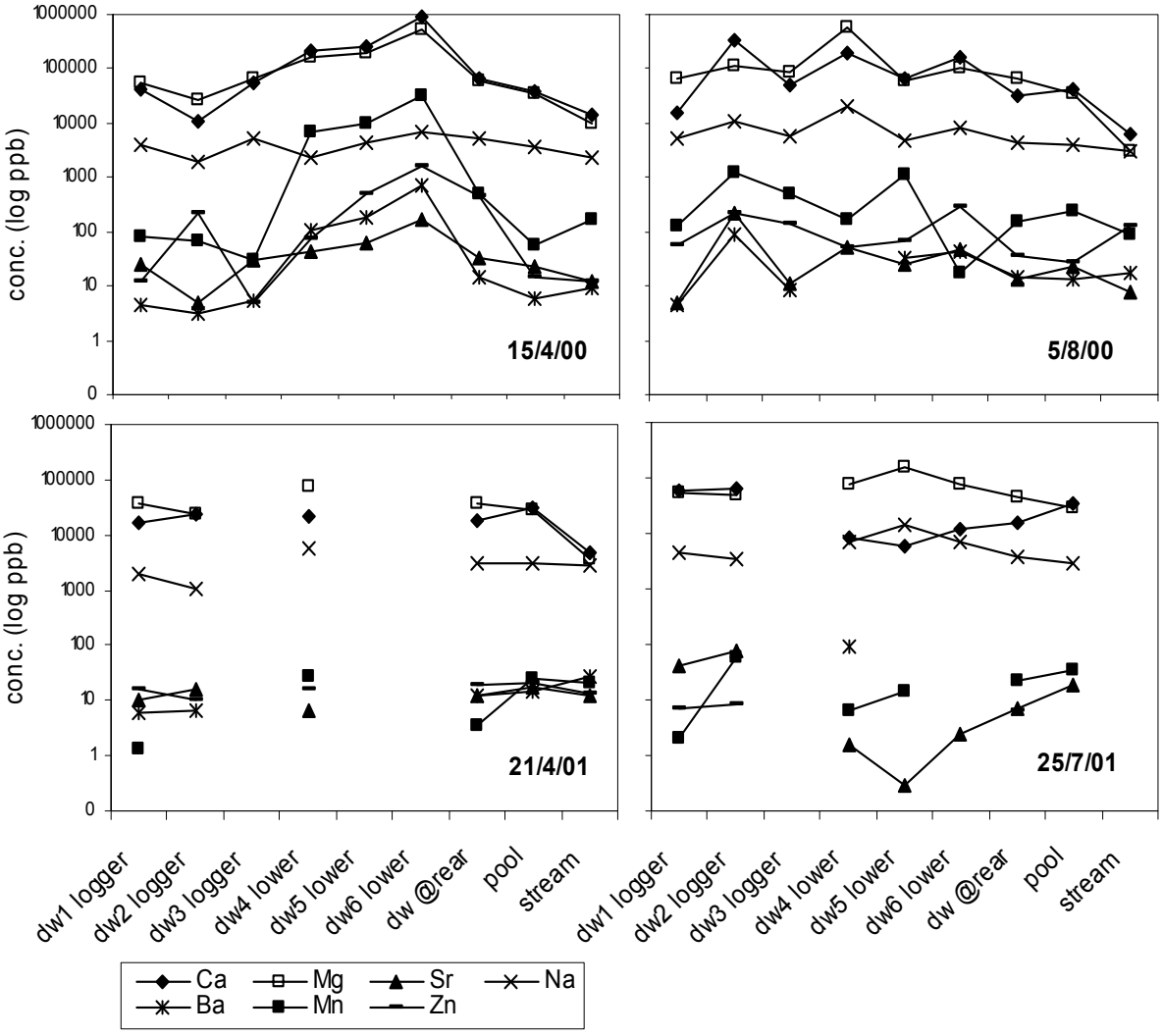

Figure 3.5. Spatial variability of significant elements in cave waters and in the stream, for four dates, reflecting 2 late summer (April 2000 and 2001) and 2 winter (Aug 2000, July 2001) seasons, respectively.

The results of the series of elemental determinations for calcium (Ca), magnesium (Mg), strontium (Sr), sodium (Na), potassium (K), barium (Ba), manganese (Mn), nickel (Ni), zinc (Zn), arsenic (As), and rubidium (Rb) are given in Appendix 1 and shown in Fig 3.5 and 3.6. The results show exceptionally high concentrations of Ca and Mg as could be predicted in a dolomitic region, as well as high concentrations of Na and K. Ca and Mg are superabundant and track well in concentrations and in variation across time and space. Sr concentration is significantly lower and it is tracked closely by Ba (not shown in figure). Transition metals are present in variable amounts. Mn, Zn and Ni track each other, as does Sr in space and time. Solutes are mostly lower in the stream and in the pool. The exception is Na which remains high in all locations and at all times. Other than these differences between stream/pool, lower level and medium level dripwaters, a smaller level of variability also exists between closely spaced drips from different fissures (eg. DW1, DW2, DW3).

Seasonal differences are observable in the dripwaters (Fig 3.5). According to data from DW1 (the site near the data-logger with the most complete data), Mn, Zn and Sr levels are low to intermediate in summer; begin to rise in May and reach higher levels by midwinter. A marked shift to lower values occurs in early spring (Sept) followed by an increase to higher values in early summer (Dec) and then again a decrease. The trends for Ca and Mg are more muted but similar. Na is less variable but does decline slightly in summer, perhaps indicating a freshening of dripwater. The pattern for DW4, although incomplete, may be offset from DW1 by approximately one month. The pool does not follow the dripwater pattern; these data show even concentrations of Mg and Ca, and essentially invariable Na apart from a slight decline in the first summer and a sharp decline in the second summer. These shifts are prior to similar trends in dripwater. However, the decline in Na in Nov 2001 may be an outlier. Mn and Zn in the stream shows similar trends as in DW1 but at least a month earlier. The data suggest that solute shifts in the dripwaters are delayed, and this delay is enhanced with increasing depth. Figure 3.4 also suggests that the amounts of solutes are enhanced at lower depths. Surprisingly, there is no variation in pool water Sr and Fig 3.4 suggests that the same is true of the stream. Therefore fluctuations in the dripwater supply of Sr, Mn, Zn, Ni to speleothems is mediated by passage through the overburden but that of for Ca and Mg is not similarly mediated.

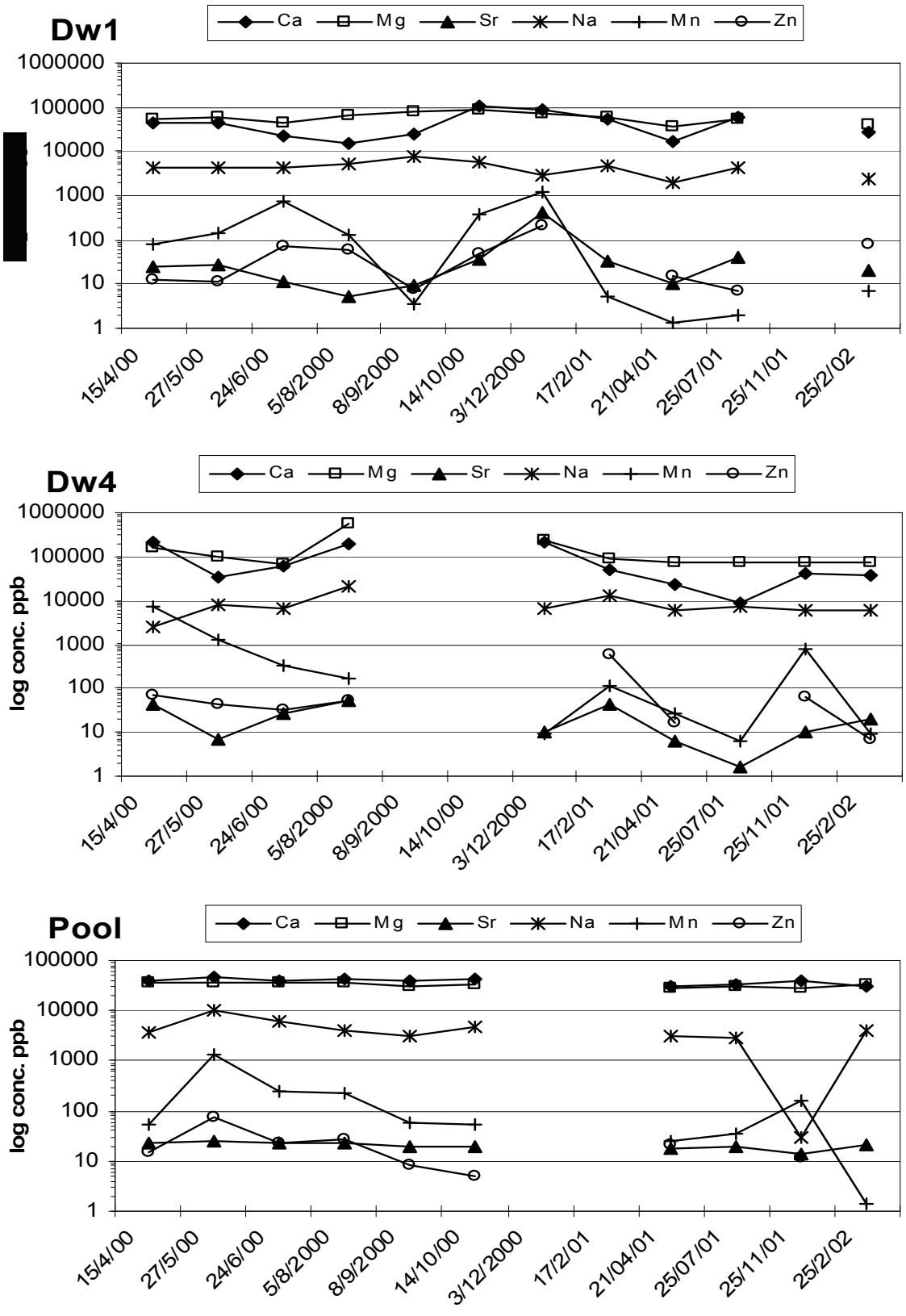

Figure 3.5. Time series of element concentrations for three sampling sites, DW1 (dripwater near logger), DW4 (dripwater in lowermost cave) and the pool.

The differences between dripwaters from the upper and lower levels of the cave, ie between the data-logger area and the pool area suggest that the thickness of the cave roof or overburden influences the concentration of trace elements dissolved in the seepage water. The differences between even relatively closely spaced collection stations can most plausibly be attributed to variations in the pathways for seepage water through fissures, which result in different amounts of solute. This observation implies that there is no reasonable expectation that the trace element composition between two close stalagmites should be exactly the same.

These data are complex and deserve closer attention at a more detailed level than can be provided here. The large excess of Mg is likely a major contributing factor in the formation of meta-stable aragonite rather than calcite. In summary, the elemental data show that a ready supply of most trace elements of interest in palaeoclimate studies, in particular Mg, Sr, possibly Ba, and the more poorly studied transition metals such as Mn. Ni, Zn is present in the dripwaters. Variability in the abundant elements in the stalagmite fabric of, for instance, Mg, must therefore be influenced by processes during the crystallisation of stalagmite carbonate. Shifts in Sr are likely to have at least two sources of variation, including supply and formation conditions (temperature and growth rate). Hence these fluctuations will be more difficult to interpret.

CHAPTER 4

CHRONOLOGY OF THE COLD AIR CAVE STALAGMITES

SAMPLING

In the case of T7, three plane-parallel slices of 10mm thickness and two outer sections were cut lengthwise. The three slices were used for dating, for petrology and stable isotope analysis, and for growth layer analysis respectively. T8 was sectioned lengthwise into 3 sections. The mid-section was used for dating, and one each of the side sections for grey scale analysis and for stable light isotope analysis respectively.

CHRONOLOGY

For both stalagmites, the first age estimations were established by means of α-spectrometry, in the Department of Geology, Bergen University by Dr Karin Holmgren under Prof. Stein-Erik Lauritzen's supervision. For T7, 21 5-15g samples were taken at regular intervals along the growth axis. Fewer samples were taken in the case of T8, where the purpose was merely to establish a rough time-scale for working purposes. Standard chemical preparation procedures and computer algorithms were used for α-particle spectrometry, as described by Lauritzen (1993). Age errors are based on counting statistics.

Uranium content for T7 was moderate to high (0.6-2.7ppm) throughout (Holmgren et al, 1999). The α-spectrometry ages indicated that T7 began growing about 6 500 years ago. An age model determined by linear interpolation of age versus depth suggested some variations in an otherwise steady growth rate, including a growth "spurt" at ~4000 years and a lesser increase at ~500 years. For T8, α-spectrometry showed that the base of the stalagmite was about 24 – 26 Ky old (uncertainty is due to large errors) and that the upper section occupied the entire Holocene. Rapid growth occurred in the Holocene compared to the Pleistocene. A sharp change in chemistry occurred at the interface between calcite and aragonite; in the calcitic section U was present in much lower amounts.

Because of the large samples required, uncertainties inherent in the α-spectrometry method, and in consideration of the goal of obtaining a high resolution record, it was decided to obtain another set of high precision dates, using the TIMS method, for T7. Fourteen thermal ionisation mass spectrometry U-series dates (Table 2) were determined from 2 g samples chipped from a wafer following procedures outlined in Lauritzen and Lundberg (1999). These refined the earlier age model, showing slightly younger dates and a nearly linear growth curve over the last ~6450 years.

Table 2. TIMS Uranium series dates for T7. Ratios are activity ratios expressed for 2σ, data reported in Lee-Thorp et al (2001).

Sample	mm	U (ppm)	$^{234}U/^{238}U$	$^{230}Th/^{234}U$	$^{230}Th/^{232}Th$	Age, yr
230/T7-25	22 ±3	0.769±0.0011	7.6635±0.03024	0.00103±0.00001	48.0±0.5	112±1
231/T7-35	44 ±3.5	0.7218±0.0005	7.564±0.01279	0.00186±0.00001	123±1.2	199±2
351T7/-50	77±2.75	0.720±0.007	8.0673±0.01877	0.00292±0.00001	41±0.4	317±1
232T7/-73	129±3.25	0.9311±0.0005	7.9176±0.01111	0.00424±0.00001	496±3.6	462±1
316T7/-90	163±2	0.609±0.0004	7.7209±0.01177	0.00540±0.00003	190±2.2	588±4
317T7/-109	197±2	0.823±0.00007	8.0134±0.01601	0.00633±0.00003	510±5.0	690±3
352T7/-151	298±2.5	0.724±0.0006	7.3754±0.01651)	0.01225±0.00005	1289±12.9	1334±5
353T7/-192	412	0.791±0.0015	7.5697±0.03118	0.01889±0.00006	197±1.3	2068±7
354T7/-223	500±2.75	1.051±0.0009	7.5382±0.01599	0.02423±0.00011	1374±13.8	2659±13
355T7/-274	597±2	1.675±0.0016	3.4783±0.01599	0.02954±0.00012	418±4.1	3251±17
356T7/-337	701±3.75	1.1259±0.0020	6.3647±0.02370	0.03696±0.00011	2859±25.0	4076±13
357T7/-403	806±2.75	1.0646±0.0018	5.2904±0.02379	0.04527±0.00045	852±10.5	5009±50
358T7/-465	905±6.5	0.9266±0.0013	5.9101±0.01752	0.05233±0.00014	1245±12.4	5805±16
359T7/-517	983±5	0.8675±0.0008	5.1668±0.01268	0.05746±0.00014	915±8.3	6388±16

The TIMS U-series determinations for T8 were performed by Dr Toni Eisenhauer, GEOMAR, Kiel. The results are shown in Table 3. No samples display sufficient ^{232}Th contamination ($^{230}Th/^{232}Th$ < 20) to affect the age determinations. Stalagmite growth occurred over the past 24.4 Ky, but a significant hiatus is evident from 12.7 to 10.2 Ky. From 0-12.7 Ky, T8 is composed of aragonite. The presence of aragonite was verified by X-ray diffraction (XRD), a method which cannot, however, detect low (<3%) amounts of calcite. Rapid growth rate (11 mm/100 yr), high chemical yields and well-resolved energy spectra resulted in precise age determinations for this period. An age model (Fig. 4.1) was produced by linear interpolation between dated intervals for the period 0-10.2 Ky. A large age interval between two closely spaced high-precision dated samples indicates the presence of a 2.5 ka hiatus at 10.2-12.7 Ky. Between 12.7 and 24.4 Ky the stalagmite is composed of calcite and dating precision is poorer, owing to the low U content and slow growth rate (2 mm/100 yr). The calcite nature of the speleothem fabric was again verified by XRD; in this case small amounts of aragonite cannot be detected. For this section the age model was derived by linear regression over the whole period. Excellent dating precision of ± 6 to160 yr is obtained for the period 0-12.7 Ky; thereafter precision declines from about ± 500 yr at 13 Ky to about ±3000 yr at 24.4 Ky.

Table 3. TIMS Uranium series dates for T8, Cold Air Cave. Activity ratios are expressed with 2σ. Numbers in brackets give the statistical uncertainty of the last significant digit.

Sample	mm	U (ppm)	$^{234}U/^{238}U$	$^{230}Th/^{234}U$	$^{230}Th/^{232}Th$	Age, yr
T8-21	21	1.502 (5)	11.78 (6)	0.00150 (3)	269±5	113±6
T8-20	43	0.942 (2)	8.72 (3)	0.0034 (1)	531±20	321±28
T8-19	62	0.854 (4)	8.95 (5)	0.00429 (10)	141±2	418±14
T8-18	101	0.911 (2)	9.66 (3)	0.00646 (4)	740±5	654±9
T8-17	117	1.095 (3)	9.61 (4)	0.00728 (10)	690±10	744±24
T8-16	181	1.026 (3)	9.57 (7)	0.01337 (10)	814±4	1411±17
T8-15	215	0.924 (3)	9.75 (5)	0.01549 (10)	959±15	1644±14
T8-14	234	1.040 (4)	10.36 (6)	0.01670 (10)	1054±5	1778±22
T8-13	258	0.909 (5)	9.9 (1)	0.01772 (20)	297±2	1890±37
T8-12	276.5	0.990 (5)	9.24 (8)	0.01903 (30)	1450±26	2034±73
T8-11	296	0.927 (2)	9.09 (4)	0.01986 (30)	859±14	2170±71
T8-29	363	1.475 (5)	10.06 (5)	0.02637 (10)	1543±8	2845±31
T8-08	502	0.968 (2)	10.57 (3)	0.03236 (30)	2624±27	3549±57
T8-07	602	1.474 (8)	10.48 (9)	0.04277 (30)	8334±56	4674±74
T8-28	650.5	2.258 (9)	10.49 (7)	0.04655 (30)	10421±50	5100±59
T8-06	812.5	2.246 (4)	9.73 (3)	0.060758 (30)	12377±65	6748±31
T8-27	887	2.56 (1)	6.78 (5)	0.06819 (40)	11717±46	7558±88
T8-05	977	1.95 (1)	6.09 (5)	0.07649 (60)	14903±127	8556±145
T8-26	1039	1.3298 (2)	6.17 (1)	0.08396 (20)	5276±28	9378±56
T8-04	1131.5	0.863 (4)	6.81 (5)	0.09016 (70)	389±3	10141±160
T8-31	1135.5	1.2349 (7)	7.70 (8)	0.11182 (70)	8867±52	12687±160
T8-03	1160	0.03703 (6)	7.39 (4)	0.10849 (580)	250±13	12280±1366
T8-32	1166.5	0.03969 (9)	7.21 (4)	0.12680 (130)	3922±177	14474±331
T8-25	1175.5	0.0380 (1)	7.06 (4)	0.11608 (250)	116±2	13145±584
T8-2b	1191	0.0983 (2)	7.59 (4)	0.11092 (180)	199±3	12580±422
T8-02	1205.5	0.02220 (6)	6.99 (6)	0.14583 (100)	394±3	16726±243
T8-24	1217.5	0.02551 (4)	7.46 (4)	0.13061 (510)	255±10	14880±1225
T8-23	1289.5	0.0426 (2)	8.05 (5)	0.16194 (300)	303±6	18691±735
T8-34	1326.5	0.0274 (3)	8.27 (12)	0.21611 (330)	1087±13	25571±854
T8-22	1360	0.0250 (2)	8.9 (1)	0.20082 (370)	242±4	23554±930
T8-01	1384.5	0.02254 (2)	7.56 (2)	0.18638 (300)	109±2	21777±759

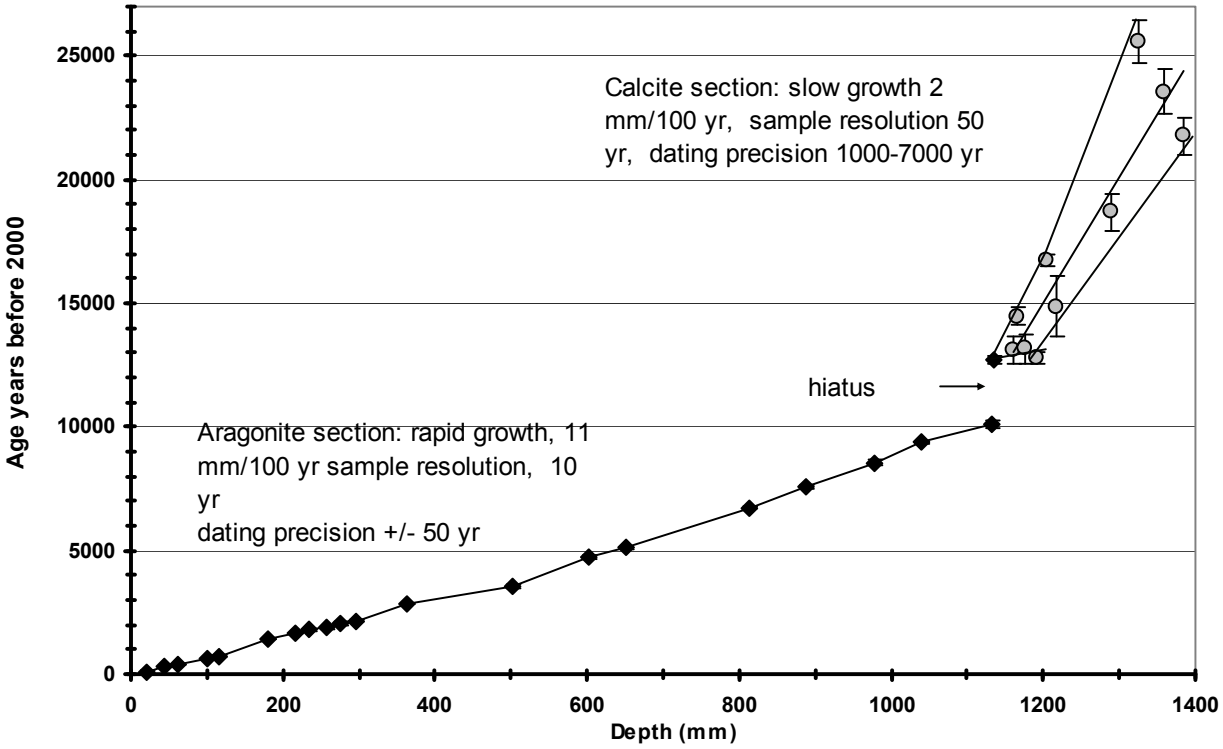

Figure 4.1. Age model for stalagmite T8 obtained from TIMS Uranium series disequilibrium dates by linear interpolation for the Holocene (solid triangles) and by regression for the Pleistocene (grey circles) sections, respectively. Growth rates, sampling and dating precision are indicated for each section. The hiatus is well-defined by two high precision dates.

The results show that the stalagmite provides a precisely dated sequence for the entire Holocene, and the relatively fast growth rate ensures that proxy data may be sampled at high resolution. Rapid growth rate is correlated with an aragonite fabric, and a markedly slower growth rate with a calcite fabric. Growth rate is nearly uniform for the Holocene, but it's not possible to determine whether growth rate is uniform or not, for the lower section. Notwithstanding the poorer precision in the late Pleistocene, this level of age control is unprecedented for Quaternary sequences in South Africa. Moreover, in spite of the problems with chemistry and dating precision of the lower section, we have been able to determine precisely the duration of a hiatus common in many records. This is possible because the age determination immediately prior to the hiatus is made on aragonite and has a high precision with a low error. The age for the lower section provides an opportunity for exploration of the pattern of the glacial maximum and subsequent warming for this region.

CHAPTER 5

PROXY PALAEOCLIMATE AND ENVIRONMENT INDICATORS

SAMPLING

As outlined earlier, stalagmites T7 and T8 were each sliced into 3 sections. Separate sections were used for dating (sampled at Stockholm University), for grey scale and incremental analyses, and for stable light isotope analyses, respectively.

Prior to sampling for stable light isotope analysis, ten or more small (≤0.1mg) samples were drilled at intervals along 10 individual growth layers of stalagmite T8 for performing "Hendy" tests to check for isotopic equilibrium conditions (Hendy, 1971). While this test is not a foolproof indicator of isotopic equilibrium, it is a minimum requirement. Care was taken to stay within the narrow limits of each of the layers – Transects A to J - as far as possible. After analysis of these transects showed that isotopic equilibrium conditions likely existed on the mid-growing face of the stalagmite, high resolution sampling was undertaken along the growth axes. Sampling and most of the isotopic analyses for T7, drilled at approximately 2mm intervals using a 0.6mm diamond-tipped drill, had been completed by the start of the current project. We did, however, re-sample a small section (~4cm) at the tip at higher resolution of 1mm intervals. High resolution sampling was attempted for the entire T8 stalagmite by drilling at as closely spaced intervals as possible, by offsetting each drilled hole. This resulted in a 'zigzag' pattern (visible in Fig 2.5). To avoid contamination between samples the drill-bit and stalagmite surface was cleaned between drillings by high pressure air, and the drill-bit was dipped in a weak HCl solution. Sampling direction lines altered slightly along the stalagmites, with small changes in the growth axis (Fig 2.4 and 2.5).

ANALYSIS

Grey scale/humates and trace elements

Grey scale analysis was performed at Stockholm University. The results for T7 have been reported (Holmgren et al, 1999; Lee-Thorp et al 2001) and are not repeated here. Grey scale analysis of T8 was less useful because of lower humate levels and considerable non-humate grey staining, likely due instead to Manganese (Mn). Hence this technique is not discussed further for T8.

Ultra-high resolution trace element analysis by means of Secondary Ion Mass Spectrometry (SIMS) was applied to two small thin-sectioned chips of T7 and a ~20mm thin section from the tip of T8. Although this study grew out of the present one and bears on the aims and results, it falls beyond the scope of this project as originally proposed. Therefore I do not report on the methods and results in any detail. The results have been published as Finch et al (2003).

Hendy tests

The intra-layer samples required for the Hendy tests were analysed for $\delta^{18}O$ and $\delta^{13}C$ according to the methods given below. The data were analysed by plotting $\delta^{18}O$ across each transect, as well as $\delta^{13}C$ versus $\delta^{18}O$ from the midpoint outwards. The data showed that $\delta^{18}O$ values remained homogenous at the centre of each growth layer, and that plots of $\delta^{13}C$ versus $\delta^{18}O$ did not show linear trends (Fig 5.1 below) which would have indicated co-fractionation.

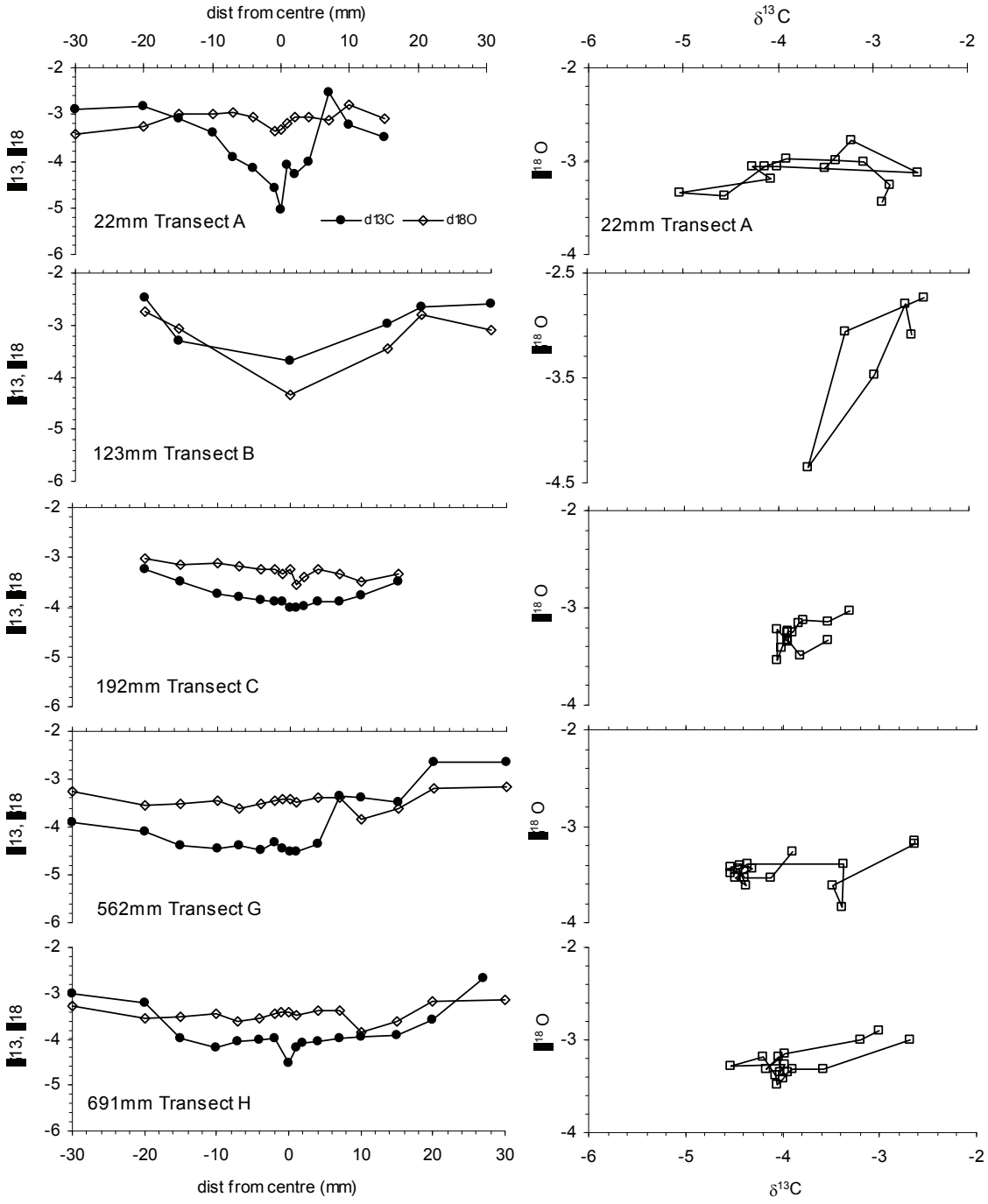

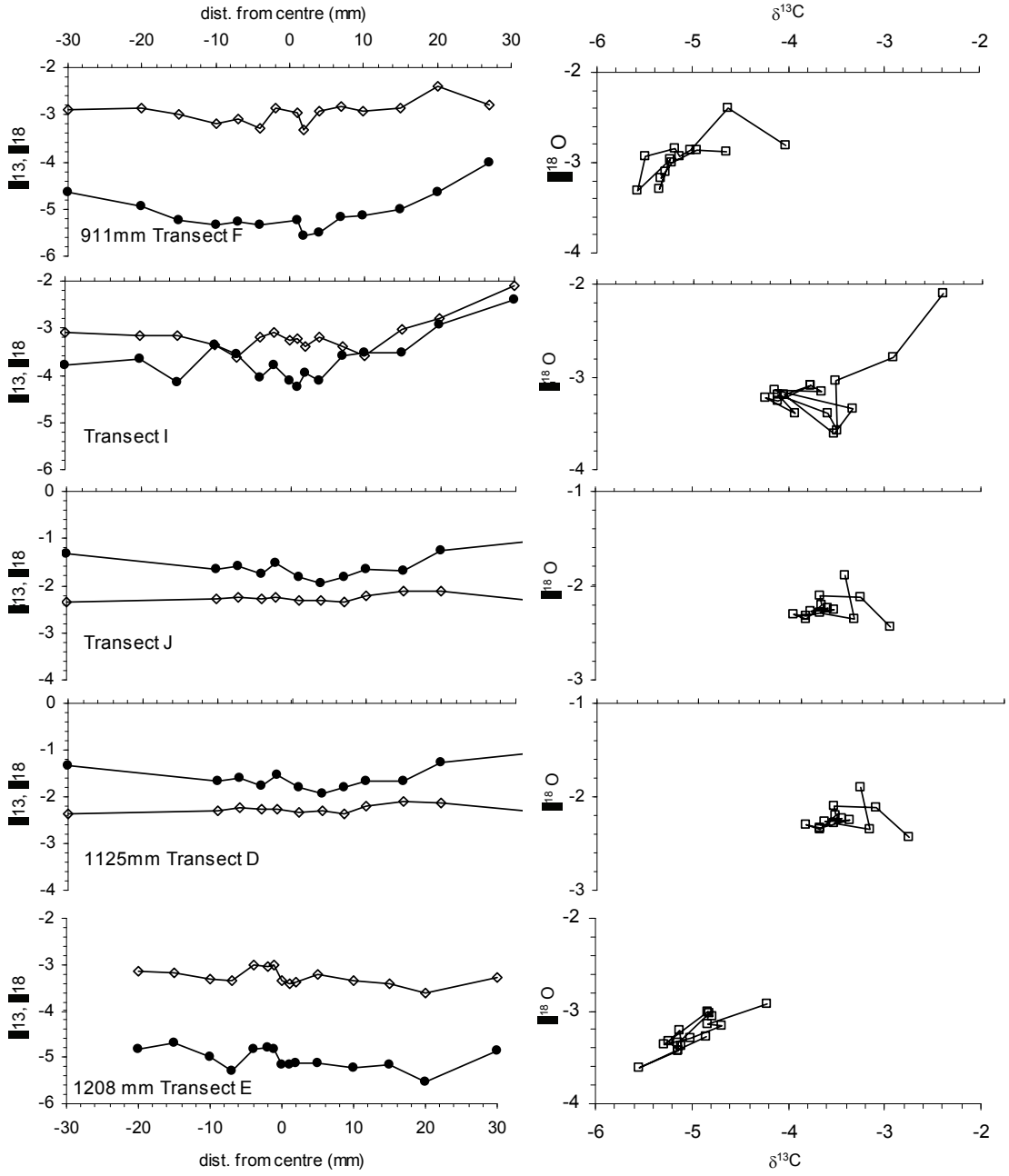

Figure 5.1. Results for 10 Hendy tests on individual growth layers A-J are shown (Hendy, 1971). To the left, $\delta^{18}O$ and $\delta^{13}C$ is plotted against position from the centre of the stalagmite mid-point. To the right, $\delta^{18}O$ is plotted against $\delta^{13}C$ to check for non-linearity.

Stable light isotopes

Samples of ~0.06mg of carbonate powder were weighed into individual sample cups and introduced into the Kiel autocarbonate device. CO_2 was produced by reaction with 100% H_3PO_4 at 70°C, and introduced to a Finnigan Mat 252 mass spectrometer after removal of H_2O by cryogenic distillation. The ratios of $^{13}C/^{12}C$ and $^{18}O/^{16}O$ in samples were determined against a reference gas, and the results

were standardised against international (NBS 18, 19) and inter-laboratory standards (CarraraZ and Lincoln Limestone) using a 3-point calibration curve. Isotope ratios are expressed in the δ convention relative to PDB, in parts per mil ($^{o}/_{oo}$).

Based on the age model for T7, sampling resolution for T7 averages just over 10 years, but in certain sections resolution dipped because of analytical errors resulting in "missed" analyses, or slight differences in growth rate. Sampling intervals for T8 were more closely spaced, but again sampling resolution for T8 averaged ~9 years for the period 0-10.2 Ky and ~50-160 years for the much slower-growing 12.7-24.4 Ky section. The latter resolution must be treated with caution because errors in the U-series dates for the lower section are large.

RESULTS

The T7 and T8 $\delta^{18}O$ and $\delta^{13}C$ records can be compared where they overlap for the past 6.5 Ky (Fig 5.2). The records compare well for both $\delta^{18}O$ and $\delta^{13}C$; frequency of occurrence of peaks or troughs of opposite sign in the two sets of series is <5 %. Their concordance suggests that the stalagmite-derived stable isotope proxies provide a robust signal of local climatic and environmental change

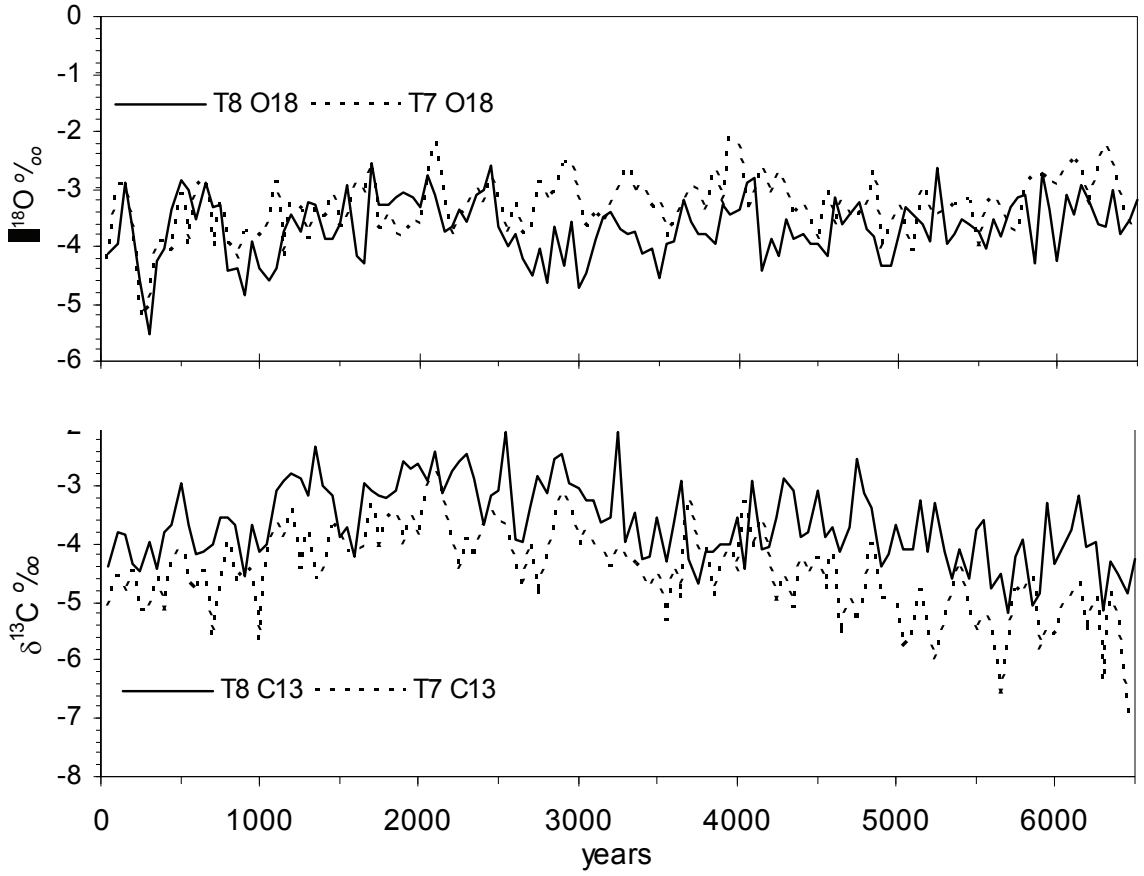

Figure 5.2. A comparison of the $\delta^{18}O$ (above) and $\delta^{13}C$ (below) time series for T7 and T8 for the period of overlap. The data are resolved at 50 year intervals.

Discrepancies, as for example in $\delta^{18}O$ at 2.6-3.5 Ky, may be a result of small differences in the age models, or they may reflect real differences between the records due to local variations. In addition to concordance for long- and short-term trends, the two records share a feature of remarkably high amplitude variability on short timescales, in comparison with the Cango stalagmite.

Although inverse temperature dependence of the fractionation between carbonate and water is the basis for conventional palaeotemperature determinations, there are a number of indications that, in this case, the thermodynamic effect is over-ridden by factors affecting meteoric water $\delta^{18}O$. First, the $\delta^{18}Oc$ series from the high resolution, re-sampled upper 4cm section of T7, and for the tip of T8, can be compared with regional instrumental temperatures records to AD 1900 (Fig 5.3).

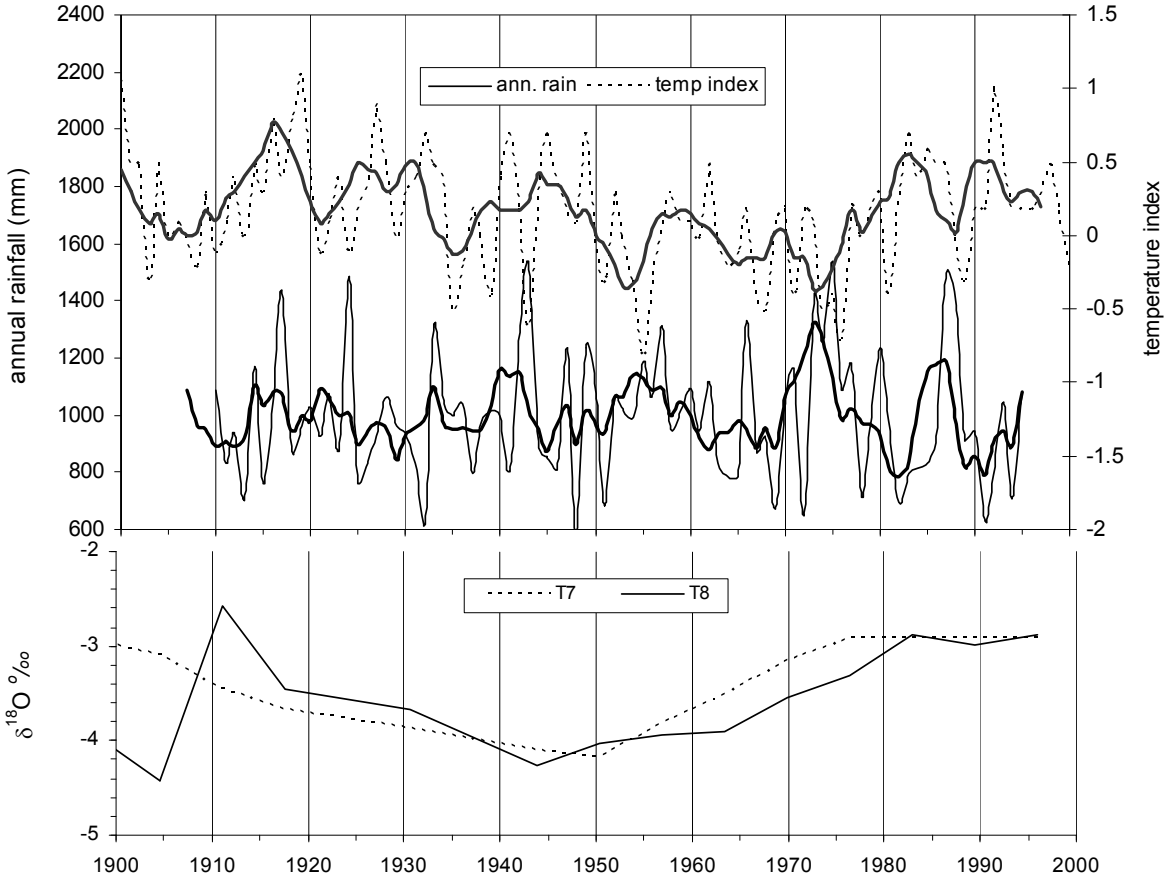

Figure 5.3. Comparison of the $\delta^{18}Oc$ series for the tips of T7 and T8, placed within their respective U-series age models (lower panel), against the regionally averaged annual rainfall (mm) and temperature indices. Four-term weighted running means are superimposed on the rainfall and temperature index series. Regional climate data were provided by the South African Weather Service.

Temperature calculations based on the palaeotemperature equation (4) for aragonite (see Chapter 1) yields a trend opposite to the instrumental record. In fact, substitution of upper T8 $\delta^{18}Oc$ and $\delta^{18}O$

values for recent groundwater into the expression yields a *cooling* of 5°C from 1950, whereas instrumental records demonstrate a warming of 1°C (Holmgren et al, 2003). Furthermore, the amplitude of exceedingly rapid $\delta^{18}O_c$ shifts, notably the shift at ca. AD1800 (Fig 5.2), yields unreasonably high temperature shifts of up to 9°C using Equation 4. The conclusion is that shifts in rainfall $\delta^{18}O$ have overprinted the temperature dependent thermodynamic fractionation from seepage water to carbonate, and that δ^{18}Omw has varied considerably over time.

Stalagmite δ^{18}Oc values nevertheless bear a relationship to temperature. Comparisons of δ^{18}Oc from T7 and T8 with the instrumental temperature records from the Polokwane (formerly Pietersburg) station described above (Fig. 5.3) , suggests a *direct,* not inverse, relationship between temperature and δ^{18}Oc (Lee-Thorp et al, 2001; Holmgren et al, 2003). The amount of rainfall, *per se*, seems to bear little relationship to isotopic composition – or at least any relationship is extremely complex - as suggested by a comparison of mean annual rainfall with δ^{18}Omw (using a weighted mean) from the Pretoria station (Fig. 5.4). In one year (1977) low δ^{18}Omw values are associated with higher rainfall, but there is no consistency.

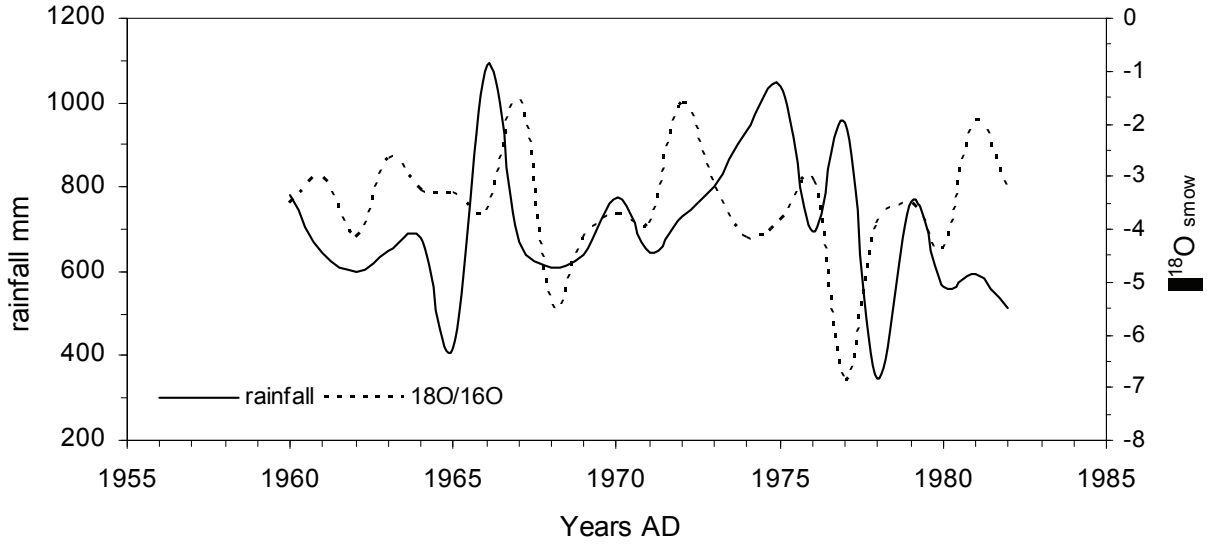

Figure 5.4. A comparison of mean annual rainfall with meteoric water $\delta^{18}O$ from Pretoria. Data courtesy of Mr Siep Talma, QUADRU, CSIR.

A consideration of current climatology provides a plausible explanation. During drier summers relatively more rain is derived from high altitude, convective storms originating in the upper troposphere (Harrison, 1986); these conditions are associated with equatorward expansion of the atmospheric circumpolar vortex leading to cooler and drier conditions over the entire summer rainfall region of South Africa (Tyson, 1986). The association between relatively cooler temperatures and meteoric water depleted in ^{18}O occurs because the temperature at which raindrops condense is lower, and because convective rain and hail from storms is markedly depleted in ^{18}O

(Rozanski *et al.* 1993). Storms are also associated with an "amount effect" which also leads to isotopic depletion. Depletion may also simply be associated with general atmospheric cooling.

The replication of the Makapansgat T7 and T8 speleothems $\delta^{13}C$ records suggests that they are robust indicators of the proportions of C_4 plants in the local environment. A clear trend towards higher $\delta^{13}C$ and hence maximum C_4 grass cover by 2-3 Ky ago corresponds to a similar trend in the Cango Cave stalagmite thousands of kilometres to the south (Talma and Vogel, 1992). Since C_4 grasses are adapted to high radiation and warm temperatures in the growing season, and CO_2 fluctuations can be excluded, it must be concluded that similar conditions favouring C_4 grasses were widespread at the time.

The 0-24.4 Ky $\delta^{18}O$ and $\delta^{13}C$ series for T8, plotted at 50 yr intervals, is shown corrected for aragonite by -0.6 ‰ for $\delta^{18}O$ and by -1.8 ‰ for $\delta^{13}C$ (Tarutani *et al.*, 1969; Grossman and Ku, 1986) for the aragonite section, to ensure that the entire record is comparable with the lower calcite section (12.7-24.4 Ky) (Fig 5.5). Since the $\delta^{18}O$ signal is derived from rainfall and ultimately an oceanic moisture source, in the lower panel $\delta^{18}O$ is further corrected for global ice volume following Guilderson *et al.* (2001), in order to ensure comparability across the entire period. A 9-term weighted running mean was applied. Surprisingly, the $\delta^{18}O$ record for the late Pleistocene does not display the well-known pattern of a steep increase after ~18 Ky. The series, however, does show patterned shifts over millennial time-scales, which are further explored in the following chapter.

An overarching problem in speleothem isotope studies is the estimation of dripwater $\delta^{18}O$ composition. In this study, $\delta^{18}O$ ratios from groundwater samples from the Springbok Flats to the South West provided some indications for meteoric water $\delta^{18}O$ values, integrated over several thousands of years. It is very unlikely, however, that $\delta^{18}O$ ratios in precipitation have remained stable over long periods, hence it is not possible to use these averaged values for estimating temperature variations at the 9-50 year resolution of the Makapansgat $\delta^{18}O$ records. However, it *is* possible to use the mean values of $\delta^{18}O$ for carbonate and groundwater for the Holocene and late Pleistocene to obtain an estimate of the gross temperature *difference* between the two periods. Using mean values for carbonate (corrected to calcite) and water of –3.86 ‰ and –4 ‰, respectively, for the Holocene, and means for the late Pleistocene of –3.21 ‰ and –4.8 ‰, average temperatures of 16.3°C and 10.6°C are obtained for the Holocene and late Pleistocene respectively. The resulting difference of 5.7°C compares well with previous estimates of 5-6°C derived from analyses of dissolved gases from fossil aquifers in South Africa and Namibia (Heaton *et al.*, 1986; Stute and Talma, 1998).

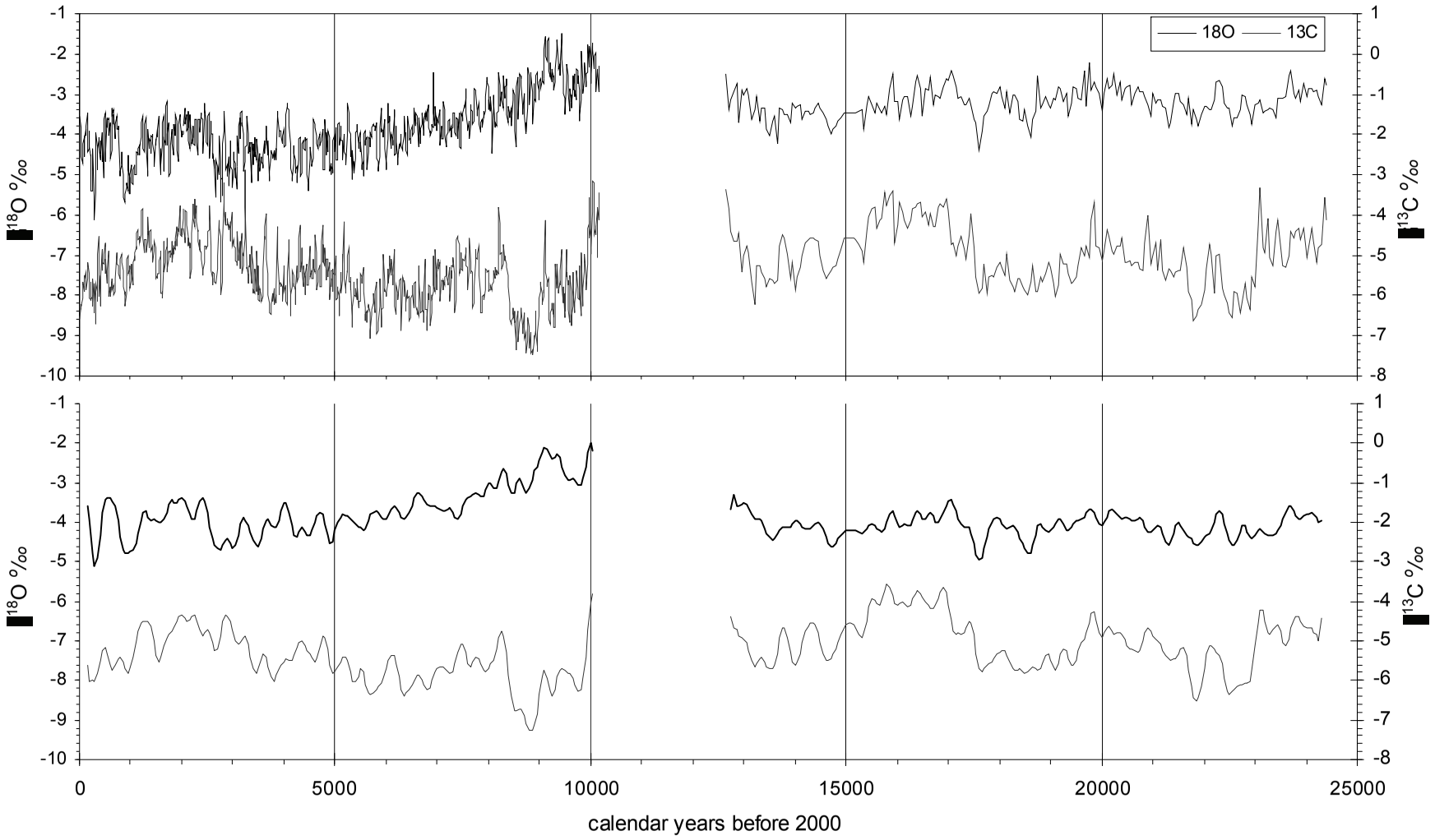

Figure 5.5. The $\delta^{18}O$ and $\delta^{13}C$ time series for T8, with data normalised to calcite as described in the text. In the upper panel the data are interpolated to average age intervals of 10 and 50 years for the Holocene and Pleistocene respectively. In the lower panel $\delta^{18}O$ is corrected for ice volume effects in ocean source, as described in the text, and a 9-term weighted running mean applied.

As we argued in the case of T7 (Holmgren et al, 1999; Lee-Thorp et al, 2001), changes in the T8 $\delta^{18}O$ record are best ascribed to shifts in the $\delta^{18}O$ composition of precipitation. As discussed above, an interpretation of this variability is sought in current rainfall patterns. Occurrence of persistent rainfall from middle-level stratiform cloud bands during generally wetter periods is argued to lead to less ^{18}O depletion in the rain than occurs in generally drier periods when rain and hail from high, cool, convective thunderstorms provides a greater proportion of precipitation. Thus both the rainfall type (storms, hail) and amount (more with a single event, but less on an annual basis) contribute to lower $\delta^{18}O$ values during these cooler and stormier, but drier periods.

The stalagmite $\delta^{13}C$ record varies between ca. –3.2 and –6.5 ‰ (Fig. 5.5), implying that C_4 grasses are always present, with moderate short-term variations reflecting changes in their relative proportions. Higher $\delta^{13}C$ values indicate predominant C_4 grass cover and suggest optimal or seasonally restricted summer rainfall conditions. Low values suggest sparse grass cover, probably associated with shrubbier vegetation cover (and in some cases, dry conditions), or with denser tree and shrub cover (and moister conditions). The slightly higher $\delta^{13}C$ overall average for the Pleistocene part of the record is best considered as a reflection of lower atmospheric CO_2 levels in which C_4 grasses are favoured in spite of lower temperatures (Ehleringer et al , 1997).

After correction for global ice volume, the mean $\delta^{18}O$ value for late Pleistocene is 0.3 ‰ lower than the Holocene mean value (Fig. 5.5). The small change in $\delta^{18}O$, despite a mean inferred temperature change of 5.7ºC between late Pleistocene and early Holocene, results from the cancelling out of several factors: slightly higher $\delta^{18}O$ oceanic sources but lower sea surface temperatures leading to greater fractionation during vaporisation, and conversely during precipitation, as well as a higher temperature dependent fractionation factor between water and calcite $\delta^{18}O$. Rather than the well-known pattern from sea levels and ice cores showing a marked Last Glacial Maximum trough followed by a warming trend, $\delta^{18}O$ record shows a series of modest quasi-periodic positive and negative inflexions during this period, coupled with similar but stronger shifts in $\delta^{13}C$. The record suggests lower temperatures and sparser grass cover at about 23-21 Ky, 19.5-17.5 Ky and 15-13.5 Ky (Fig. 5.5). The nearby Wonderkrater pollen sequence suggests a 1000m altitudinal lowering of vegetation zones, corresponding to a 5-6 °C drop in temperature at ~18 Ky (Scott, 1982). Drier conditions are also inferred from other less detailed regional proxy records (Partridge, 1997).

Clearly, a considerable, abrupt change in climate and environment occurred at 12.7 Ky. A sharp change in crystal form from calcite to aragonite was followed by a 2.5 Ky hiatus, after which higher growth rates, higher concentrations of uranium and enrichment of stable isotopes are observed. The sudden shift in stalagmite composition from calcite to aragonite at 12.7 Ky implies that a threshold was breached. The

balance between the two forms is controlled both by Mg composition and temperature/evaporation (Murray, 1954). Since Mg is always present in super-abundance from the dolomite bedrock, it may be concluded that temperature or evaporation is the driving factor for the change from calcite to aragonite. The hiatus from 12.7-10.2 Ky prevents observations of this period, but the Wonderkrater pollen-derived temperature index shows an interruption in the warming trend, centred around 11.3 Ky (Scott, 1999). High amounts of the Chenopodiacae and Amaranthaceae pollen taxa indicate the prevalence of strongly evaporative but not necessarily low-rainfall, conditions between ca. 12 and 10 Ky. The hiatus in stalagmite growth is most likely due to a cessation of drip water, due in turn to these evaporative conditions.

A marked feature in the early Holocene immediately after the hiatus is the period from 10.2 to ~ 8Ky showing lower $\delta^{13}C$ coupled with significantly higher $\delta^{18}O$. $\delta^{18}O$ values are high enough to suggest processes related to evaporation. Coupled with lower $\delta^{13}C$, showing grass-poor conditions, these data suggest an evaporative, dry environment with sparse, mostly shrubby vegetation cover. The rest of the T8 Holocene record follows the T7 pattern well. The period from ~7-5.2 Ky, with moderately higher $\delta^{18}O$ coupled with lower $\delta^{13}C$, is interpreted as relatively wetter and warmer with denser C_3 (trees and shrub) vegetation. After 5.2 Ky, the overall but highly variable trends are towards higher $\delta^{13}C$ showing increasing proportions of grasses culminating at ~2200 years, and towards lower $\delta^{18}O$ culminating at AD1700.

CHAPTER 6

Variability and longterm trends

One of the problems in palaeoclimatology concerns the nature of the links between external forcing, for instance solar radiation, and non-linear feedback mechanisms within the climate-ocean system. Climate signals are complex in space and time, representing a culmination of feedbacks and interactions between a number of physical processes operating over a wide range of spatial and temporal scales (Bolton et al, 1995). These signals are not stationary in time because they comprise frequency regimes that may span longer and shorter periods. Hence analysis of long proxy data series to extract information about variability or periodicity, and temporal and spatial evolution of periodic elements, is an important component of palaeoclimate studies. Determination of frequency and evolution of the South African climate is severely constrained by the scarcity of long, continuous records of sufficiently high resolution.

Studies of recent climates have relied extensively on variability analysis as a way of determining periodicity, leads and lags and teleconnections in signals from different places. Traditionally, spectral analysis has been applied to time series data to determine dominant frequencies (eg. Mann and Park, 1994). However, the major constraint of this tool is the inability to examine shifts in variability over time. Wavelet analysis offers a useful tool for determining variance spectra; it clearly shows frequency and amplitude modulation of climatic oscillations over time. Wavelet analysis is better suited to the study of multi-scale, non-stationary processes (Lau and Weng, 1995; Torrence and Compo, 1998).

EXISTING VARIABILITY STUDIES OF LOCAL CLIMATE AND SPELEOTHEMS

Tyson has observed, in instrumental rainfall and temperature records for South Africa for the past century, a pattern of quasi-periodic cycles of ~18 years, and hints of the existence for a longer period of cycles of the order of 80 years (Tyson, 1986; Tyson and Preston White, 2001). The existence of the 18-20 year cycle in the summer rainfall region of South Africa has not been confirmed, however, in an examination of records from 1921 across *all* summer rainfall zones (Rouault and Richard, 2003). This study used a Standardised Precipitation Index (SPI) to catalogue major droughts during the 20th century. It was concluded that the ~20 year pattern was restricted to a limited number of districts, and that since 1960 droughts corresponded well with ENSO-type events (Rouault and Richard, 2003). Clearly, variability of South African rainfall is a complex matter, and discernment of patterns requires longer records than those which presently exist for instrumental records. Strong periodicity on much longer time-scales, following a precessional (~23 Ky) pattern clearly related to Milankovitch orbital forcing, is observed in the singular Tswaing Crater record (Partridge et al, 1997). Currently an exceptionally large gap exists between observations of variability on short, recent time-scales, and the longer period Tswaing

Crater series. The determination of high resolution proxy climate data from the Cold Air Cave speleothems provides an opportunity to bridge this gap.

As noted earlier the Cold Air Cave speleothems exhibit high amplitude variability, and provide suitable subjects for frequency analyses. In an earlier study we applied multi-taper spectral analysis to examine variability in the $\delta^{18}O$, $\delta^{13}C$ and grey scale series for the continuous 6.5 Ky-old T7 stalagmite (Lee-Thorp et al, 2001). The data was interpolated to a regular 1-year grid, but only periods of >40 years, approximating the Nyqvist frequency, were examined. The spectra showed a red noise character with a number of superimposed peaks, occurring at different frequencies for the different proxies. Significant (99.5% level) F-tests for periodic components occur at 57 years in the $\delta^{18}O$ spectrum, and 334, 83, 52 and 42 years in the $\delta^{13}C$ spectrum. Subsequent analyses using wavelet analysis has shown that frequency and amplitude modulation is a prime reason for the poorly resolved results from traditional spectral analysis.

Tyson et al (2002a) were the first to apply wavelet transform analysis to examine variability in a Cold Air Cave speleothem, together with several existing scattered tree ring and river runoff series, to determine whether patterns of variability seen in the instrumental record also existed further back in time. They applied wavelet analysis to the upper half (~3500 years) of the T7 stalagmite $\delta^{18}O$ record, interpolated to regular time intervals, using a Morlet wavelet and continuous wavelet transform and the real wavelet function. Details of the method of analysis are given in Torrence and Compo (1998). The result is a continuous wavelet transform, whose coefficients were contoured as a function of time and frequency following an adjustment to convert scale to the centre frequency of the wavelet. The signed coefficients were contoured to highlight phase relationships between the different frequency components and to provide a distinction between positive- and negative-amplitude peaks (Tyson et al, 2002a). The results are discussed along with those for T8.

A similar wave transform analysis was applied to the full T7 and T8 $\delta^{18}O$ series by Cooper and Tyson (reported in Holmgren et al, 2003). The analysis showed that greatest changes in variability occurred in the range 2.5-4.0 Ky. Frequency modulation of this oscillation occurred over the entire period of 24 Ky, but amplitude modulation was more pronounced in the late Pleistocene. Variability in this range has been variously ascribed to non-linear responses of the precession cycle (Pestiaux *et al.*, 1988), solar forcing (Stuiver *et al.*, 1995), and stochastic resonance of Dansgaard/Oeschger events every 1.5 Ky or multiples thereof (Ganopolski and Rahmsdorf, 2002). An oscillation from 0.75-1.25 Ky, the "quasi-1 Ky" oscillation, was less developed, undergoing frequency modulation with the shortest period of ~750 years prior to 20 Ky and the longest in the early Holocene. A change in the pattern of variability occurred ~6 Ky. At the higher frequency end, a quasi-100-year oscillation, found during the upper 3.5 Ky of the T7

record (Tyson *et al*., 2002a), was discerned weakly and intermittently in the 24.4 Ky T8 record. It has been suggested that variability at about 100 years, observed around the world in ocean and atmospheric records, may be related to changes in solar output associated with the ~80 year Gleissberg cycle, which is, in turn, linked to high and low phases of the 11-year solar cycle (Lean *et al.*, 1992; Hoyt and Schatten 1997; Harrison and Shine, 1999). It was concluded that the ~100 year rhythm in southern African climates was considerably more long lived than was previously realised.

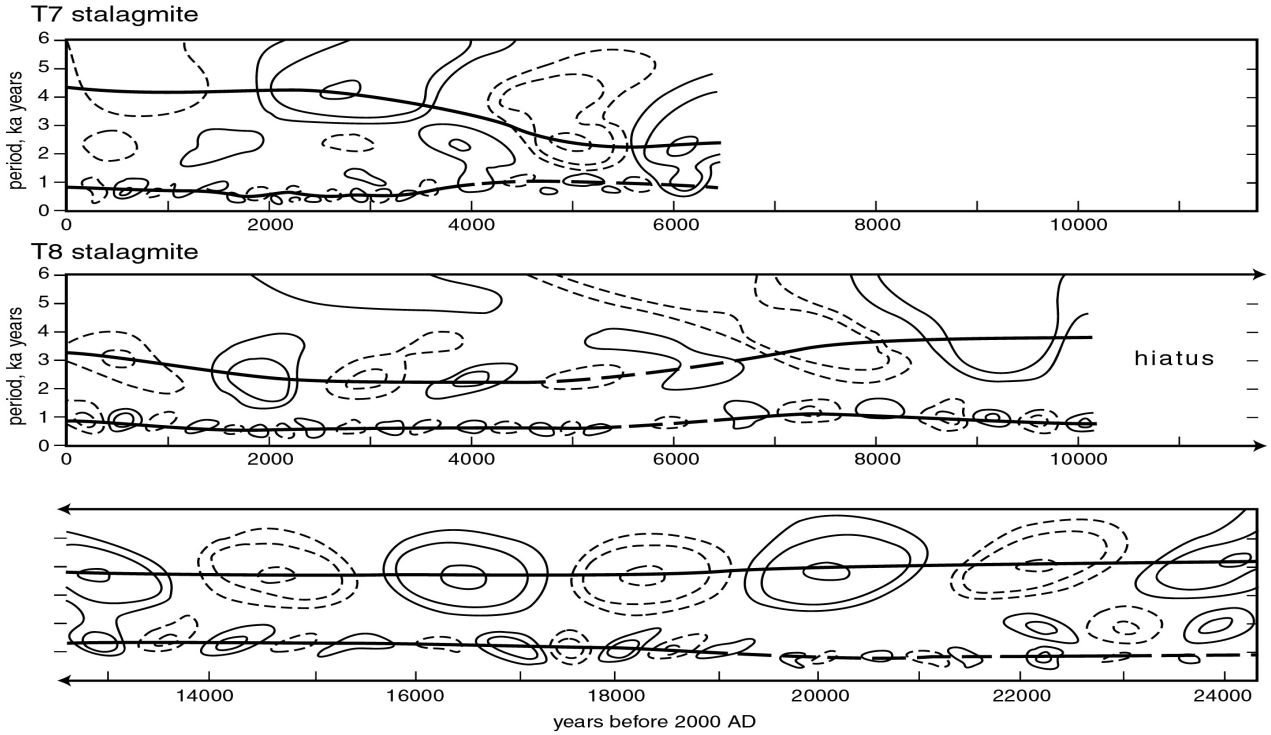

Figure 6.1. Wavelet analysis of the 6.5 Ky T7 and 24.4 Ky T8 $\delta^{18}O$ records from Holmgren et al (2003). Contours are bounded by values of -1.7 to +1.6 (top panel), -3.1 to +3.7 (middle panel) and -2.5 to +2.4 (lower panel), positive continuous wavelet transform coefficients are enclosed by solid lines, negative coefficients by broken lines.

NEW TIME SERIES ANALYSES OF T8

In an effort to ascertain patterns of variability in the $\delta^{13}C$ series (reflecting vegetation changes), as well as those for the $\delta^{18}O$ series described above from Holmgren et al (2003), further continuous wavelet transform analysis of the T8 data was undertaken. The Morlet wavelet and continuous wavelet transform (Lau and Weng, 1995; Mélice et al, 2001) was applied, but in this case the real *and* imaginary wavelet functions were retained, using the following equation.

$$W_{a,b} = 1/a \int_{-\infty}^{\infty} x(t)\, \Psi^*((t-b)/a)\delta t \qquad (6)$$

The data were analysed using a program written by J.-L. Mélice (Mélice et al, 2001). $\delta^{18}O$ and $\delta^{13}C$ data were analysed separately for the Holocene and Pleistocene. Since a complex series of frequencies which modulate in time and amplitude are obtained using this method, the CWT for each proxy data series is shown separately, in the lower left, together with the data series (blue) and 3 most important frequency extractions (red) in the other panels. Frequency is shown on the y-axis on a log scale. Colour changes in the CWT spectrum indicate signal amplitude, from deep blue (low) to red (high).

The results for $\delta^{18}O$ show similar patterns to those reported earlier (Holmgren et al 2003), although there are some differences. Figure 6.2 shows that the low frequency bands are more intense during the period ~16-20 Ky, during which time several bands occur. The ~4000 year band is present throughout; although never strong it modulates slightly in amplitude and in frequency from >4000 year (at 24 Ky and 13 Ky) to <4000 years (centred on 18 Ky). The millennial band is more intermittent, but modulates more strongly in both frequency and amplitude. Lower frequencies (~1500 years) are less intense and occur in the earlier (23-24 Ky) and later (12.6-14 Ky) periods, while a relatively stronger ~900-1000 year frequency band occurs during the period 17-19 Ky. Whether variation in other bands at ~500-700 years should be included as modulations of this band, as presented in the earlier analysis (Holmgren et al 2003), is a matter of preference, and it was not done here. Higher frequency variability is noisy. Strength is present intermittently for the 200-300 year band, most noticeably at ~19, 16 and 12.6 Ky (Fig 6.2, lower right panel), and some of the most intense bands in the spectrum occur discretely in the 150 year region. It's not possible to resolve variability at higher frequencies due sampling resolution constraints (nominally 50 years), and uncertainties in the age model for the Pleistocene time series.

During the Holocene, the multi-millennial $\delta^{18}O$ frequency band modulates in frequency to ~3000 years; it is discontinuous and more intense in the earlier and later periods (Fig. 6.3, left panels). The same phenomenon occurs for the millennial-scale band which modulates to a higher frequency centred on 800 years during the Holocene (Fig. 6.3, upper right). The 800 year band modulates strongly in amplitude, again showing most strength during the earlier and later periods. It exhibits the most power in the Holocene $\delta^{18}O$ spectrum, although it is intermittent. Higher frequency variability is noisy but indicates some intermittent power in the range 200-300 years, and below 100 years. The 200-300 year band is strongly modulated in frequency and amplitude throughout the Holocene (Fig 6.4, lower panels); it is more strongly developed ca. 8-9 Ky, in the mid-Holocene ca 6-2.5 Ky, and from about 1 Ky to the present. In order to examine in more detail the variability at higher frequencies beyond 200 years, the extracted frequency bands for 150 and 100 years are shown in Fig 6.4. The two extracted frequency bands illustrate frequency modulation from 150 -100 years by showing increased power at different points in time. Decadal-scale variability is even noisier, but again shows intermittent but poorly resolved power in a domain between ~50 and 100 years throughout the Holocene.

The CWT spectra for $\delta^{13}C$ in the Pleistocene shows strong, continuous power in a low frequency band centred on ~4000 years (Fig 6.5). This variability is similar in frequency but much more strongly resolved than the 4000 year band in the $\delta^{18}O$ spectrum. It is the most intense of the frequency bands for the $\delta^{13}C$ Pleistocene spectrum. Some limited variability resides in the 1000-1500 range, restricted to the upper section, but variability in the region 500-750 years shows more power (although nevertheless intermittent). The extracted 750 year frequency spectrum and its "fit" to the data are shown in the upper right panel of Figure 6.5. Bands at higher frequencies show intermittent strength in the 150-300 year region (Fig. 6.5 lower right), with highest frequency and power near 23 Ky.

In the Holocene, the $\delta^{13}C$ spectrum (Fig 6.6) appears different mostly because the continuous, strong 4000 year frequency band observed in the Pleistocene has modulated to more intermittent, and weaker variability at ~ 2500 years. No variability occurs in the lower frequencies below this band, hence the frequency scale for Fig 6.6 has been cropped at 3000 years. More power in fact lies in the discontinuous band centred on 750 years (Fig 6.6, upper right). Frequency modulation occurs between 600 and 800 years, and greatest power is shown in the early (8-10 Ky) and late Holocene. This band is probably the most striking feature of the Holocene $\delta^{13}C$ spectrum. Intermittent power is also shown in the 200-300 frequency region (Fig 6.6 shows the 300 year spectrum at lower right) during discrete periods more prominent in, but not restricted to, 2 to 4 Ky ago. The higher frequencies are noisy, but some power is present in a broad domain between 150 and 50 years, intermittently and more noticeably from 3-4 Ky, 6-7 Ky, and 9-10 Ky.

Hence, the pattern seen for both the $\delta^{18}O$ and $\delta^{13}C$ CWT spectra is for frequency modulation of Pleistocene bands to shorter wavelengths in the Holocene, while at the same time these multi-centennial bands (~800 years for $\delta^{18}O$ and ~ 750 years for $\delta^{13}C$) become prominent features in the spectra. Variability in the higher frequency domains below 300 years is clearly noisier and less predictable for both $\delta^{18}O$ and $\delta^{13}C$ series in the Holocene, although the latter spectrum is undoubtedly the most complex. A similar conclusion was reached by a different method of time series analysis of the T7 isotope series, in which spectral analysis showed few significant peaks for $\delta^{18}O$ but a complex series of significant peaks for $\delta^{13}C$ (Lee-Thorp et al, 2001). These occurred, moreover, at different frequencies differing from those of the $\delta^{18}O$ series. Neither conventional nor continuous wavelet time series analysis is able to resolve variability at frequencies less than 150 years for the Pleistocene, and 30-50 years for the Holocene, where mean sample resolutions are ~50 years (at best) and 10 years respectively. Hence it is not possible to ascertain whether the 50-120 year quasi-periodicity suggested by Tyson in various publications (eg. Tyson et al, 2002a) extended into the Pleistocene. Some variability in this domain undoubtedly occurs in the Holocene T8 $\delta^{18}O$ record, although it is poorly resolved and eclipsed by

stronger variability at the multi-centennial scales. For the same reason, using the stalagmite $\delta^{18}O$ data, we are unable at present to test the longevity of the proposed 18-year rainfall cycle for South Africa. Hence a gap still remains between the instrumental variability studies and the palaeoclimate proxy series.

One important conclusion to be drawn from CWT analysis of the isotope proxy data is that lower frequency variability at multi-centennial scales appears to be more dominant and hence predictable that high frequency variability. This is true for the climate proxy series from $\delta^{18}O$ as well as the floral composition series from $\delta^{13}C$.

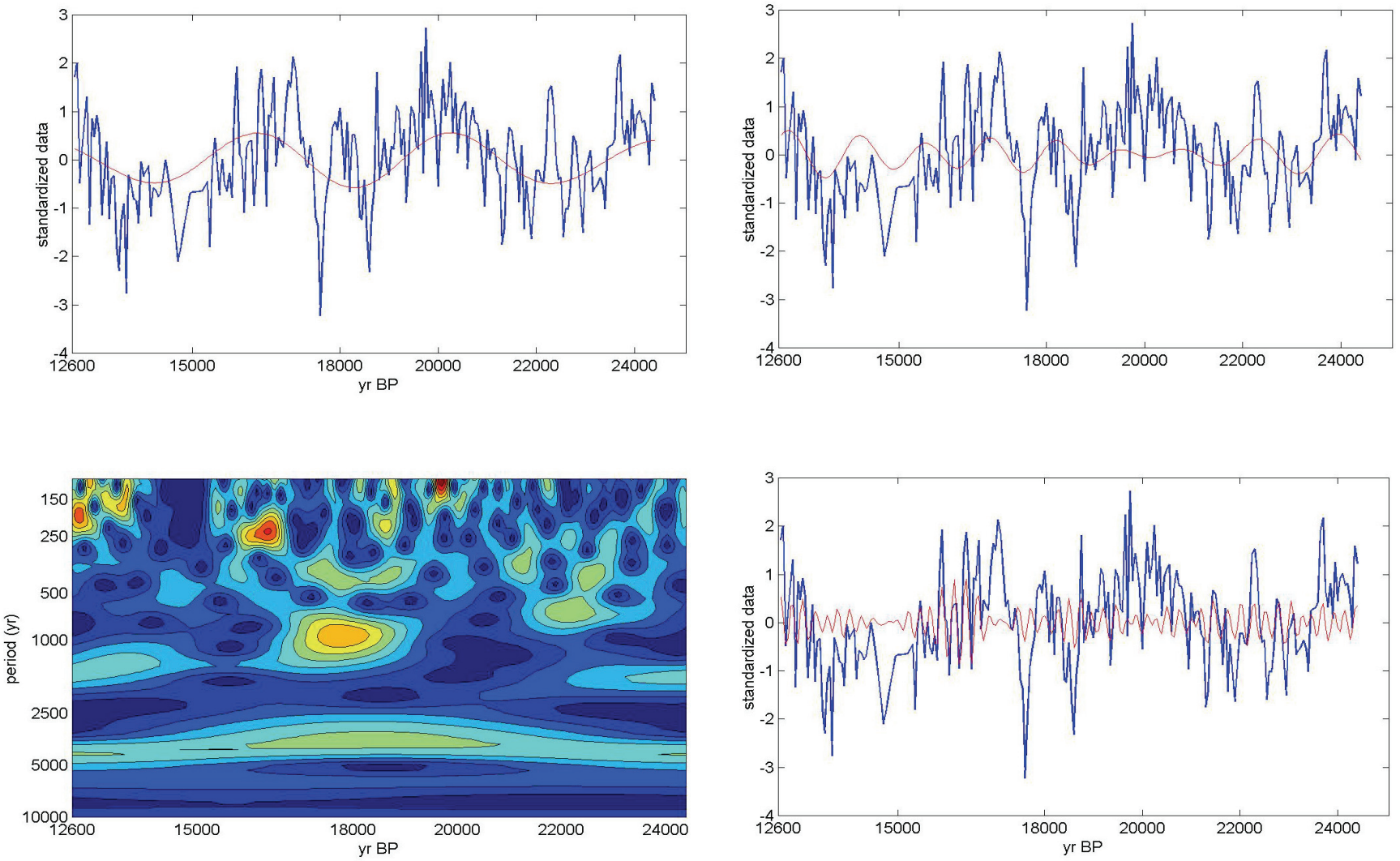

Figure 6.2. Continuous wavelet transform spectrum for $\delta^{18}O$ from 12 700 to 24 400 yr (lower left). The extracted frequency spectra for the bands 4000, 1500 and 250 years are shown (red) against the standardized data (blue) above left, above right and lower right, respectively. Flattening indicates that the signal weakens or disappears at certain points, or has modulated in frequency.

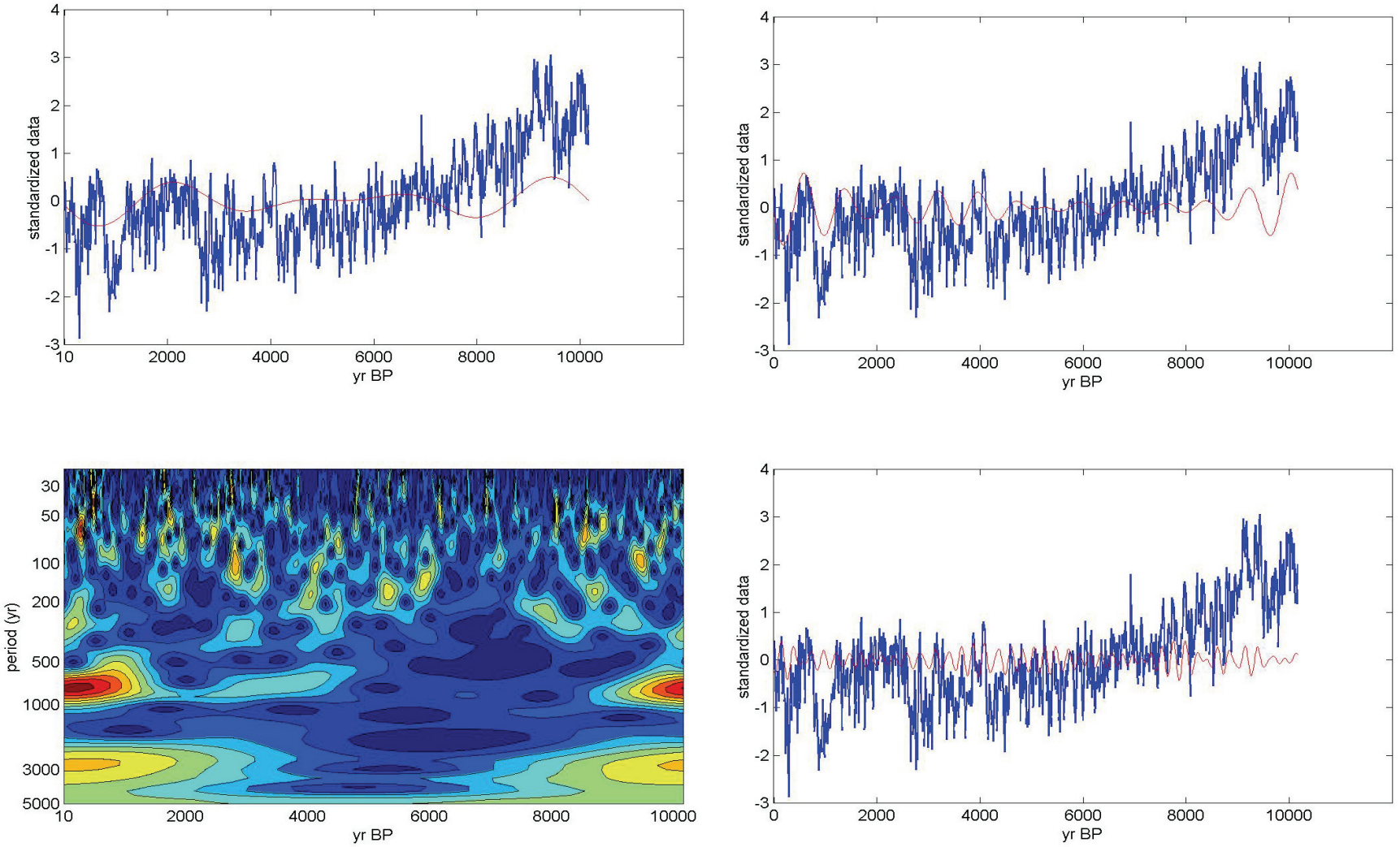

Figure 6.3. Continuous wavelet transform spectrum for $\delta^{18}O$ for the Holocene (lower left). Data were not detrended prior to analysis. Note that the vertical (time) scale for the Holocene differs from Fig 6.2 (see text) The extracted bands for frequencies 3000, 800, and 225 years are shown above left, above right and below right respectively.

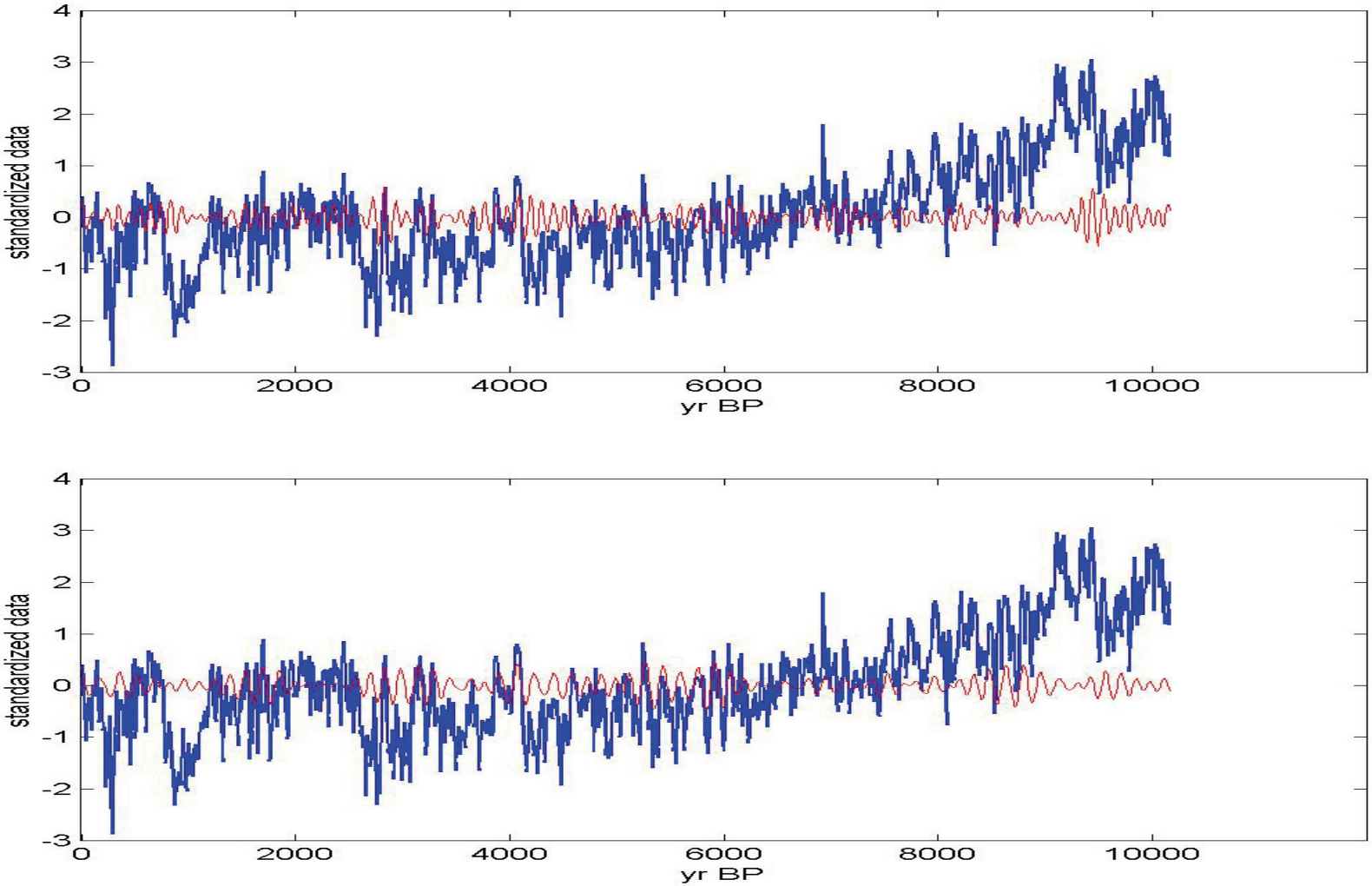

Figure 6.4. Extracted higher frequency bands for Holocene $\delta^{18}O$ data have been elongated in order to show the higher frequency bands. The upper and lower panels show frequency bands for 150 and 100 years, respectively, indicating frequency modulation in this region. This level of detail cannot be observed in the Pleistocene section because of the grosser time-scale.

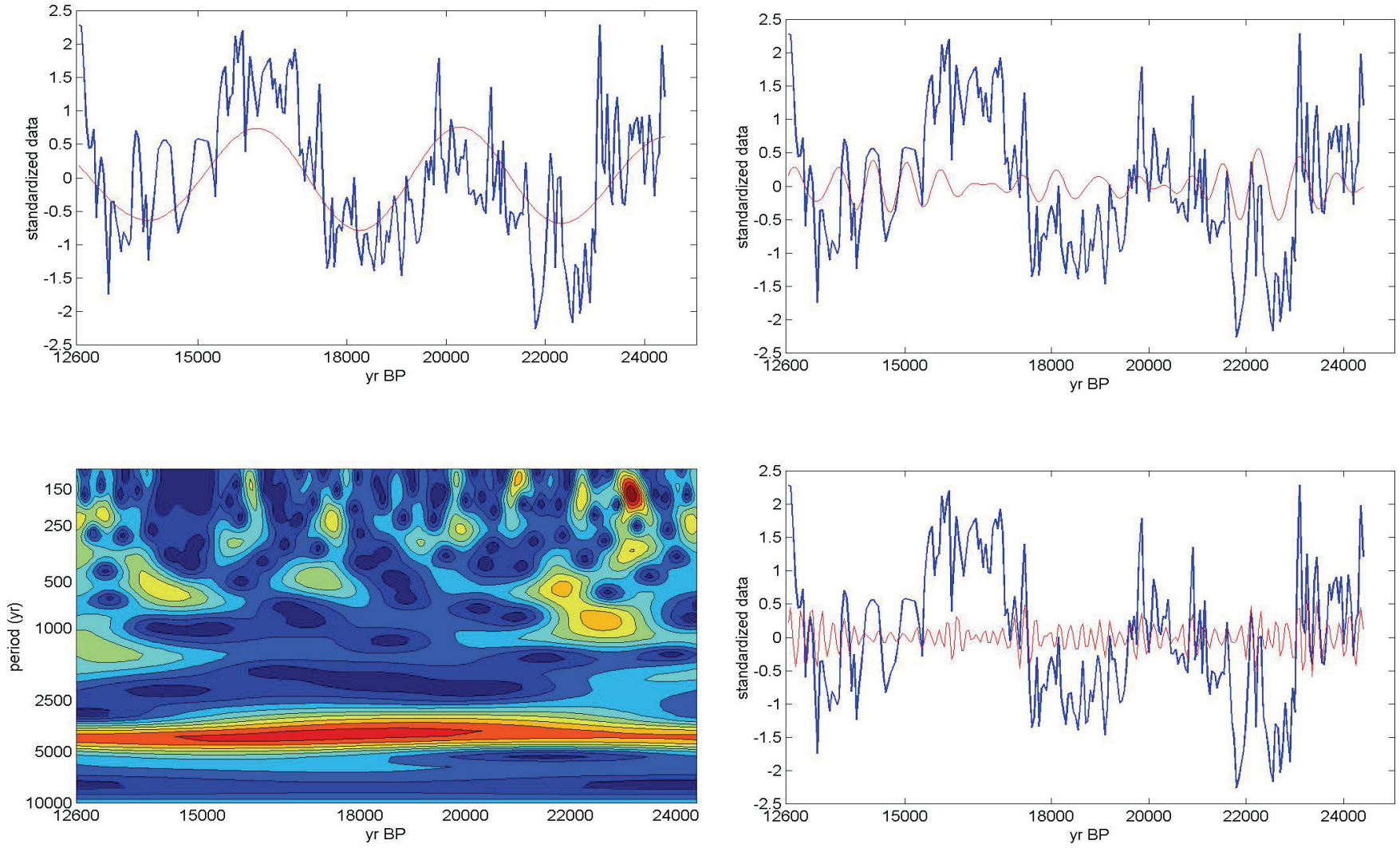

Figure 6.5. Continuous wavelet transform spectrum for $\delta^{13}C$ from 12 700 to 24 400 years, showing the strong, continuous variability centred on ~4000 years. The extracted bands for frequencies 4000, 750, and 200 years are shown above left, above right and below right, respectively. The vertical frequency timescales are the same as for Fig 6.2.

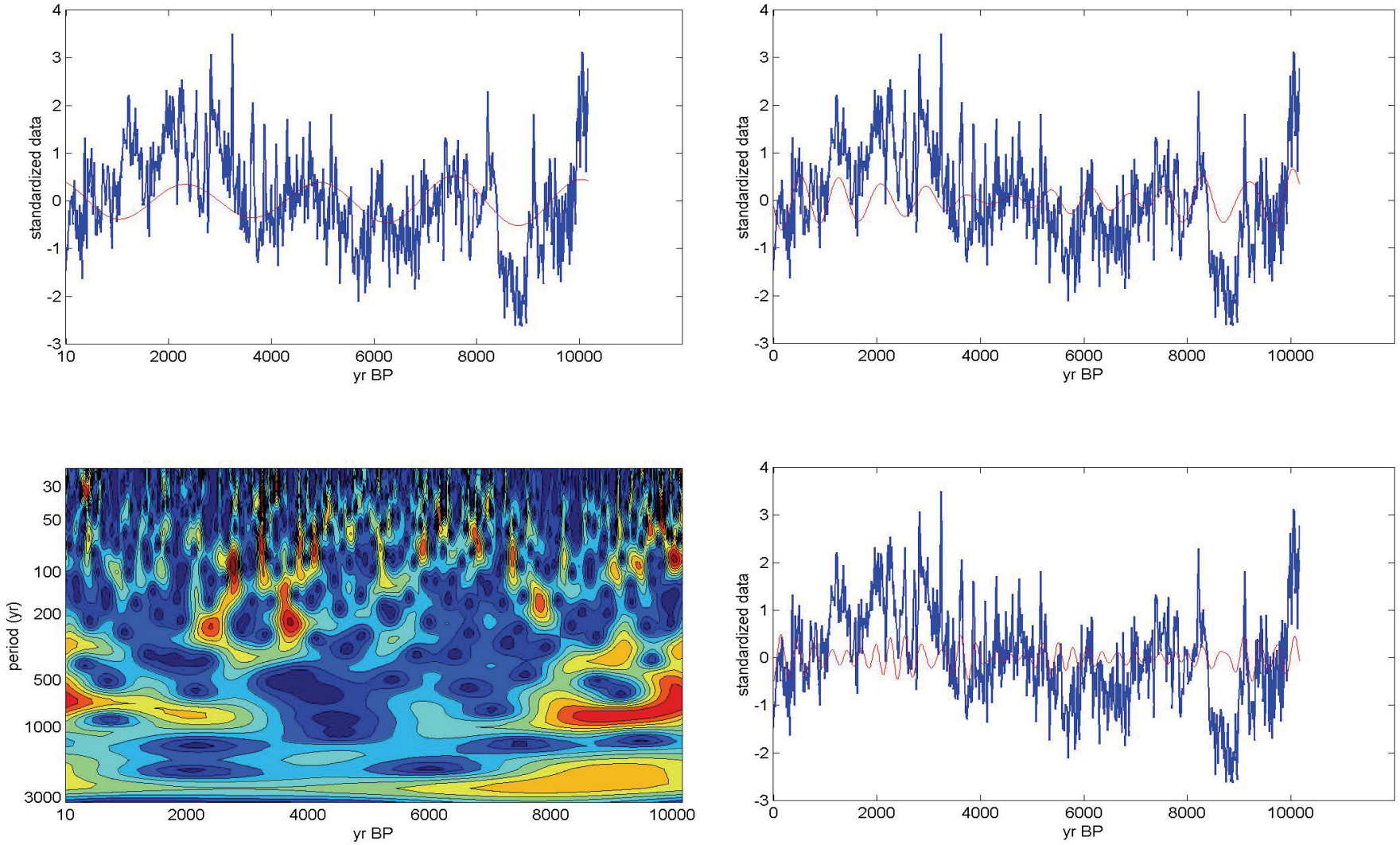

Figure 6.6. Continuous wavelet transform spectrum for $\delta^{13}C$ during the Holocene (lower left). Note that the vertical scale of the CWT is cropped at the lower end. The extracted bands for lower frequencies 2500, 750 and 300 years are shown above left, above right and below right, respectively..

CHAPTER 7

SYNTHESIS AND COMPARISONS

A range of issues related to the ground-truthing and application of proxy records from the Cold Air Cave speleothems have been covered in the preceding chapters. Here an attempt is made to draw together the various strands of the project, including the palaeorecords, the monitoring study and other recent evidence, and to place the results into a regional, and finally, a broader global context. Some of the problems encountered during the course of this project point to a number of gaps in our understanding with implications for interpretations of the records and their broader significance, and hence to directions for future research.

INFERENCES FROM THE MODERN CAVE CLIMATE DATA

The cave climate and water monitoring study provides crucial baseline information. One immediate goal was to establish whether conditions in Cold Air Cave were appropriate for yielding reasonable climate data from the stalagmites. This was found to be the case. Relative humidity in the cave has remained uniformly ~100% throughout several years that encompassed several dry winter-wet summer seasonal shifts, a flood and a drought. Therefore we can be confident that it remained so in the past. We also know that temperature in the inner cave reflects faithfully the mean annual exterior temperature and that it remains almost uniform throughout the year in spite of larger intra-annual seasonal fluctuations.

We now have some understanding of the nature of dripwater supply in terms of amounts, response times and in stable light isotope and elemental composition. The response time after initiation of rain is on the order of 6 weeks. A good supply into the cave seems to demand a high moisture level in overlying soils since lesser amounts at the end of the season hardly register. Dripwater supply declines markedly in the dry winter period. Some fissures do remain active but are not recorded by the logger because of its placement. Hence at least some stalagmites are vulnerable to cessation of growth in winters, and even more so over prolonged dry spells. This observation may explain discontinuities in the T5 stalagmite.

If growth ceases in winter, it is, however, unlikely to affect the isotopic composition because $\delta^{18}O$ in dripwaters reflects the bulk of rainwater supply, and shows a smoothing effect over the year. In other words, dripwater $\delta^{18}O$ reflects summer rainfall whenever it arrives in the cave. Although dripwater $\delta^{13}C$ was not monitored, a similar pattern is likely to hold. The isotopic values obtained for dripwater samples, together with the temperature data, provide a basis for checking whether the $\delta^{18}O$ composition of the stalagmite tips obeys the rules for fractionation under isotopic equilibrium, and what the controls on $\delta^{18}O$ variation are. $\delta^{18}O$ of dripwaters in locations near the stalagmites were ~ -3 to -3.4 ‰ at first, later shifting to values nearer -4 ‰. These values accord well with the composition of the stalagmite tips and

cave temperature when substituted into the aragonite palaeotemperature equation. They are also in accordance with isotopic composition of regional rainfall (sampled at Pretoria to the south) averaging –3.7‰ for 1958–1985 (IAEA, 1992) as well as for late Holocene–age underground waters at nearby Bela Bela of –3.6 to –4.4 ‰ (Holmgren et al, 2003). Dripwater values clearly differ from those of environmental waters in the immediate vicinity, including the river and the cave pool, which must derive directly from an external source.

In detail, there are no clear patterns in shifts in dripwater $\delta^{18}O$ through seasons and climate events. Correlations are made more difficult because key (winter) data are missing. From the existing data it seems that dripwater $\delta^{18}O$ shifts are muted through the year compared to the rapid responses and shifts of river and pool water. A shift to a lower dripwater value (-4 ‰) nearer river and pool values is observed after the flood of 2000, and dripwater values remain lower from April 2001. When δD for all cave and environmental waters is plotted against $\delta^{18}O$, most values fall above the International Meteoric Water Line, suggesting fractionation processes resulting in higher δD values and/or slightly lower $\delta^{18}O$ values. The higher slope suggests condensation effects, possibly reflecting the tropical nature of the rainfall. Since the effect is more pronounced in the dripwaters, some exchange effects could occur during passage through the bedrock or in the cave. All of this suggests that the offset between rainwater and dripwater results from the extra processes undergone by dripwaters.

These short-term *patterns* of change of the dripwater do not accord comfortably with interpretations of longer term $\delta^{18}O$ shifts in the stalagmites. The monitoring study simply was not long enough to make firm deductions about the longer time-scales in the stalagmites.

A number of observations support the conclusion that rainwater $\delta^{18}O$ fluctuations dominate stalagmite $\delta^{18}O$. Firstly, the observed variability in the stalagmites on short (decadal) time-scales is too high to be interpreted in terms of the inverse water-carbonate temperature isotope effect (Lee-Thorp et al, 2001). The assumption that the $\delta^{18}O$ composition of rainwater has remained constant on shorter timescales in the past was tested by comparing temperatures calculated from substituting groundwater and speleothem data into the palaeotemperature equation, with the observed meteorological record for the last century. The curve thus constructed shows a *cooling* of 5°C from 1950 in contrast to the observed warming of nearly 1°C for the same period (Holmgren et al, 2003). Hence the conclusion is that shifts in $\delta^{18}O$ of rain have overprinted the temperature dependent fractionation, implying considerable isotopic variation in the rain.

Comparison of the temperature index for the twentieth century with stalagmite $\delta^{18}O$ shows a weak, direct relationship (Fig 5.3). Since $\delta^{18}O$ of precipitation is controlled by Rayleigh distillation of atmospheric vapour, driven mainly by changes in air-mass temperature (Rozanski *et al.*, 1993), we can conclude that

$\delta^{18}O$ variability in the stalagmites is a consequence of changes in the nature of rainfall. Proportionately more convective rain and hail originating in the upper troposphere, along with cooler temperatures, provides the most plausible explanation for the $\delta^{18}O$ troughs in the stalagmite record. The monitoring study clearly does not reflect the amplitude of variation seen in the longer record.

Significant seasonal fluctuations do occur in trace element composition of dripwater and these changes are likely to be reflected in small-scale subannual to annual shifts in trace element composition, together with processes at the water-carbonate interface reflecting temperature and/or growth rate. The pilot studies (Finch et al, 2001; Finch et al, 2003) on small chips of T7 and T8 using SIMS indicated that subannual (seasonal) patterns are indeed observed. At present, however, the interpretation of trace element shifts in the fabric of stalagmites is still uncertain. This is particularly the case for aragonitic stalagmites which have been poorly studied. Trace element fluctuations in the upper tips of T7 and T8, specifically for Sr and Ba expressed as Sr/Ca and Ba/Ca, show links to mean regional rainfall fluctuations over the last ~40 years (Finch et al, 2003).

These observations must still be linked more securely with seasonal cave water compositions to ascertain the influence of supply and residence time in the overburden. Our current modern dripwater data presents a rather complex picture over the short period of measurement. The data show that Ca and Mg are always super-abundant in dripwater, while Sr and Ba and other trace metals are present in lower amounts. Although seasonal-scale fluctuations in these ions are observed, the main influences are difficult to discern. For instance there are some hints of a "flushing" effect after the first substantial rains, but the signals are not consistent. Furthermore, dripwater variability is but one control. Strong controls are exerted over inclusions in the calcium carbonate fabric during calcification, and they differ between calcite and aragonite. Mg, for instance, is present in the stalagmite fabric at orders of magnitude lower than in dripwater. If these problems can be resolved, the implication is that fine-scale trace element fluctuations may the key to determination of higher resolution rainfall records than has proved possible from the isotopic composition.

THE SPELEOTHEM RECORDS IN A REGIONAL FRAMEWORK

A guideline for evaluating robusticity of proxy climate indicators from stalagmites series is that the results must be replicable. Agreement between the Makapansgat T7 and T8 $\delta^{18}O$ and $\delta^{13}C$ records (Fig 5.2) (and for the shorter, discontinuous T5 where applicable), strongly suggests that the Cold Air Cave speleothems provide robust palaeo-rainfall and environmental proxies. How well do these records match with others in the region, and beyond?

A surprising feature of the Late Pleistocene section of the T8 $\delta^{18}O$ curve is the lack, apart from the quasi-periodic shifts at frequencies of ~4 Ky (Fig 6.1, 6.2), of the familiar pattern in Oxygen Isotope Stage 2, of

a severe depression at the Last Glacial Maximum ca. 19-20 Ky, followed by warming. Lowest $\delta^{18}O$ occurs at two points at ~17.5 and 18.5 Ky, but they do not present a very substantial feature in relation to other similar low points in the record. The familiar pattern is observed in sea-level curves and some ice core $\delta^{18}O$ and δD sequences, and reflects global ice volume and temperature. However, a closer examination of other regional records shows that the T8 series is not unusual. Late Glacial *warming* after ~15 Ky is widely evident in proxies such as the Uitenhage aquifer dissolved gas record, in the relevant section of the Cango Cave speleothem (Fig 7.1), and in the Mocambique Channel marine core MD 9257 foraminifera $\delta^{18}O$ and alkenone-derived SST series (Bard et al, 1997). The rather gradual shift in the foraminifera $\delta^{18}O$, decreasing after 15 Ky to achieve ~Holocene values 1.5$^{o}/_{oo}$ lower by ~9 Ky (Fig 7.1), largely reflects an ice volume effect on the ocean values.

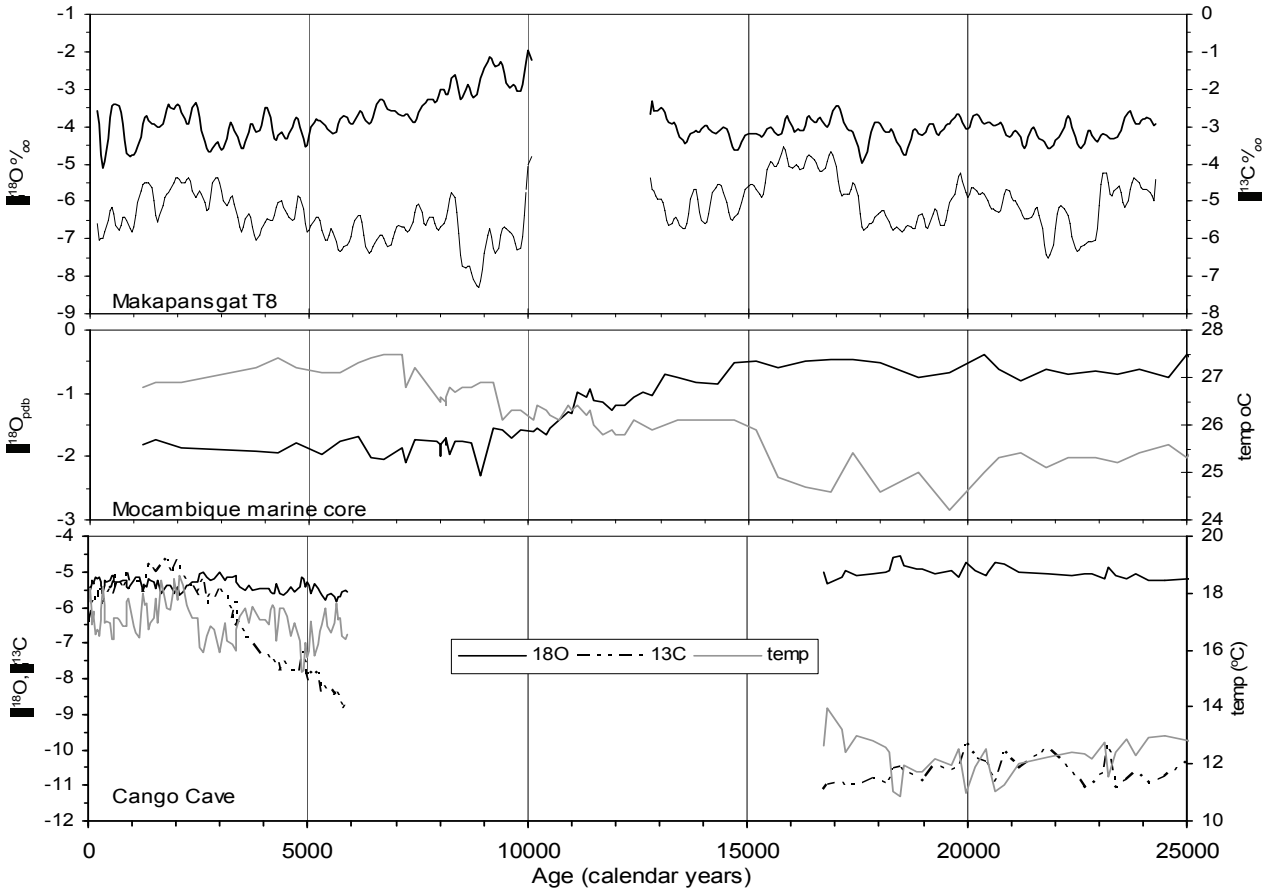

Figure 7.1. The smoothed T8 $\delta^{18}O$ and $\delta^{13}C$ series (top panel) compared with the MD 9257 $\delta^{18}O$ and alkenone sea surface temperature (SST) record (grey line) (middle panel) (Bard et al, 1996), and the $\delta^{18}O$, $\delta^{13}C$ and temperature series from Cango (lower panel). The original data for the last two were kindly supplied by E. Bard and S. Talma respectively.

With the exception of the SST record, which shows lowest temperatures from 17-19.5 Ky, followed by

stepwise warming (Bard et al, 1997), the other proxy series are rather "flat" during the period commonly considered as the LGM, ie 19-20 Ky. The Uitenhage aquifer shows lowest temperatures much earlier, at ~26 Ky, and the $\delta^{18}O$ curve for the Cango speleothem is also flat with little difference in absolute values compared to the Holocene. Even the derived temperature curve is relatively monotonous until slight warming is indicated after ~18 Ky. A substantial hiatus obscures subsequent patterns.

Although the MD 9257 $\delta^{18}O$ series lacks high resolution for both the data and the radiocarbon chronology, it suggests that the overall curve for T8 $\delta^{18}O$ in this period is strongly influenced by $\delta^{18}O$ in the oceanic source area. In the stalagmite the curve is inverted due to influence of temperature on water-vapour, and vapour-water isotope effects. Deviations at and within the 4 Ky cycles must reflect isotope effects related to drivers other than ice volume.

The pollen record from the Wonderkrater spring site ~100 Km to the west provides an opportunity for comparison with a nearby, independent source. The pollen record has a lower resolution but it provides continuous and direct evidence for vegetation shifts. Available moisture and temperature indices were derived from principal components analysis (Scott, 1999), and an age model was recently defined using a revised set of calibrated radiocarbon dates (Scott et al, 2003). Overall, the suggestion from the T8 $\delta^{13}C$ record for generally grassier conditions in the Late Pleistocene compared to the Holocene, is consistent with the Wonderkrater record, which shows that woody components are lower in the Pleistocene and higher in the Holocene (Fig 7.2). This general pattern accords in some measure with predictions and observations of higher proportions of C_4 grasses in periods with lower atmospheric CO_2 conditions in glacials (Ehleringer et al, 1997; Cerling *et al.*, 1997). The T8 $\delta^{13}C$ and the Wonderkrater pollen data, however, show that the environment never became completely dominated by C_4 grasses. Fluctuations in the T8 Late Pleistocene record suggest sparser grass cover coupled with lower temperatures at ~ 23-21, ~19.5-17.5, and ~15-13.5 Ky (Fig 7.1, 7.2). Based on a new age model for Wonderkrater (Scott et al, 2003), maximum cooling corresponding to a 1000m altitudinal drop in vegetation zones or a temperature depression of 5-6 °C compared to the present, occurred at ca. 17.5 Ky (Fig 7.2). The temperature index shows rapid warming after this event, a return to colder conditions ~15 Ky and renewed warming after ~13.5 Ky. The general pattern agrees well with the stalagmite data, lending support to the interpretation that periodic episodes with lower $\delta^{18}O$ were cooler. The discrepancies in timing are likely the result of differences in the chronologies.

The switch to aragonite at 12.7 Ky suggests the breaching of a temperature threshold. The speleothem hiatus from 12.7-10.2 Ky precludes the reconstruction of environmental conditions from stable isotope proxies for this period. The Wonderkrater temperature index shows an interruption in the warming trend at 11.3 Ky where high abundances of Chenopodiaceae and Amaranthaceae pollen suggest the prevalence

of strongly evaporative, but not necessarily dry, conditions between ca. 12 and 10 Ky (Scott, 1982; Scott et al, 2003). Hence the hiatus in the Makapansgat stalagmite growth likely reflects a cessation of dripwater due to a soil water deficit associated with evaporative conditions. These findings accord with a number of less chronologically secure, regional proxy records indicating generally drier and colder conditions at about this time (Partridge, 1997; Thomas et al. 2000).

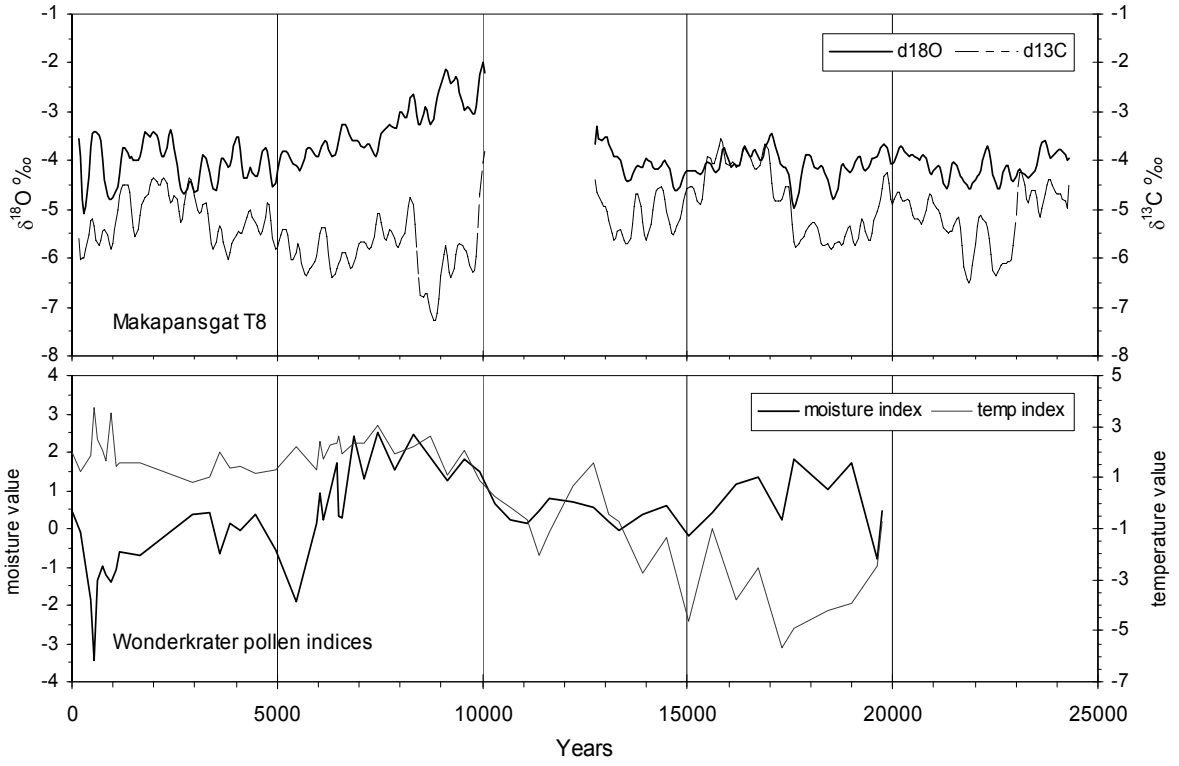

Figure 7.2. The smoothed T8 $\delta^{18}O$ and $\delta^{13}C$ record compared with the Wonderkrater pollen-derived moisture and temperature indices plotted on the revised, calibrated radiocarbon-derived age-scale (from Scott et al, 2003).

The $\delta^{13}C$ record shows a rapid decrease after 10.2 Ky to reach lowest values for the last 25 Ky at ~9 Ky, indicating increased abundance of C_3 woody or shrubby vegetation and/or a sharp reduction in C_4 grass cover (Fig. 7.2). Since the $\delta^{13}C$ minimum coincides with an exceptionally white section of the stalagmite, reflecting low organic content, a vegetation-poor environment may be inferred. At the same time, $\delta^{18}O$ values are very high, implying evaporative conditions and concurring with the indication for continued warm, evaporative conditions from the Wonderkrater pollen record (Fig. 7.2). In the Eastern Highlands of the Free State to the south, proportions of C_3 grasses vary sharply on high altitude slopes arguing for at least 2 temperature minima between 9 Ky and ~ 7.9 Ky, suggesting that continuous warm conditions were not present everywhere in the summer rainfall region (Smith et al, 2002). After 8.5 Ky increased C_4 grass cover is indicated at Makapansgat while the Wonderkrater moisture index, which is independent of grass

pollen, suggests a continuation of dry conditions. The pollen spectra indicate a dry, grassy, sparsely wooded ecosystem similar to that of the present semi-arid Kalahari Thornveld, while Cyperaceae pollen decreases sharply indicating a shrinking of the Wonderkrater swamp (Scott, 1982). From 7 to nearly 5 Ky, slightly lower $\delta^{13}C$, combined with higher $\delta^{18}O$ and higher concentrations of humates, particularly in the T7 record, indicate warmer, moister and more vegetated conditions (Lee-Thorp et al, 2001). These conditions correspond with the warming of sea surface temperatures in the Mocambique Channel (Fig 7.1) (Bard et al, 1997).

The subsequent increase in $\delta^{13}C$ in both T7 and T8, to a peak at ~2.5 Ky, is matched in the Cango Cave speleothems record. The Cango Caves lie several thousand kilometres to the south of the Makapansgat Valley in a relatively dry region which today experiences both summer and winter rains. Its geographical position places it in a zone which can sensitively reflect intensity or spatial shifts in the winter (westerly) and summer (tropical) zones of influence. Accordingly, there are several predictable differences in the two sets of speleothem records. For one, Cango $\delta^{13}C$ in the Late Pleistocene reflects entirely C_3 vegetation cover (Talma and Vogel, 1992), in contrast with that of T8 (Fig 7.1). A long hiatus exists for the Cango speleothem from ca 17 to 6 Ky. However, the $\delta^{13}C$ pattern after 6 Ky shows a clear trend towards higher $\delta^{13}C$ and hence maximum C_4 grass cover for the same period in both T7 and T8. Taken together, the two regional speleothem records suggest that conditions for C_4 grasses were optimal across a wide area at this time (Lee-Thorp et al, 2001). High grass and Asteraceae pollen counts at Wonderkrater between 2 and 3 Ky support the inference for a grassy, very slightly cooler environment, and show warmer, moister conditions with greater bushiness from 1.2 to 0.6 Ky.

The T7 and T8 $\delta^{18}O$ series show a clear, marked, negative excursion centred on 1700 AD. As we have argued elsewhere(Tyson et al, 2000; Lee-Thorp et al, 2001 Tyson et al, 2002b), this likely represents a regional manifestation of the Little Ice Age. As outlined above, strong negative shifts in $\delta^{18}O$ are most plausibly interpreted as indications of cooler conditions with greater influence of convective storms, and according to current climate models, also drier conditions. Close inspection shows that the other regional records are not necessarily in good agreement with these stalagmites, as to the directions, or timing, of climate changes. The Wonderkrater pollen moisture index shows a sharp negative excursion – but earlier at ~1500 AD, while the temperature index, although variable and showing a small dip after ~1600 AD, indicates mostly warmer conditions (Scott et al, 2003). While difference in timing of the arid episode could be ascribed to poorer chronological control, the lack of a clear temperature depression at Wonderkrater is more difficult to explain. The Cango $\delta^{18}O$ series and its derived temperatures varies very little at all, *contra* an earlier emphasis on this record (see Tyson and Lindesay, 1992). The Karkloof tree ring record from Natal, which is well-dated, seems to indicate steadily improving conditions for tree-ring

growth from ca. 1300 AD with just a slight interruption at 1700 AD and a more marked interruption at 1850 AD. Clearly, regional rainfall patterns were complex and very likely not synchronous across the summer rainfall areas around this time. Lack of agreement amongst different, widely spaced proxies, is not surprising given that the recent Standard Preciptation Index survey showed similar complexity across all entire summer rainfall regions in historical times (Rouault and Richard, 2003).

THE GLOBAL FRAMEWORK, VARIABILITY AND FORCING

Bearing in mind the large age uncertainties for the oldest part of the Makapansgat T8 stalagmite, the record can nevertheless be compared with others beyond South Africa. Comparisons with the Antarctic ice core records are particularly useful, since not only do they sensitively reflect atmospheric temperatures on high resolution timescales, but some, for instance the Taylor Dome core, provide information on the intensity of the Antarctic vortex from Na and Ca composition (Steig et al, 2000).

The Pleistocene section.

The T8 $\delta^{18}O$ curve corresponds in a general way to the relatively poorly resolved Vostok ice core temperature index (shown in Fig 7.3 as "temperature difference") derived from deuterium). Slight negative inflexions in the Vostok series, on either side of 22 and 18 Ky, correspond to the 4 Ky cyclical low points in the T8 $\delta^{18}O$. The apparently lagged warming trend in the Vostok core is likely due to chronological differences, since the temperature difference curve also differs from the well-dated Byrd $\delta^{18}O$ (Blünier *et al.,* 1998), in a similar fashion. Furthermore, according to the time model used here for Vostok (Jouzel et al, 1993), the Antarctic Cold Reversal occurs at 10.5-13 Ky which is slightly too young compared to most Antarctic records.

Correspondence with the Byrd ice core $\delta^{18}O$ is good (Fig 7.3) as one might expect since, unlike Vostok in the central interior of Antarctica, Byrd is located in Eastern Antarctica near the coast. Conditions reflected in near coastal ice cores like Byrd and Taylor Dome can be expected to correlate more strongly to circumpolar circulation in the low to mid-latitudes of the Southern Hemisphere (as noted, for instance, by Pahnke et al, 2003). Comparison of T8 $\delta^{18}O$ with the well-dated Byrd ice core (which has been fine-tuned to yield excellent comparison with GISP II in Greenland (Blunier et al, 1998), suggests remarkably close correspondence until the point (ca. 16 Ky) at which oceanic $\delta^{18}O$ shifts as a result of melting ice, as seen in the Moçambique core (Bard et al, 1997) (Fig 7.3). Low frequency shifts at ca. 4 Ky are noted in both the stalagmite and Byrd $\delta^{18}O$ series. The clear Antarctic Cold Reversal from ~12.5-14 Ky in Byrd is reflected in lower $\delta^{18}O$ stalagmite values at about the same time, although the period is somewhat extended. This discrepancy may be due to errors in the chronology or age model of the T8 stalagmite.

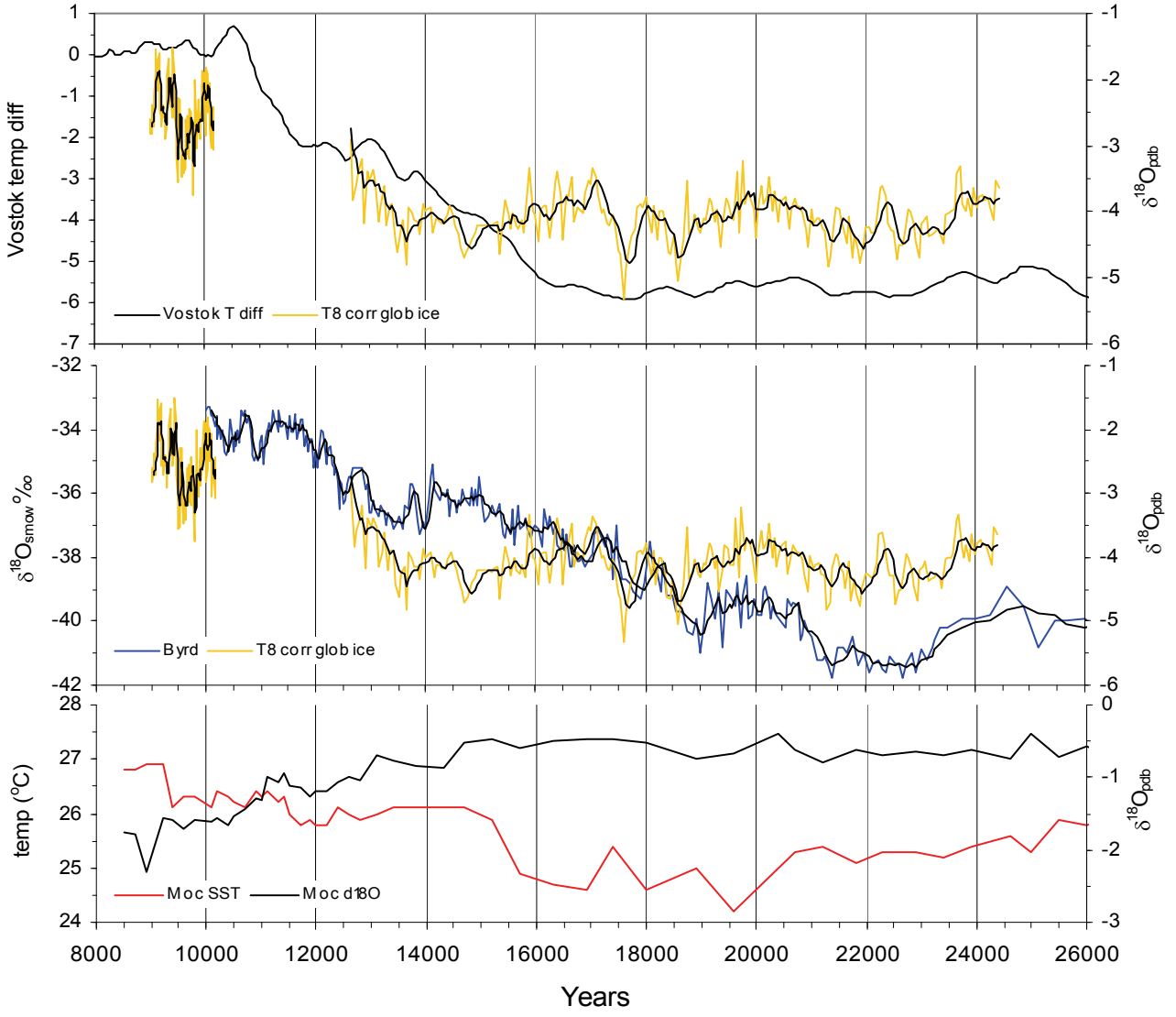

Figure 7.3. The T8 stalagmite $\delta^{18}O$ record compared against Antarctic ice core records. In the upper panel, T8 $\delta^{18}O$, interpolated to 10 year intervals (pale line) and smoothed using a 5-point running mean (dark line), is shown against the Vostok deuterium-derived temperature index (expressed as temperature difference). The EGR age model is used for the Vostok curve (Jouzel et al, 1993). In the middle panel T8 is compared against the Byrd ice core $\delta^{18}O$ curve which has been similarly smoothed (dark line) (Blunier et al, 1998). SST and $\delta^{18}O$ from the Mocambique marine core (Bard et al, 1997) is shown in the lower panel for comparison. Ice core data were obtained from www.ngdc.noaa.gov/paleo/icecore/antarctica.

The Holocene

The onset of Holocene conditions coincides closely with the spectacular collapse of the intense Antarctic circumpolar vortex evident in the Taylor Dome ice-core Na record (Steig et al, 2000). Both T8 and the Wonderkrater temperature index indicate generally warmer (but variable) conditions between 10 and 6 Ky as outlined above (Fig. 7.2). Linear dune construction in Zambia at 10-8 Ky (O'Connor and Thomas, 1999) argues for widespread arid conditions. These conditions correspond to a period of low sunspot activity (Stuiver *et al.*, 1998) preceding the "8.2 Ky cold event" observed in the North Atlantic (e.g. Alley *et al.*, 1997; deMenocal et al, 2000; Peterson et al, 2000). In contrast, further north in Africa, equatorial and northern Africa lake records (Gasse, 2000) and the Kilimanjaro ice core record (Thompson *et al.,* 2002) document a short but strong dry event at about 8.2-8.3 Ky within an overall humid Early Holocene. The two stalagmite records suggest denser vegetation (higher grey scale/humate mobilisation), more trees and/or shrubs, and slightly wetter conditions from ~7 to ~5.5 Ky.

Both the Makapansgat $\delta^{18}O$ records and the Wonderkrater temperature index suggest cooling and drying after ~5.5 Ky (Fig. 7.2), while a sharp $\delta^{18}O$ minimum occurs at 5.2 Ky in the T7 stalagmite. Elsewhere in the Southern Hemisphere, a temperature decline has been documented in 11 Antarctic ice cores at this time (Masson *et al.*, 2000), in South Atlantic marine sediments (Hodell *et al.*, 2001) and in glacier expansion in New Zealand (Porter, 2000). The dune record from Zambia (O'Connor and Thomas, 1999) indicates arid conditions after 6 Ky. Many lake level records from equatorial and northern Africa, however, suggest that widespread aridity did not take hold until after ca 5 Ky (Gasse 2000). The mid-late Holocene trend towards lower $\delta^{18}O$ values at Makapansgat occurs at roughly the same time as annual sodium (Na) concentrations and variability increases after a long period of early to mid-Holocene quietitude, in the Taylor Dome ice core (Steig *et al.*, 2000). The correspondence points to a strong connection between an intensified or enlarged circum-Antarctic vortex and declining temperatures over South Africa (Fig 7.4).

The availability of highly resolved and reproducible records from the Makapansgat Valley, with excellent time control during the Holocene, permits comparisons with similarly well-dated records globally. A great deal of argument has surrounded the question of whether climate shifts are asynchronous between the Northern and Southern Hemispheres or not, but data series, particularly terrestrial ones, with the requisite resolution to resolve the synchroneity problem are rare. Comparison of the stalagmite evidence presented here, together with Antarctic and Greenland ice cores, suggests that at least some events or trends are globally synchronous.

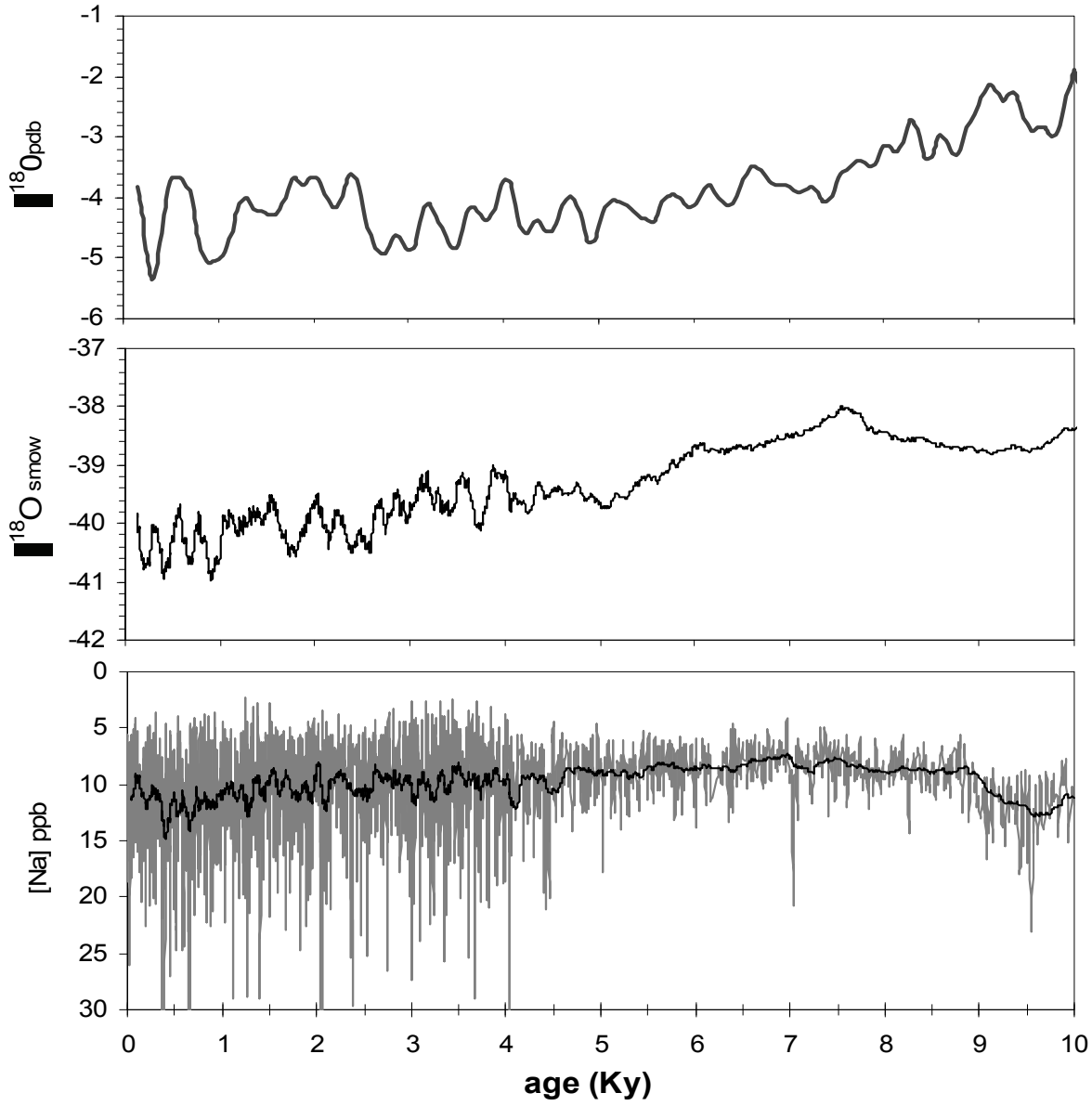

Figure 7.4. The smoothed T8 $\delta^{18}O$ record (9 point weighted running mean) (upper panel) compared with the $\delta^{18}O$ (25 point weighted mean) (middle panel) and sodium (Na) concentration series for the Taylor Dome ice core (Steig et al, 2000; Grootes et al, 2000)). Na concentration is expressed in ppb (note inverse scale), with the original data series in grey, and smoothed with a 25 point weighted running mean shown as a solid black line. www.ngdc.noaa.gov/paleo/icecore/antarctica

Variability and forcing

Wavelet analysis of $\delta^{18}O$ and $\delta^{13}C$ variations in the 24.4 Ky T8 record underscores the complexity of the climate variability suggested by visual observation of the data. Low frequency variability on millennial and multi-centennial scales seems, in general, to be more predictable for both the $\delta^{18}O$ and $\delta^{13}C$ series. All

bands showed strong frequency and amplitude modulation. Amongst the lower frequency bands in the multi-millennial to multi-centennial scales, frequency modulation occurs from longer periods in the Pleistocene to shorter periods in the Holocene. For $\delta^{18}O$ this is from a rather weak ~4000 to stronger but discontinuous ~3000 years, and moderate to weak, intermittent ~1000 to intense but intermittent ~800 years. For $\delta^{13}C$, an intense, continuous band at ~4000 modulates to a weaker band at ~2500 years, and a highly discontinuous ~750 to a broad, intermittent, but intense band between 1000 and 500 years. Amplitude shifts for $\delta^{13}C$ bands are generally in the same direction, ie the most intense band in the Pleistocene is at 4000 years, but at ~750 in the Holocene. Both series show a noisy Holocene higher frequency spectrum with variability in broad bands from ~50-150 years. These bands are more intense for the $\delta^{13}C$ series. Few significant bands are observed in the last 2000 years for either series, with the exception of variability around the period of the "LIA".

A number of inferences and points for discussion can be drawn from the CWT results. The results suggest that most power occurs in the low frequency bands: at multi-millennial (4000-3000 years), but more especially at multi-centennial (1000-700 years), scales. It would appear that variability in rainfall patterns (from $\delta^{18}O$) and proportions of tropical C_4 grasses in the floral mix (from $\delta^{13}C$) is more predictable at lower frequencies than at high frequency, multi-decadal scales. Variability in $\delta^{13}C$ is stronger than it is for $\delta^{18}O$.

Elsewhere, variability of ~4.7 Ky has been detected in Indian Ocean (Pestiaux *et al.*, 1988**)** and North Atlantic (Bond *et al.*, 1997; Alley *et al.*, 2001) marine cores. A global ~2.5 ka oscillation has been reported from glacier fluctuation (Denton and Karlén, 1973), ice cores (O´Brien *et al.*, 1995) and marine cores (Pestiaux *et al.*, 1988; Rohling *et al.*, 2002). Variability in this range has been ascribed to non-linear responses to the precession cycle (Pestiaux *et al.*, 1988) and solar forcing (Davis *et al.*, 1992; Stuiver *et al.*, 1995), but the causes are not well-understood. The greater intensity of $\delta^{13}C$ variability at these scales would affirm both of these factors, since proportions of C_4 grasses in the floral environment are sensitive to solar radiation and seasonality (that is, when pCO_2 is held constant).

It must be noted that there is *no sign*, in the Makapansgat isotope series, of Dansgaard/Oeschger events, so prominent in the Greenland ice cores and North Atlantic marine records. D/O events are quite precisely paced at regular 1470-year intervals (Schulz, 2002; Rahmstorf, 2003), but their cause remains a mystery (Rahmstorf, 2003). Schulz et al (2003) noted that D/O paced events (they are regarded as events rather than cycles) are 10x less prominent in Antarctic ice cores compared to the North Atlantic records. Nevertheless, if D/O events are paced by external solar forcing, one might reasonably expect to see some trace of them, even if only in the $\delta^{13}C$ record, which should be sensitive to solar radiative shifts.

The 0.5-1 Ky band, more prominent in the Holocene section of the Makapansgat records, finds some parallels in other, geographically widely separated palaeoclimate records. Geochemical indicators for variability in the strength of westerlies circulation in marine cores from the continental slope off Chile suggest variability at ~0.9 and 1.5 Ky years (Lamy *et al.*, 2001). Eleven ice cores from a variety of coastal and central Antarctic sites typically show oscillations of 0.8-1.2 Ky, with a reduced spacing (~800 years) between warm events and an enhanced spacing (~1200 years) during cooler periods (Masson *et al.*, 2000). It is however, a little difficult to compare these results, obtained from standard spectral analysis, with those obtained in this study by CWT analysis. If this was done, these climate series *might* show the same degree of frequency modulation as does the Makapansgat series. Notwithstanding these problems, climate oscillations in the range 1.5+/-0.5 Ky have been variously ascribed to changes in the thermohaline circulation of the North Atlantic and its connectivity with the global conveyor (Bond *et al.*, 1997; Bianchi and McCave, 1999), to vegetation-albedo positive feedbacks (deMenocal *et al.*, 2000), and to stochastic resonance (Ganopolski and Rahmstorf, 2002). Given widespread observations, the most plausible and basic explanation likely remains that of variations of solar output (Stuiver *et al.*, 1995).

One important implication of the noisiness of the high frequency part of the CWT spectrum, is that patterns of rainfall would appear to be unpredictable on short time-scales. Nevertheless, bands in the region 50-150 years are present intermittently throughout the Holocene T8 record. Attention has been drawn previously to similar observed variability in tree-ring records from South Africa, and in a run-off record for the Zambezi River at the Victoria Falls (Tyson *et al.*, 2002). Elsewhere its presence has been detected in the Greenland Camp Century oxygen isotope record (Dansgaard *et al.*, 1993). Significant variability has been found to reside in the 60-80 year band in simultaneous historical North Atlantic surface air temperature and sea level pressure (Mann and Park, 1994), in global sea surface temperature data (Folland *et al.*, 1998) and in joint empirical orthogonal function analysis of historical sea surface temperatures and mean sea level pressures around the globe. Variability at this scale may be related to changes in solar output associated with the Gleissberg cycle of around 80 years, which is, in turn, linked to high and low phases of the 11-year solar cycle (Hoyt and Schatten, 1993, 1997; Lean *et al.*, 1992, 1996; Harrison and Shine, 1999). Hence, although the quasi-100 year rhythm in the Makapansgat series is indeed noisy, widespread global observations suggest that they are firstly, real, and secondly, reflecting global variations.

SUMMARY

The long, high resolution Makapansgat stalagmite records have permitted the determination of detailed records of climate and environmental change over the last 24 400 years, their analysis for patterns of variability, and comparisons with other appropriate climate records, most notably the Antarctic ice cores.

Many of the interpretations used in this analysis have been by now reasonably well 'ground-truthed'. This study represents an enormous leap in our understanding of the evolution of the South African climate and its responses to external forcing – solar forcing either directly or via associated ocean and Antarctic climate circulation forcing. The trends within the sequence, and their patterns of variability, suggest that climate -specifically rainfall patterns - and floral composition of the northeastern interior of South Africa responds to a complex interplay between solar forcing, and influences from the circum-Antarctic atmospheric circulation and regional elements of the global thermohaline system.

Teleconnections with Antarctic circulation patterns are clearly visible in the correspondences between the T8 record with Antarctic ice-core temperature ($\delta^{18}O$ or δD) records, and vortex intensity (Na) in Taylor Dome. On present evidence, owing to uncertainties in the T8 (Late Pleistocene period) chronology, its impossible to detect the timing offset between shifts in the Makapansgat record and those in the well-dated Byrd ice-core. Oceanic influences most visible in the Makapansgat and Wonderkrater records comes from the Mozambique Channel marine core record (Bard *et al*., 1997) where warmer SST correlates with evidence for increased moisture between ~ 5.5-7 Ky.

Since the predictivity of regional climate is an important issue in a generally dry sub-continent, one of the aims of the study was to examine variability of the proxies with an eye to establishing cyclical regularality of these climate indicators. The results suggest that the lower frequency bands have modulated in frequency and intensity, in a reasonably predictable way from the late Pleistocene to the Holocene period. These bands, particularly at multi-centennial scales, appear to offer the strongest and most "reliable" of periodic features over the last several thousand years. The CWT pattern for both $\delta^{18}O$ and $\delta^{13}C$ over the last 2 Ky suggests that we are midway or so in a ~750 year climate cycle. In contrast, higher frequency variability in the region 50-150 years, is noisy and hence less predictable. Nevertheless these bands, which after all are those on the scale of (recent) human experience and approach the instrumental records, are present intermittently througout the last 10 Ky. This would suggest that current understanding of South African climate as based on roughly 80 year cycles has some worth. Due to limitations in sampling precision, the stalagmite data cannot provide information on the continued presence, or not, of 20 year cycles that have been derived from analyses of the instrumental records.

FUTURE DIRECTIONS

A number of important gaps remain to be addressed, or have newly arisen during the course of this study as is inevitable as our understanding increases.

Persistent questions remain about the connections between rainfall patterns and isotopic composition of rainfall and dripwater supply to stalagmites. Only when this problem is thoroughly addressed, by means

of long-term monitoring of rainfall or dripwater $\delta^{18}O$ composition can we be completely confident that our interpretations of stalagmite shifts are correct. In the same vein, and in spite of the progress made in this study, we lack a sound, medium-term understanding of the relationship between climate features such as rainfall amounts, patterns, and temperatures, and the delivery of trace elements to speleothems. I would identify this problem as being of particular importance because our results hint that trace element fluctuations likely provide the best opportunity for obtaining annual scale longterm climate records. Both of these questions are complex and require further cave climate monitoring studies.

Next, variability analysis has pointed to a number of frequency modes which modulate in frequency and in intensity. On their own they provide some suggestions for possible external forcing mechanisms, but the available comparisons are geographically too broad and produced using different techniques that are likely to affect the results. Firming the comparisons remains a priority for the purposes of examining forcing, but also may allow us establish more firmly some indications of lags and leads. These leads and lags could be Anarctica to southern Africa, and also Southern Hemisphere to Northern Hemisphere. Several high resolution series, including the Makapansgat $\delta^{18}O$ and $\delta^{13}C$ series as well as some of the ice-core records, should be subjected to the same continuous wavelet transform analysis. Once that is achieved cross-wavelet analysis may throw some sharper light on the question of lags or leads, rather than the eyeballing required at present.

Finally, I believe that the success of this study points to a need to apply similar techniques more broadly across southern Africa to obtain a more regionally coherent framework. For instance, if, as the climate models suggest, the western winter rainfall region is indeed in anti-phase relationship to the eastern summer rainfall region, the prediction would be that this relationship should have obtained in the past and under different boundary conditions. We can test this prediction by analysis of stalagmites from that region. The next problem would be to find suitable subject material! Above all, we urgently require many more continuous as well as detailed and well-dated proxy climate sequences to allow us to examine the evolution of climate and environments in southern Africa. Sequences have up to now been extremely scarce.

REFERENCES

Acocks, J.P.H., 1953. Veld types of South Africa. Memoirs of the Botanical Survey of South Africa 28, 1-192.

Alley, R.B., Mayewski, P.A., Sowers, T., Stuiver, M., Taylor, K.C., Clark, P.U., 1997. Holocene climatic instability: A prominent, widespread event 8200 yr ago. Geology 25(6), 483-486.

Baker. A., Smart, P.L., Edwards, R.L. and Richards, D.A. 1993. Annual growth banding in a cave stalagmite. Nature, 364, 518-520.

Baker, A., Ito, E., Smart, P.L., McEvan, R.F., 1997. Elevated and variable values of ^{13}C in speleothems in a British cave system. Chemical Geology 136, 263-270.

Baldini, J.U., McDermott, F, and Fairchild, I.J. 2002. Structure of the 8200-year cold event revealed by a speleothem trace element record. Science, 296, 2203-2206.

Bard, E., Rostek, F., Sonzogni, C., 1997. Interhemispheric synchrony of the last deglaciation inferred from palaeothermometry. Nature 385, 707-710.

Bar-Matthews, M., A. Ayalon, A. Kaufman, 1997. Late Quaternary Paleoclimate in the Eastern Mediterranean Region from Stable Isotope Analysis of Speleothems at Soreq Cave, Israel. Quaternary Research, 47, 2, 155.

Bianchi, G.G., McCave, I.N., 1999. Holocene periodicity in North Atlantic climate and deep-ocean flow south of Iceland. Nature 397, 515-517.

Blunier, T., Chappellaz, J. Schwander, J., Dällenbach, A., Stauffer, B., Stocker, T.F., Raynaud, D., Jouzel, J., Clausen, H.B., Hammer, C.U., Johnsen, S.J., 1998. Asynchrony of Antarctic and Greenland climate change during the last glacial period. Nature 394, 739-743.

Bolton, E.W., Maasch, K.A. and Lilly, J.M. 1995. A wavelet analysis of Plio-Pleistocene climate indicators: a new view of periodicity evolution. Geophysical Research Letters, 22 (20), 2753-2756.

Bond, G., Showers, W., Cheseby, M., Lotti-Bond, R., Almasi, P., deMenocal, P., Priore, P., Cullen, H., Hajdas, I., Bonani, G., 1997. A pervasive millennial-scale cycle in North Atlantic Holocene and glacial climates. Science 278, 1257-1266.

Bond, G., Showers, W., Elliot, M., Evans, M., Lotti-Bond, R., Hajdas, I., Bonani, G., Johnson, S., 1999. The North Atlantic's 1-2 kyr climate rhythm: relation to Heinrich events, Dansgard/Oeschger cycles and the Little Ice Age. In: Mechanisms of global climate change at millennial time scales. Geophysical Monograph 112, 35-58.

Brook, G. A., Burney, D.A., and Cowart, J.B. 1990. Desert palaeoenvironmental data from cave speleothems with examples from the Chihuahuan, Somali-Chalbi and Kalahari deserts. Palaeogeography, Palaeoclimatology, Palaeoecology, 76, 311-329.

Coleman, M.C., Sheppard, T.J., Durham, J.J., Rouse, J.D., and Moore, G.R., 1982. Reduction of water with zinc for hydrogen isotope analysis. Analytical Chemistry, 54, 993-995.

Coplen, T.B. 1988. Normalisation of oxygen and hydrogen isotope data. Chemical Geology (Isotope Geoscience Section) 72, 293-297.

Craig, H. 1965. The measurements of oxygen isotope palaeotemperature: stable isotopes in oceanographic studies and paleotemperatures. In Proceedings of the Third Spoleto Conference, Spoleto, Italy (E. Tongiori, Ed) pp.161-182. Sischi and Figli, Pisa.

Dansgaard, W., 1964. Stable isotopes in precipitation. Tellus, 16 (4), 436-468.

Dansgaard, W., Johnsen, S.J., Clausen, H.B., Dahl-Jensen, D., Gundestrup, N.S., Hammer, C.U., Hvidberg, C.S., Steffensen, J.P., Sveinbjörnsdóttir, A.E., Jouzel, J., Bond, G.C. 1993. Evidence for general instability of past climate from a 250 kyr ice-core record. Nature 264:218-220.

deMenocal, P., Ortiz, J., Guilderson, T., Sarnthein, M., 2000. Coherent high- and low-latitude climate variability during the Holocene warm period. Science 288, 2198-2202.

Denton, G., Karlén, W., 1973. Holocene climatic variations – Their pattern and possible cause. Quaternary Research 3, 155-205.

Dreybrodt, W. 1980. Deposition of calcite from thin films of natural calcareous solutions and the growth of speleothems. Chemical geology, 29, 89-105.

Ehleringer, J.R., Cerling, T.E., Helliker, B.R., 1997. C_4 photosynthesis, atmospheric CO_2, and climate. Oecologia 112, 285-299.

Finch, A.A., Shaw, P.A., Weedon, G.P. and Holmgren, K. 2001. Trace element variation in speleothem aragonite: potential for palaeoenvironmental reconstruction. Earth Planetary Science Letters, 186, 255-267.

Finch, A.A., Shaw, P.A., Holmgren. K and Lee-Thorp, J.A. (2003) Corroborated rainfall records from aragonitic stalagmites. *Earth and Planetary Science Letters*, 215, 265-273.

Fairchild, I.J., Baker, A., Borsato, A., Frisia, S., Hinton, R.W., McDermott, F., Tooth, A.F. 2001. Annual to sub-annual resolution of multiple trace-element trends in speleothems. J. Geol. Soc. London 158, 831-841.

Folland, C.K., Parker, D.E., Colman, A.W., and Washington, R. 1998. Large scale modes of ocean surface temperature since the late nineteenth century. Climate Research Technical Note CRTN18, Hadley Centre, Meteorological Office, UK, 21 pp.

Ganopolski, A., Rahmstorf, S. 2002. Rapid changes of glacial climate simulated in a coupled model. Nature, 409, 153-158.

Gasse, F., 2000. Hydrological changes in the African tropics since the Last Glacial Maximum. Quaternary Science Reviews 19, 189-211.

Grootes PM, Steig EJ, Stuiver M, Waddington ED, Morse DL. (2000). Taylor Dome ^{18}O record indicates global synchrony of climate change. Quaternary Research.

Grossman, E.L., Ku, T.-L., 1986. Oxygen and carbon isotope fractionation in biogenic aragonite: Temperature effects. Chemical Geology 59, 59-74.

Guilderson, T.P., Fairbanks, R.G., Rubenstone, J.L., 2001. Tropical Atlantic coral oxygen isotopes: glacial-interglacial sea surface temperatures and climate change. Marine Geology 172, 75-89.

Harrison, M. S. J., 1986. A synoptic climatology of South African rainfall variability, Unpublished Ph D thesis, University of the Witwatersrand , Johannesburg, 341pp.

Harrison, R.G., Shine, K.P., 1999. A review of recent studies of the influence of solar changes on the earth's climate. Technical Note 6, Hadley Centre, U K Meteorological Office, 64pp.

Heaton, T.H.E., Talma, A.S., Vogel, J.C. 1986. Dissolved gas paleotemperatures and 18O variations derived from groundwater near Uitenhage, South Africa. Quaternary Research 25, 79-88.

Hendy, G.H. 1971. The isotopic geochemistry of speleothems - 1. The calculation of the effects of different modes of formation on the isotopic composition of speleothems and their applicability as palaeoclimatic indicators. Geochimica et Cosmochimica Acta, 35, 801-824.

Hodell, D.A., Kanfoush, S.L., Shemesh, A., Crosta, X., Charles, C.D., Guilderson, T.P., 2001. Abrupt cooling of Antarctic surface waters and sea ice expansion in the South Atlantic sector of the Southern Ocean at 5000 cal yr B.P. Quaternary Research 56, 191-198.

Holmgren, K. 1995. Late Pleistocene climatic and environmental changes in central southern Africa. PhD thesis, Stockholm University.

Holmgren, K, Karlén, W., Lauritzen, S.E., Lee-Thorp, J.A., Partridge T. C., Piketh, S. Repinski, P., Stevenson, C., Svanered, O.,Tyson, P.D., 1999. A 3000-year High-Resolution Record of Palaeoclimate for North-Eastern South Africa. The Holocene 9,3, 295-309.

Holmgren, K., Tyson, P.D., Moberg, A., Svanered, O. 2001. A preliminary 3000-year regional temperature reconstruction for South Africa. South African Journal of Science, 97, 49-51.

Holmgren, K., Lee-Thorp, J.A., Cooper, GRJ, Lundblad, K., Partridge, T.C., Scott, L., Sithaldeen, R., Talma, A.S., and Tyson, P.D. (2003) Persistent millennial-scale variability over the past 25 thousand years in southern Africa. Quaternary Science Reviews 22, 2311-2326

Hoyt, D.V., Schatten, K.H., 1993. A discussion of plausible solar irradiance variations, 1700-1992. Journal of Geophysical Research 98, 18,895-18,906.

Hoyt, D.V., Schatten, K.H., 1997. The Role of the Sun in Climate Change. Oxford University Press: New York, 279pp.

IAEA, 1992. Statistical Treatment of Data on Environmental Isotopes in Precipitation. Technical Reports Series. Vienna: International Atomic Energy Agency. 331, 1992.

Jouzel J., Barkov, N. I., Barnola, J. M., Bender, M., Chappelaz, J., Genthon, C., Kotlyakov, V. M., Lipenkov, V., Lorius, C., Petit, J. R., Raynaud, D., Raisbeck, G., Ritz, C., Sowers, T., Stievenard, M., Yiou, F., Yiou, P. 1993, Extending the Vostok ice-core record of paleoclimate to the penultimate glacial period, Nature, 364, 1993, 407-412

Lamy, F., Hebbeln, D., Röhl, U., Wefer, G., 2001. Holocene rainfall variability in southern Chile: a marine record of latitudinal shifts of the Southern Westerlies. Earth and Planetary Science Letters 185, 369-382.

Lau, K.-M., Weng, H.-Y., 1995. Climate signal detection using wavelet transform: how to make a time series sing. Bulletin of the American Meteorological Society 76, 2391-2402.

Lauritzen, S.E., 1993. Age4U2U' Program for reading ADCAM energy spectra , integration peak correctoin and calculation of {+230}Thorium/{+234} Uranium ages. Computer Program, Dept of Geology, Bergen.

Lauritzen, S.E., 1995. A high resolution palaeotemperature proxy record during the last interglaciation in Norway from speleothems. Quaternary Research 43, 133-46, 1995.

Lauritzen, S.E. and Lundberg, J. 1999 Calibration of the speleothem delta function: an absolute temperature record for for the Holocene in northern Norway. The Holocene. 9, 659-669.

Lean, J., Skumanich, A., White, O., 1992. Estimating the sun's radiative output during the Maunder Minimum, Geophysical Research Letters 19, 1591-1594.

Lean, J., 1996. Reconstructions of past solar variability. In: Jones, P.D., Bradley, R.S., Jouzel, J. (Eds.), Climatic Variations and Forcing Mechanisms of the Last 2000 years. NATO ASI Series 1, Springer Verlag, Berlin, 41, 519-532.

Lee-Thorp, J.A., Holmgren, K., S.E. Lauritzen, Linge, H., Moberg, A., Partridge, T.C., Stevenson, C., Tyson P., 2001. Rapid climate shifts in the southern African interior throughout the mid to late Holocene. Geophysical Research Letters 28, 4507-4510.

Mann, M.E., Park, J., 1994. Global-scale modes of surface temperature variability on interannual to century time scales. Journal of Geophysical Research 99, 25819-25833.

Masson, V., Vimeux, F., Jouzel, J., Morgan, V., Delmotte, M., Ciais, P., Hammer, C., Johnsen, S., Lipenkov, V.Y., Mosley-Thompson, E., Petit, J.R., Steig, E.J., Stievenard, M.,Vaikmae, R., 2000. Holocene climate variability in Antarctica based on 11 ice-core isotopic records. Quaternary Research 54, 348-358.

Mélice, J.-L., Coron, A. and Berger, A. 2001. Amplitude and frequency modulations of the Earth's obliquity for the last million years. Journal of Climate, 14, 1043-1054.

Murray, J.W., 1954. Deposition of calcite and aragonite in caves. Journal of Geology 62, 481-492.

O`Brien, S.R., Mayewski, P.A., Meeker, L.D., Meese, D.A., Twickler, M.S., Whitlow, S.I., 1995. Complexity of Holocene climate as reconstructed from a Greenland ice core. Science 270, 1962-1964.

O´Connor, P.W.,Thomas, D.S.G., 1999. The timing and environmental significance of late Quaternary linear dune development in western Zambia. Quaternary Research 52, 44-55.

Pahnke, K., Zahn, R., Elderfriield, H., Schulz, M. 2003. 340,000-year centennial -scale maine record of Southern Hemisphere climatic oscillation. Science, 301, 948-952.

Partridge, T.C. 1997. Cainozoic environmental change in southern Africa, with special emphasis on the last 200 000 years. Progress in Physical geography, 21 (1), 3-22.

Partridge, T.C. 2000. Hominid-bearing Cave and Tufa deposits. In Partridge, T.C. and Maud,R. R. (Eds) The Cenozoic of South Africa. Oxford University Press, Oxford, pp.100-125.

Partridge, T.C., Demenocal, P.B., Lorentz, S.A., Paiker, M.J., Vogel, J.C., 1997. Orbital forcing of climate over South Africa: A 200,000-year rainfall record from the Pretoria Saltpan. Quaternary Science Reviews 16, 1125-1133.

Pestiaux, P., Van Der Mersch, I., Berger, A., Duplessy, J.C., 1988. Paleoclimatic variability at frequencies ranging from 1 cycle per 10000 years to 1 cycle per 1000 years: Evidence for a nonlinear behaviour of the climate system. Climate Change 12, 9-37.

Peterson, L.C., Haug, G.H., Hughen, K.A., Röhl, U., 2000. Rapid changes in the hydrologic cycle of the tropical Atlantic during the last Glacial. Science 290, 1947-1951.

Porter, S.C., 2000. Onset of neoglaciation in the southern hemisphere. Journal of Quaternary Science 15, 395-408.

Rahmstorf, S. 2003. Timing of abrupt climate change: a precise clock. Geophysical Research Letters, 30 (10), 1510-13.

Railsback, L.B., Brook, G.A., Chen, J., Kalin, R., Fleischer, C.J. 1994. Environmental controls on the petrology of a late Holocene speleothem from Botswana with annual layers of aragonite and calcite, Journal of Sedimentary Research A64, 147-155.

Repinski, P., Holmgren, K., Lauritzen, S.-E., Lee-Thorp, J.A. 1999. A late Holocene climate record from a stalagmite, Cold Air Cave, Northern Province, South Africa. Palaeoceanography, palaeoclimatology, Palaeoecology, 150, 269-277.

Roberts, M.S., Smart, P.L., Hawkesworth, C., Perkins, W.T., Pearce, N.J.G. 1999. Trace element variations in coeval Holocene speleothems from GB Cave, southwest England. The Holocene, 9 (6), 707-713.

Rohling, E.J., Mayewski, P.A., Abu-Zied, R.H., Casford, J.S.L., Hayes, A., 2002. Holocene atmosphere-ocean interactions: records from Greenland and the Aegean Sea. Climate Dynamics 18, 587-593.

Rouault, M. , Richard, Y. 2003. Intensity and spatial extension of drought in South Africa at different time scales. Water SA, 29, 489-500.

Rozanski, K., Araguás-Araguás, L., Gonfiantini, R., 1993: Isotopic patterns in modern global precipitation. In: Swart, P.P., Lohmann, K.C., McKenzie, J., Savin, S. (Eds.), Climate change in Continental Isotopic records. Geophysical Monograph 78, 1-36.

Schulz, M. 2000. On the 1470-year pacing of Dansgaard-Oescher events. Palaeoceanography, 17 (2), 1029-1037.

Schulz, M., Paul, A., Timmermann, A. 2002. Relaxation oscillators in concert: a framework for climate change at millennial timescales during the last Pleistocene. Geophysical Research Letters, 29 (24) 2193-6.

Schulze, B. R.,1984. Climate of South Africa, Part 8: General Survey, WB 28, South African Weather Bureau, Pretoria, 5th Edition, 330pp.

Schwarcz, H.P., 1986. Geochronology and isotopic geochemistry of speleothems. In: Fritz, P., Fontes, J. Ch. (Eds.), Handbook of Environmental Isotope Geochemistry 2,271-303. Elsevier, Amsterdam.

Scott, L. 1982. A Late Quaternary pollen record from the Transvaal bushveld, South Africa. Quaternary Research 17, 339-370.

Scott, L., 1999. The vegetation history and climate in the Savanna Biome, South Africa, since 190 000 KA: A comparison of pollen data from the Tswaing Crater (the Pretoria Saltpan) and Wonderkrater..Quaternary International 57-58, 215-223.

Scott, L., Holmgren, K., Talma, S., Woodborne, S,. Vogel, J.C. 2003. Age interpretation of the Wonderkrater spring sediments and vegetation change in the Savanna Biome, Limpopo Province, South Africa. South African Journal of Science, 99, 484-7.

Smith, B.N., Epstein, S. 1971. Two vategories of $^{13}C/^{12}C$ ratios for higher plants. Plant Physiology, 47,380-384.

Smith, Jeannette, J.A. Lee-Thorp and Judith Sealy (2002) Stable carbon and oxygen isotopic evidence for late Pleistocene and early - middle Holocene climatic fluctuations in the Caledon River Valley, southern Africa. *Journal Quaternary Science* 17 (7), 683-695.

Steig, E.J., Morse, D.L., Waddington, E.D., Stuiver, M., Grootes, P.M., Mayewski, P.A., Twickler, M.S., Whitlow, S.I., 2000. Wisconsian and Holocene climate history from an ice core at Taylor Dome, Western Ross Embament, Antarctica. Geografiska Annaler 82 A, 2-3, 213-235.

Stevenson, C., Lee-Thorp, J.A., Holmgren, K. 1999. A 3000-year isotopic record from a stalagmite in Cold Air Cave, Makapansgat Valley, Northern Province, South African Journal of Science 95, 46-48.

Stuiver, M., Grootes, P.M., Braziunas, T.F., 1995. The GISP2 $\delta^{18}O$ climate record of the past 16,500 years and the role of the sun, ocean, and volcanos. Quaternary Research 44, 341-354.

Stuiver, M., Reimer, P.J., Bard, E., Beck, J.W., Burr, G.S., Hughen, K., Kromer, B., McCormac, G., van der Plicht, J., Spurk, M., 1998. INTCAL98 radiocarbon age calibration, 24,000-0 cal BP. Radiocarbon 40(3): 1041-83.

Stute, M., Talma, A. S. 1998. Glacial temperatures and moisture transport regimes reconstructed from noble gases and $\delta^{18}O$, Stampriet aquifer, Namibia. In: Isotope techniques in the study of environmental change: Proceedings of a symposium in Vienna, 14-18 April 1997. Vienna, IAEA, 307-318.

Svanered, O. 1998. Growth layet analysis of a stalagmite from South Africa. Unpublished report, Department of Physical Geography, Stockholm University, 28pp.

Talma, A.S., Vogel, J.C., 1992. Late Quaternary paleotemperatures derived from a speleothem from Cango Caves, Cape Province, South Africa. Quaternary Research 37, 203-213.

Tarutani, T., Clayton, R.N., Mayeda, T.K., 1969. The effect of polymorphism and magnesium substitution on oxygen isotope fractionation between calcium carbonate and water. Geochimica et Cosmochimica 33, 987-996.

Thomas, D.S.G., O'Connor, P.W., Bateman, M.D., Shaw, P.A., Stokes, S., Nash, D.J., 2000. Dune activity as a record of late Quaternary aridity in the Northern Kalahari: new evidence from northern Namibia interpreted in the context of regional arid and humid chronologies. Palaeogeography, Palaeoclimatology, Palaeoecology 156, 243-259.

Thompson, L.G., Mosley-Thompson, E., Davis, M.E., Lin, P.-N., Henderson, K.A., Brecher, H.H., Zagorodnov, V.S., Mashiotta, T.A., Lin, P.-N., Mikhalenko, V.N., Hardy, D.R., Beer, J., 2002. Kilimanjaro ice core records: Evidence of Holocene climate change in tropical Africa. Science 298, 589-593.

Torrence, C., Compo, G.P., 1998. A practical guide to wavelet analysis. Bulletin of the American Meteorological Society 79, 61-78.

Tyson, P.D., 1986. Climatic Change and Variability in Southern Africa. Oxford University Press, 220pp.

Tyson, P.D. and Lindesay, J. A. 1992. The climate of the last 2000 years in South Africa. The Holocene, 2, 271-78.

Tyson, P.D., Karlén, W., Holmgren, K., and Heiss, G.A. 2000. The Little Ice Age and Medieval Warming in South Africa. South African Journal of Science 96, 121-126.

Tyson, P.D., Preston-Whyte, R.A., 2000. The Weather and Climate of Southern Africa, Oxford University Press, Cape Town, 396pp.

Tyson, P. D., Cooper, G. R., and McCarthy, T.S. 2002a. Millennial to multi-decadal variability in the climate of Southern Africa. International Journal of Climatology 22, 1105-1117.

Tyson, P. D., Lee-Thorp, J., Holmgren, K., and Thackeray, J. F. 2002b. Changing gradients of climate change in southern Africa during the past millennium: their implications for population movements. Climatic Change 52, 129-135.

Vogel, J.C., Fuls, A., and Ellis, R.P. 1978. The geographical distribution of Kranz grasses in South Africa. South Africa Journal of Science 74, 209-215.

Vogel, J.C. 1983. ^{14}C variations during the Upper Pleistocene. Radiocarbon, 25, 213-218.

Appendix 1. Results of elemental analyses by date and location. Dripwaters are denoted by dw. The lowermost dripwaters in the cave system are labelled dw @lower; dw @rear refers to samples from the upper section well behind the logger and stalagmite sites. All measurements are given in parts per billion (ppb).

Date/location	Ca	Mg	Sr	Na	K	Ba	Mn	Ni	Zn	As	Rb
15/4/00											
dw1 logger	43115	55262	26	4109	517	5	80	8	12	2	2
dw2 logger	10456	26040	5	2020	608	3	68	5	224	5	2
dw3 logger	53476	65263	30	5148	439	6	30	2	5	0	1
dw4 lower	208834	159322	44	2412	550	105	7153	19	71	5	2
dw5 lower	264546	191803	60	4387	1616	180	9577	124	520	12	7
dw6 lower	897161	538568	173	6735	3299	735	33133	241	1675	30	14
dw @rear	68826	62438	32	5213	1226	15	512		443	1	2
pool	39188	35132	24	3663	1139	6	55		15	1	1
stream	13753	9993	12	2246	1483	9	171		12	1	3
27/5/00											
dw1 logger	45833	57198	27	4364	590	9	146	3	12	2	2
dw2 logger	34787	60540	18	4311	623	7	163	6	19	3	2
dw3 logger	39967	60344	23	4352	589	9	102	2	8	2	1
dw4 lower	33926	97196	7	7630	606	37	1277	4	42	5	2
dw5 lower	18783	70516	8	6853	444	7	222	2	18	3	1
dw6 lower	84170	84317	26	8063	945	20	371	2	26	2	1
dw @rear	16824	59608	9	4658	494	2	7	1	12	0	1
pool	45915	35735	25	9837	2242	44	1308	9	76	1	3
24/6/00											
dw1 logger	22402	45921	11	4143	1251	18	754	6	70	19	3
dw2 logger	51123	57927	38	4125	2319	16	286	3	26	8	3
dw3 logger	131306	58030	91	5256	875	19	266	6	26	9	2
dw4 lower	62331	69638	27	6571	526	13	336	6	32	4	1
dw5 lower	57580	67849	20	6458	559	5	97	2	11	4	1
dw6 lower	238963	80597	61	6593	647	23	335	3	21	5	1
dw @rear	28098	59339	15	4558	764	10	439	3	50	4	1
pool	40288	34758	23	6027	1824	12	253	2	22	1	2
stream	15893	12262	12	2906	1144	7	63	4	200	2	1
5/8/2000											
dw1 logger	15460	64821	5	5030	792	5	129	5	57	6	2
dw2 logger	344838	118563	224	10334	1991	91	1215	26	222	7	5
dw3 logger	50216	85402	12	5855	635	9	484	11	146	5	2
dw4 lower	189480	565311	54	20890			171	10	53	7	13
dw5 lower	64397	62675	25	4881	1309	32	1081	21	71	12	4
dw6 lower	164076	101955	48	8583	917	43	18	1072	286	3	2
dw @rear	33421	65936	13	4507	684	14	159	3	35	1	1
pool	43137	35152	22	3909	1367	13	231	5	27	2	2
stream	6084	2933	8	2954	2188	18	92	15	123	2	3
8/9/2000											
dw1 logger	24196	81246	10	7831	1324	5	4	3	8	2	2

dw2 logger	344838	118563	224	10334	1991	91	1215	26	222	7	5
dw3 logger	188317	177045	60	15498	2351	17	830	19	90	4	3
dw4 lower	ns										
dw5 lower	5620	80017	25	6587	855	21	1217	7	20	2	1
dw6 lower	22036	10654	3	8995	766	13	12	690	27	4	1
dw @rear	20185	53671	9	3558	494	9	7	1	7	1	1
pool	39819	31813	20	2994	2051	6	56	3	9	1	1
stream	4268	3058	9	2635	3225	18	7	2	11	1	3
14/10/00											
dw1 logger	104155	86641	36	5957	1210	13	363	9	48	3	2
dw2 logger	31894	74633	12	5424	1615	27	1176	27	185	7	3
dw3 logger	40261	65490	24	5311	1120	5	37	2	5	1	1
dw4 lower											
dw5 lower	101674	109530	23	5466	974	19	2604	11	52	3	3
dw6 lower	335702	101942	9	7594	946	2	4	33	7	1	1
dw @rear	18550	58207	7	4029	1448	3	5	1	2	1	1
pool	42130	31970	20	4828	1919	4	53	2	5	0	2
stream	5537	3566	11	4925	3295	25	157	21	95	1	4
3/12/2000											
dw1 logger	919071	72814	411	2941	5584	88	1265	33	215	22	8
dw2 logger	1167708	62682	187	3156	2013	5	163	12	69	6	2
dw3 logger	19202	56097	7	5142	2132		82	2	6	3	2
dw4 lower	2151047	244673	10	6275	8063	191	9			2	1
dw5 lower	61178	83001	55	6395	1267		602	8	38	2	3
dw6 lower	34965	81571	7	6829	1067		1	137	101	1	2
dw @rear	21148	58253	8	4760	1019		3			0	1
pool											
stream	5671	3775	8	2138	2131		112			1	3
17/2/01											
dw1 logger	54373	61690	32	4799	1744	90	5	6		24	1
dw2 logger	46539	23387	28	3125	8213	67	43	3	87	16	1
dw3 logger	5366	3744	16	5299	2095	99	4	14	72	65	5
dw4 lower	47720	91477	42	12831	1944	7	116	26	594	18	7
dw5 lower	28902	76431	9	10889	2658	74	30	6	1054	10	2
dw6 lower	24493	84596	8	9101	1203	74	1	3	n.d	15	1
dw @rear	15483	48214	13	10966	1146	249	6	1	260	74	1
pool	nd										
stream	nd										
21/04/01											
dw1 logger	17050	36413	10	2006	2014	6	1	2	16	1	1
dw2 logger	22744	23893	16	1060	1593	7		2	11	1	1
dw3 logger											
dw4 lower	22630	72419	7	5813	1106		28	2	16	n.d	1
dw5 lower											
dw6 lower											
dw @rear	18280	35921	12	2964	1326	13	4	5	20	1	1
pool	31611	28570	18	3078	2132	15	25	3	22	n.d	1

stream	4921	3750	12	2884	2457	28	21	2	13	0	3
25/07/01											
dw1 logger	58160	55405	41	4458	4100		2	9	7	1	1
dw2 logger	62285	49229	78	3394	1815		57	2	8	1	2
dw3 logger	ns										
dw4 lower	8498	75065	2	7156	8691	91	7			0	1
dw5 lower	6123	151864	0	13695	1467		14			1	1
dw6 lower	11968	75649	3	6803	1029			74		1	1
dw @rear	14992	47083	7	3722	1161		23	36	6	0	1
pool	34505	29778	19	2965	1873		34			0	1
stream	ns										
25/11/01											
dw1 logger											
dw2 logger	25615	51226	9	3821	3735	31	12	3		4	2
dw3 logger	30254	51860	7	13665	5929	13	158	3	11	6	2
dw4 lower	41827	77175	10	6001	890	*n.d.*	786	13	64	10	5
dw5 lower	ns										
dw6 lower	ns										
dw @rear	30237	23181		1874	5821	n.d	28	5	2	1	13
pool	38348	28003	14	31	5517	25	163	13	12	4	2
stream	7368	3669	13	2547	7296	49	21	3		4	4
25/2/02											
dw1 logger	27397	38886	21	2489	745	28	7	2	83	0	1
dw2 logger	11965	41756	8	2434	605	*n.d.*	2	7	13	1	1
dw3 logger	17529	30646	10	1542	740	*n.d.*	6	5	3	1	1
dw4 lower	36048	70492	20	6065			9	3	7	1	1
dw5 lower	32727	71513	23	6306	992	*n.d.*	2	6	4	0	1
dw6 lower	9144	72535	3	5810	612	*n.d.*	*n.d.*	11	*n.d.*	1	1
dw @rear	15092	33860	9	2617	689	*n.d.*	0	3	*n.d.*	0	0
pool	30297	32404	21	3973	1788	4	1	3	*n.d.*	0	1
stream	4544	3245	11	3931	3524	28	8	4	*n.d.*	1	4